2011

Isolation and characterization of compounds from Zanthoxylum setulosum in the development of novel structures for chemotherapeutic drugs

Tameka M. Walker

ISOLATION AND CHARACTERIZATION OF COMPOUNDS FROM *ZANTHOXYLUM SETULOSUM* IN THE DEVELOPMENT OF NOVEL STRUCTURES FOR CHEMOTHERAPEUTIC DRUGS

by

TAMEKA M. WALKER

A DISSERTATION

Submitted in partial fulfillment of the requirements
for the degree of Doctor of Philosophy
in
The Biotechnology Science & Engineering Program
to
The School of Graduate Studies
of
The University of Alabama in Huntsville

HUNTSVILLE, ALABAMA

2011

In presenting this dissertation in partial fulfillment of the requirements for a doctoral degree from The University of Alabama in Huntsville, I agree that the Library of this University shall make it freely available for inspection. I further agree that permission for extensive copying for scholarly purposes may be granted by my advisor or, in his/her absence, by the Chair of the Department or the Dean of the School of Graduate Studies. It is also understood that due recognition shall be given to me and to The University of Alabama in Huntsville in any scholarly use which may be made of any material in this dissertation.

Tonika Walker 6-28-11

(student signature) (date)

DISSERTATION APPROVAL FORM

Submitted by Tameka M. Walker in partial fulfillment of the requirements for the degree of Doctor of Philosophy in Biotechnology Science & Engineering and accepted on behalf of the Faculty of the School of Graduate Studies by the dissertation committee.

We, the undersigned members of the Graduate Faculty of The University of Alabama in Huntsville, certify that we have advised and/or supervised the candidate on the work described in this dissertation. We further certify that we have reviewed the dissertation manuscript and approve it in partial fulfillment of the requirements for the degree of Doctor of Philosophy in Biotechnology Science & Engineering.

6-27-11 Committee Chair
(Date)

6-27-11

6-28-11

6/28/11

6-27-11 Department Chair

6/28/11 College Dean

Rhonda Kay Gaede 8/7/11 Graduate Dean

ABSTRACT
The School of Graduate Studies
The University of Alabama in Huntsville

Degree Doctor of Philosophy Program Biotechnology Science & Engineering

Name of Candidate Tameka M. Walker

Title Isolation and Characterization of Compounds from *Zanthoxylum setulosum* in the Development of Novel Structures for Chemotherapeutic Drugs

Breast cancer is one of the leading causes of cancer death in American women and unfortunately, current chemotherapy protocols still have limitations: 1) most chemotherapy destroys not only cancer cells, but also many rapidly dividing normal cells and 2) cancer cells can develop resistance to chemotherapeutic agents through mutation. Thus, there is a crucial need to find new chemical agents which 1) exploit differences between normal cells and breast cancer cells in order to selectively kill the breast cancer cells and 2) provide new, complementary chemotherapeutic techniques to be used in conjunction with other breast cancer treatments or in combination with other anticancer drugs. Tropical rainforest plants have evolved chemical defensive mechanisms to avoid herbivory and resist pathogens. *Zanthoxylum* is a genus of about 250 species in Rutaceae that contain a rich source of lignans, alkaloids, coumarins, amides, flavonoids, terpenes and other metabolites with pharmacological properties. Therefore, there are beneficial novel chemical agents present in *Zanthoxylum* that can be studied for human maladies, such as cancer. In this work, the fractionation of active materials, screening of cytotoxicity, determination of isolated chemical structures, and binding energies of human DNA topoisomerase I of *Zanthoxylum setulosum* were evaluated. *Zanthoxylum*

setulosum was notably cytotoxic (100% kill at 100 μg/ml) on MCF-7, MDA-MB-231, and MDA-MB-468 cells *in vitro*. The cytotoxic effects of isolated compounds from *Zanthoxylum setulosum* were tested against MCF-7 and MDA-MB-231 breast cancer cell lines. Chemical structures of cytotoxic compounds were determined through NMR, HPLC, and X-ray crystallography spectroscopic techniques. Lupeol, sesamin, lichexanthone, and sesquichamaenol were isolated from *Zanthoxylum setulosum*. Lupeol exhibited high cyctotoxic killing against MCF-7 and MDA-MB-231 cells at 100% kill at 100 mg/ml, with a LC_{50} value of 85.3 μM and 453.9 μM, respectively. Molecular docking studies for binding energies of lichexanthone with five DNA structures, PDB: 1k4t, 1z3f, 1al9, 1t8i, and 1sc7 were calculated using ArgusLab and Molegro Virtual Docker. The primary objective was to isolate fractions from *Zanthoxylum setulosum* and identify the active components and mechanism for new potential chemotherapeutic drugs.

Abstract Approval:

Committee Chair S Sivanesan

Department Chair S Sivanesan

Graduate Dean Rhonda Kay Hoede 8/7/11

ACKNOWLEDGMENTS

I would like to start by thanking God for giving me the strength and patience to complete my Doctor of Philosophy. I would like to thank my parents, Mrs. Mary Williams and Mr. Ezell Walker, for their support and love in my many endeavors throughout my education. To my family and friends, I would like to say thanks for all of your prayers and encouraging words throughout my struggles; thanks for believing in me.

I would like to thank my advisor, Dr. William N. Setzer, for his guidance with my research and obstacles. It has been a long journey and I have enjoyed working with you in the study of natural products. Thank you for the opportunity to work and research natural products and breast cancer and your advisement throughout my graduate studies. I am grateful to the Monteverde Cloud Forest Preserve and the Tropical Science Center for granting me permission to collect plant materials under a cooperative rights agreement and to the Commission for the Development of Biodiversity of Costa Rica's Ministry of the Environment, Energy, and Telecommunications for Research Permit R-001-2006-OT-CONAGEBIO. I would like to thank my committee members, Dr. Vogler, Dr. Lawton, Dr. Moriarity, and Dr. Waddell for their help in preparing my research proposal. I would also like to thank Dr. Vogler for his guidance and knowledge with NMR. I would like to thank Dr. Moriarity for her help with cell culture and biological assays, along with students Brenda Wright and Gabrielle Hill. I would like to thank Madan Gopal for X-ray crystrallography data. I would also like to thank the graduate students of the Natural Products Research Group at UAHuntsville for help along the way with questions and tips. I would like to thank MGSA for their support and guidance throughout my graduate studies.

I would like to thank the LSAMP, graduate studies, and the ACS Organic Chemistry Division Fellowship for funding my doctoral studies. I would like to thank Dr. Emanuel

Waddell, advisor of the UAH LSAMP program, for his guidance throughout my graduate education and for accepting the challenge of leading the LSAMP program after traumatic events. Dr. Waddell, your leadership has allowed me to continue in the doctoral program. I would like to thank the faculty members that were involved in the tragedy on campus for having the strength to continue and for supporting the graduate students in completion of their degrees, including my doctoral degree.

To the late Dr. Adriel D. Johnson, Sr., I would like to thank you for your commitment in producing graduate students in the STEM areas and for instilling the importance of reaching back to help others. Thank you for believing in me and encouraging me to apply for the Biotechnology Science & Engineering, Ph.D. program. Throughout the obstacles I have made it and will soon be your colleague. Thank you for your motto, "Success = Graduation". To my aunts, Dessie Brown Maxie and Annie Brown who lost the battle with breast cancer, thank you for giving me inspiration to center my doctoral research on breast cancer. To those that I have lost that have been important factors in my life, thank you for paving the way. You are never forgotten but always loved.

TABLE OF CONTENTS

Page

List of Figures xi

List of Tables xv

List of Abbreviations/Symbols xvi

Chapter

I. INTRODUCTION 1

1.1 Cancer 1

1.1.1 Breast Cancer 2

1.2 Natural Products 3

1.2.1 Monteverde Cloud Forest 4

1.3 *Zanthoxylum* 5

1.3.1 Lignans of *Zanthoxylum* 5

1.3.2 Alkaloids of *Zanthoxylum* 6

1.3.3 Coumarins of *Zanthoxylum* 8

1.3.4 Amides of *Zanthoxylum* 9

1.3.5 Flavonoids of *Zanthoxylum* 10

1.3.6 Terpenes of *Zanthoxylum* 12

1.4 Zanthoxylum setulosum 13

1.5 Triterpenoids Antineoplastic Properties 16

1.6 DNA Topoisomerase 16
1.6.1 Anti-cancer DNA Topisomerase Inhibitors 17
1.7 Molecular Docking 20
1.7.1 Molecular Docking Software 21
II. MATERIALS AND METHODS.....23
2.1 Plant Collection and Extraction 23
2.2 Chromatographic Separation 24
2.3 Cytotoxicity Assay.....25
2.4 Gas Chromatography-Mass Spectrometry.....26
2.5 Structural Determination.....26
2.6 Molecular Docking 26
III. RESULTS 30
3.1 Chromatographic Separation 30
3.2 Cytotoxicity Screening Data.....31
3.3 Spectroscopic Data.....33
3.4 Molecular Modeling Data 42
IV. DISCUSSION.....49
4.1 Analysis of Lupeol.....49
4.2 Analysis of Sesamin.....52
4.3 Analysis of Lichexanthone 53
4.4 Analysis of Sesquichamaenol 54
4.5 Analysis of Molecular Docking.....55

V. CONCLUSIONS 69

APPENDIX A: NMR Spectra.....73

APPENDIX B: Mass Spectra.....80

REFERENCES 83

LIST OF FIGURES

Figure Page

1.1 Structures of lignans from *Zanthoxylum* 6

1.2 Structures of alkaloids from *Zanthoxylum* 7

1.3 Structures of coumarins from *Zanthoxylum* 8

1.4 Structures of amides from *Zanthoxylum* 10

1.5 Structures of flavonoids from *Zanthoxylum* 11

1.6 Structures of triterpenoids from *Zanthoxylum* 13

1.7 Chemical constituents from *Zanthoxylum setulosum* 14

1.8 *Zanthoxylum setulosum* deposited in Smithsonian Tropical Research Institute 15

1.9 Anti-cancer topoisomerase inhibitor drugs 18

1.10 X-ray crystal structure of human topoisomerase I bound to DNA (PDB: 1k4t) 19

1.11 X-ray crystal structure of human topoisomerase II bound to DNA (PDB: 2rgr) 19

1.12 X-ray crystal structure of *Saccharomyces cerevisiae* ATPase region of topoisomerase II (PDB: 1pvg) 20

3.1 Chromatographic separation scheme for *Zanthoxylum setulosum* extract 31

3.2 Lupeol 34

3.3 Sesamin 36

3.4 X-ray crystal structure of sesamin 37

3.5 Lichexanthone 40

3.6 Sesquichamaenol 41

3.7 X-ray crystal structure of human topoisomerase I (ribbon structure)-DNA complex (wire figure) PDB: 1k4t with docked lichexanthone (CPK model) from Molegro Virtual Docker molecular docking analysis 44

3.8 X-ray crystal structure of DNA complex (wire figure) PDB: 1z3f with docked lichexanthone (CPK model) from Molegro Virtual Docker molecular docking analysis.... 45

3.9 X-ray crystal structure of DNA complex (wire figure) PDB: 1al9 with docked lichexanthone (CPK model) from Molegro Virtual Docker molecular docking analysis 46

3.10 X-ray crystal structure of human topoisomerase I (ribbon structure)-DNA complex (wire figure) PDB: 1t8i with docked lichexanthone (CPK model) from Molegro Virtual Docker molecular docking analysis 47

3.11 X-ray crystal structure of human topoisomerase I (ribbon structure)-DNA complex (wire figure) PDB: 1sc7 with docked lichexanthone (CPK model) from Molegro Virtual Docker molecular docking analysis 48

4.1 Hydrogen bonding (blue dashed lines) of lupeol (red) with amino acids of the DNA binding site of yeast topoisomerase II (PDB: 1bjt) 51

4.2 Hydrogen bonding (blue dashed lines) of lupeol (red) with amino acids of the ATP binding site of yeast topoisomerase II (PDB: 1pvg) 52

4.3 Overlay of docked lichexanthone (red) and topotecan (purple) in the DNA of human topoisomerase I (PDB:1k4t)..... 57

4.4 Hydrogen bonding between lichexanthone and the C-G base pair of PDB: 1z3f..... 59

4.5 Hydrogen bonding between lichexanthone and the C-G base pair ofPDB: 1z3f..... 60

4.6 LUMO of lichexanthone (left) and HOMO of guanine-cytosine orientation 1 (right) from M06/6-31G* calculations 61

4.7 LUMO of lichexanthone (left) and HOMO of guanine-cytosine orientation 2 (right) from M06/6-31G* calculations 62
4.8 Geometry optimized (M06/6-31G*) structure for interactions of lichexanthone with C-G orientation 1 63
4.9 Geometry optimized (M06/6-31G*) structure for interactions of lichexanthone with C-G orientation 2 63
4.10 Dipole-dipole interactions between lichexanthone and the C-G base pair of orientation 1. 64
4.11 Dipole-dipole interactions between lichexanthone and the C-G base pair of orientation 2. 64
4.12 Electrostatic potential map for lichexanthone (left) and C-G base pair (right) orientation 1. 65
4.13 A. Electrostatic potential map of the complex lichexanthone (below) and the C-G base Pair (above) for orientation 1. B. Electrostatic potential map of the complex lichexanthone (below) and the C-G base Pair (above) for orientation 1 rotated 180° 66
4.14 Electrostatic potential map for lichexanthone (left) and C-G base pair (right) orientation 2 67
4.15 Electrostatic potential map of the complex lichexanthone (below) and the C-G base Pair (above) for orientation 2. B. Electrostatic potential map of the complex lichexanthone (below) and the C-G base Pair (above) for orientation 2 rotated 180° 68
A.1 ^{1}H NMR for lupeol in $CDCl_3$ 74
A.2 ^{13}C NMR for lupeol in $CDCl_3$ 75
A.3 ^{1}H NMR for sesamin in $CDCl_3$ 76
A.4 ^{13}C NMR for sesamin in $CDCl_3$ 77

A.5 ^{1}H NMR for lichexanthone in $CDCl_3$ 78

A.6 ^{1}H NMR for sesquichamaenol in $CDCl_3$ 79

B.1 Mass spectrum of lichexanthone 81

B.2 Mass spectrum of sesquichamaenol 82

LIST OF TABLES

Table Page

3.1 Cytotoxicity of $CHCl_3$ fractions of *Zanthoxylum setulosum* on MCF-7 cells in culture 32

3.2 Cytotoxicity of $CHCl_3$ fractions of *Zanthoxylum setulosum* on MDA-MB-231 cells in culture 33

3.3 Spectroscopic data for Lupeol (F14) 34

3.4 Spectroscopic data for sesamin (F29) 36

3.5 X-ray atomic coordinates for sesamin 38

3.6 Atomic bond (Å) lengths for sesamin 39

3.7 Spectroscopic data for lichexanthone (F20-23F1) 40

3.8 Spectroscopic data for sesquichamaenol 41

3.9 ArgusDock binding energies (kcal/mol) of best binding poses for ligands into DNA of human topoisomerase I 42

3.10 Molegro binding energies (kcal/mol) of best binding poses for ligands into human DNA topoisomerase I 43

4.1 LC_{50} values of compounds from *Zanthoxylum setulosum* and standard deviation of those values against two tumor cell lines compared to anticancer drugs 50

4.2 LC_{50} values of lupane triterpenoids against various cell lines. 50

4.2 Calculated electronic properties for lichexanthone and DNA base pair 59

LIST OF ABBREVIATIONS/SYMBOLS

α .....alpha

Å .....angstrom

Ala.....alanine

Arg .....arginine

Asn .....asparagines

Asp .....aspartic acid

ATCC.....American Type Culture Collection

ATP.....adenosine triphosphate

β .....beta

bp .....base pair

B2LYP .....Becke-three-parameter-Lee-Yang-Parr

BRAC1.....breast cancer susceptibility gene 1

BRAC2.....breast cancer susceptibility gene 2

^{o}C .....celsius

C..... carbon

C-G.....cytosine-guanine

$CDCl_3$.....deuterated chloroform

$CHCl_3$.....chloroform

CHO.....aldehyde

CH_2O.....formaldehyde

^{13}C-NMR.....carbon nuclear magnetic resonance

CO.....carbonyl

CO_2.....carbon dioxide

gCOSY.....gradient correlation spectroscopy

CPK.....space-filling model, Corey, Pauling, Koltun

δ.....delta

d .....doublet

dd .....doublet of doublet

DFT.....density functional theory

DMSO.....dimethylsulfoxide

DNA.....deoxyribonucleic acidE energy

E_{aq}.....aqueous energy

EGFR .....epidermal growth factor receptor

ER .....estrogen receptor

EtOAc .....ethyl acetate

F .....fraction

FGFR .....fibroblast growth factor receptor

g .....gram(s)

GC-MS.....gas chromatography-mass spectrometry

GEMDOCK .....generic evolutionary method for molecular DOCKing

Glide.....grid-base ligand docking with energetics

Gln .....glutamine

Glu .....glutamic acid

Gly .....glycine

GOLD .....genetic optimization for ligand docking

GTPase.....guanosine triphosphate enzyme

H.....hydrogen

Hep G2.....human liver carcinoma cell line

HER2/neu.....human epidermal growth factor receptor 2

His.....histidine

HPLC .....high-performance liquid chromatography

gHMBC.....gradient heteronuclear multiple bond correlation

^{1}H-NMR.....proton nuclear magnetic resonance

HOMO .....highest occupied molecular orbital

gHSQC.....gradient heteronuclear single quantum coherence

IIe .....isoleucine

kcal.....kilocalorie

kD.....kilodalton

LC_{50} .....lethal concentration, 50%

LUMO.....lowest unoccupied molecular orbital

Lys .....lysine

m .....multiplet

M+.....molecular ion peak

MEL-2.....human embryonic stem cell line

MHz .....megahertz

MMFF.....Merck molecular force field

mol .....mole

MSD.....mass selective detector

m/z .....mass-to-charge ratio

µg.....microgram(s)

µL.....microliter(s)

µm.....micrometer(s)

µM.....micromolar(s)

mg .....milligram(s)

ml .....milliliter(s)

mm .....millimeter(s)

min .....minute

MCF-7.....Michigan Cancer Foundation-7 cell line

MDA-MB-231 .....M.D. Anderson-Metastatic Breast-231 cell line

MDA-MB-468 .....M.D. Anderson-Metastatic Breast-468 cell line

MTT .....3-(4,5-dimethylthiazol-2-yl)-2,5-diphenyltetrazolium

MVD .....Molegro Virtual Docker

$NaHCO_3$ .....sodium bicarbonate

NF-κB .....nuclear factor-kappa beta

NSAIDs.....non-steroidal anti-inflammatory drugs

NMR .....nuclear magnetic resonance

nm .....nanometer

NT .....not tested

O.....oxygen

π-π.....pi-pi

PDB.....Protein Data Bank

PFG .....pulsed field gradient

Phe .....phenylalanine

PKC.....protein kinase C

PLP.....piecewise linear potential

R_f.....retention factor

RMSD.....root-mean-square deviation

RPMI-1640.....Roswell Park Memorial Institute

s.....singlet

Ser.....serine

SiO2.....silicon dioxide

Std. Dev. .....standard deviation

Thr.....threonine

TLC.....thin layer chromatography

Tyr.....tyrosine

UV.....ultraviolet

VT.....variable temperature

ZASEBC.....*Zanthoxylum setulosum* chloroform extrac

CHAPTER I

INTRODUCTION

1.1 Cancer

Cancer is the second most common cause of death and accounts for 1 of every 4 deaths in the United States (U.S.) [1]. In 2010, approximately 1.5 million individuals in the U.S. are expected to be diagnosed with cancer, not including noninvasive cancers, and approximately 569,490 individuals are expected to die [1]. Cancer is a disease that involves uncontrolled growth, invasion, and metastasis of a group of cells. Environmental and hereditary genetic causes are two factors that result in cancerous cells. Tobacco, diet, obesity, radiation, and pollutants are all causes related to environmental factors, which lead to hereditary genetic abnormalities [2]. Cancer is caused by a series of mutations that inactivate tumor suppressor genes that regulates cell reproduction. Inactivation of tumor suppressor genes cause cells to proliferate, or grow, leading to further inactivation of DNA repair genes, to create oncogenes that will lead to more inactivation and will ultimately lead to cancerous cells. Oncogenes are classified into several categories involved in the pathway to cell proliferation including growth factors, receptor tyrosine kinases, cytoplasmic tyrosine kinases, cytoplasmic serine/threonine kinases, regulatory guanosine triphosphate enzymes (GTPases), and transcription factors [3]. Cancer treatment includes chemotherapy, radiotherapy, and surgery chosen by the relevance of

the type and progression of the tumor. Chemotherapy is often the most effective treatment for cancerous cells. However, chemotherapy action involves killing cells that rapidly divide, including normal cells such as bone marrow, digestive tract and hair follicles resulting in the, common side effects of treatment [1]. Therefore, there is a crucial need to find new chemotherapeutic agents that will 1) selectively kill cancer cells, 2) provide complementary chemotherapeutic techniques, and 3) reduce chemotherapy resistance.

1.1.1 Breast Cancer

According to the 2010 Cancer Statistics 1 in 4 deaths in the United States is due to cancer, with breast cancer leading and accounting for 28% of new cancer cases among women [4]. Breast cancer is the second most common cancer in American women, with about a one in eight chance of being diagnosed during a women's lifetime. Breast cancer is also the second leading cause of cancer death in women, with a death rate of about one in thirty-five [5]. The death rate largely affects women of minority race/ethnicity and medically underserved. There is a significant disparity among the deaths between African American and Caucasian women [6,7]. African American women have a 7% lower incidence rate but a 17% higher rate of death than Caucasian women. Racial disparities in mortality are contributed by a number of factors, including quality of screening, timely diagnosis and treatment, and more aggressive form of cancer at time of treatment [4]. Breast cancer is a carcinoma that is classified as a malignant tumor derived from epithelial cells influenced by several hormones and receptors. Mutations inactivate

genes such as breast cancer susceptibility gene 1 (BRCA1) and breast cancer susceptibility gene 2 (BRCA2), which have been linked to estrogen exposure [8]. There are various signal transduction pathways involved where mutations effect apoptosis and lead to tumorigenesis: survival factors, hormones, growth factors, cytokines and death factors [9]. Several cancer drugs have been developed as treatment, such as Taxol, Tamoxifen, and Herceptin. Tamoxifen is used to treat estrogen receptor (ER)-positive breast cancers and Herceptin is used in human epidermal growth factor receptor 2 (HER2/neu)-positive cancers [10,11].

1.2 Natural Products

Tropical areas of the world are incredibly diverse biologically; some 70% of the earth's plants and animals exist in the tropics. Unfortunately, tropical areas of the world are in serious jeopardy due to human population growth and rainforest destruction. In addition, we know little of the chemical composition of tropical rainforest plants. It is estimated that only about 5,000 of the estimated 250,000-300,000 plant species have been systematically studied for medicinal application. As of 1993, it has been estimated that more than half of tropical rainforest plants have never even been described, much less surveyed for chemical constituents [12]. Thus, active components of plants are an important source of new drugs, and will continue to serve as source to increase the pool of compounds available for cancer treatment.

Plants are an excellent source for anticancer drug development some of the available anticancer drugs are derived from plants, such as paclitaxel and etoposide

[3,10]. Various chemotherapy agents have been derived from plant material, directly or indirectly. There is also an abundance of extremely bio-diverse populations of plant species that have not been subjected to anti-tumor activity testing for the advancement of cancer treatment. For thousands of years, higher plants have served as sources of medicinal agents. Plant extracts have been a source of drug leads for many years, adding to the arsenal of chemotherapeutic agents [13]. Various classes of compounds have been isolated from tropical plants that exhibit biological properties. These include antioxidants, phenolics, and triterpenoids [14]. Therefore, the continued search for new compounds from tropical rainforest plants may lead to new and better anticancer drugs for breast cancer.

1.2.1 Monteverde Cloud Forest

The montane cloud forest in Monteverde, Costa Rica, contains extremely biodiverse populations of plant species, most of which have not been tested for any biological activity. A cloud forest is a tropical highland forest located below the subalpine zone with low-level cloud cover at the canopy level. The rich unexplored variety of plant species covers only 1% of the global woodland [15]. This area contains a variety of tropical flora, pathogens, parasites, and herbivores against which the plants must defend themselves [16]. Therefore, the plants in this region have developed chemical defensive mechanisms for survival that might open the door to solve human maladies.

1.3 *Zanthoxylum*

Zanthoxylum is a genus of the Rutaceae that contains about 250 species, where most species have spiny trunks and/or branches [17]. The genus is a rich source of lignans, alkaloids, coumarins, amides, flavonoids, terpenes and other metabolites [18]. Members of the genus consist of 150 genera and around 900 species are used in traditional medicine around the world [19]. The bark of species within the genus is widely used to treat ailments such as toothache, colic, and rheumatism [53]. Monteverde, Costa Rica is home to numerous species of *Zanthoxylum* that contain common bioactive constituents and various traditional uses [20].

1.3.1 Lignans of *Zanthoxylum*

Lignans are a group of phytoestrogen compounds found in plants, which also exhibit antioxidant properties [21]. Sesamin is a lignin that is important in plant defense that exhibits antioxidant, anti-inflammatory, and anti-allergic properties [22]. Sesamin also has been shown to reduce the incidence of chemically induced tumors through modulation of the nuclear factor kappa-light-chain-enhancer of activated B cells (NF-κB) pathway [23]. Other medicinal effects of sesamin include cholesterol reduction, increased fatty acid β-oxidation, and enhancement of vitamin E [22]. Asarinin biological activities include, antitumor and antiallergenic [24]. Asarinin has demonstrated inhibitory effects on two-stage carcinogenesis of skin and pulmonary tumors in mice [25]. Syringaresinol has been reported to have cytotoxic activity [26]. Hinokinin exhibits anti-inflammatory, analgesic, and cytotoxicity against lymphoblastic and human

colon adenocarcinoma cell lines [27]. Some examples of lignans found in *Zanthoxylum* are shown below in Figure 1.1.

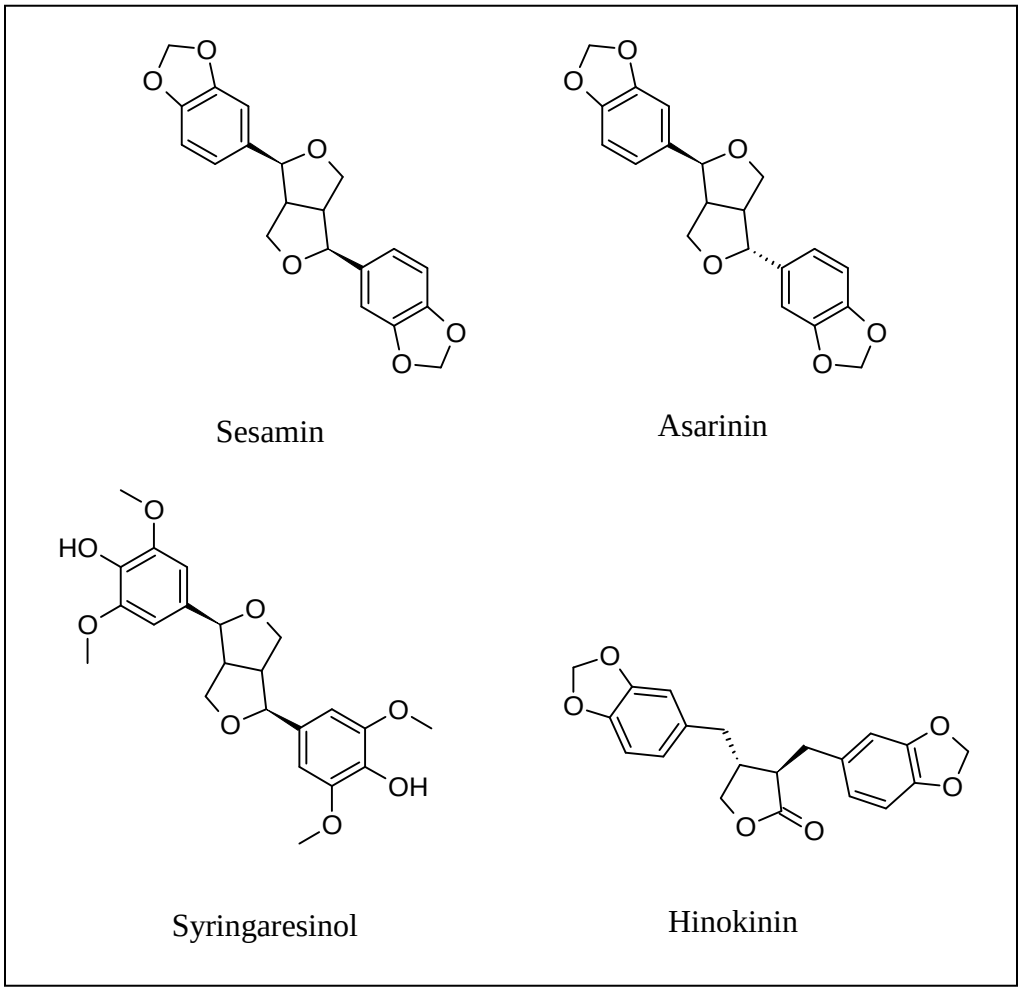

Figure 1.1 Structures of lignans from *Zanthoxylum* [27-30].

1.3.2 Alkaloids of *Zanthoxylum*

Alkaloids are a group of compounds found in nature that contain basic nitrogen atoms with pharmacological effects [31]. Berberine has been shown to be cytotoxic

against colorectal, breast, larynx, and gastric cancers [32]. Berberine has been reported to be an inhibitor of cyclooxygenase 2-transcriptional activity in human colon cancer [79]. Kokusaginine has been reported to have photo-activated antimicrobial activity against *S. aureus* [33]. Chelerythrine and nitidine have been identified as an inhibitor of topoisomerase I DNA relaxation [34]. Some examples of alkaloids found in *Zanthoxylum* are shown in Figure 1.2.

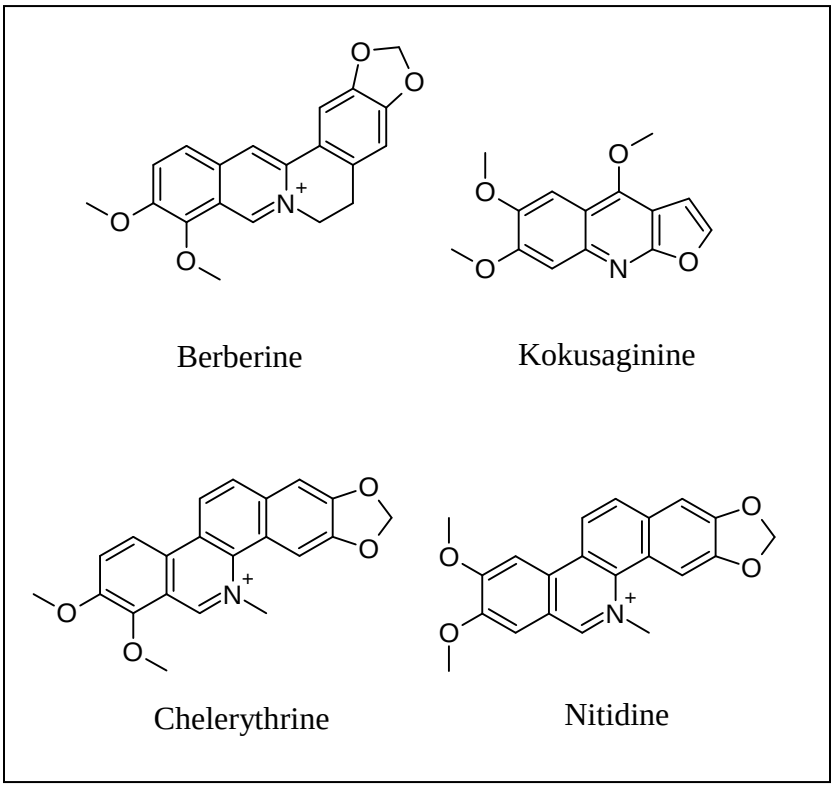

Figure 1.2 Structures of alkaloids from *Zanthoxylum* [29,32,34].

1.3.3 Coumarins of *Zanthoxylum*

Coumarins are a group of benzopyrones and fragrant phytoalexins produced in nature used as defensive mechanisms against wounds or attacks by other organism [35]. Coumarins also contain broad pharmacological activities such as anticancer, carcinogenic, and antiviral and are widely distributed [36]. Dipetaline is a pyranocoumarin that has shown cytotoxicity against human leukemia cells along with other pyranocoumarins, alloxanthoxyletin, xanthoxyletin, and xanthyletin through inhibition of DNA synthesis [36]. Some examples of coumarins found in *Zanthoxylum* are shown in Figure 1.3.

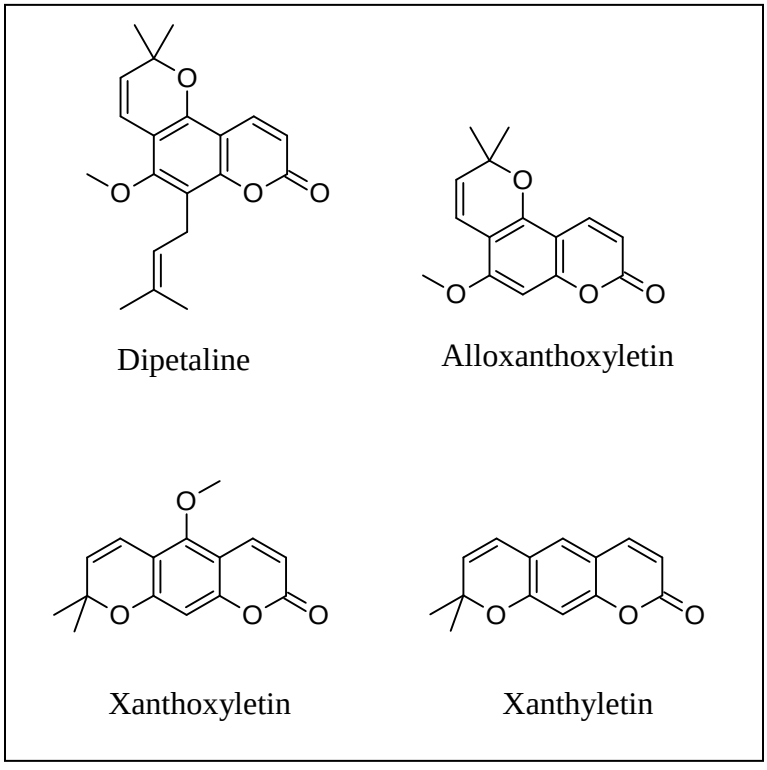

Figure 1.3 Structures of coumarins from *Zanthoxylum* [36].

1.3.4 Amides of *Zanthoxylum*

Amides are organic compounds consisting of a carbonyl group linked to nitrogen creating an amide bond. The amide bond restricts motion and provides rigidity in the formation of peptides, proteins, and enzymes. Distortion of the amide bond has been found to occur in nature through the bulkiness of substituent groups [37]. Fenoprofenamides and ketoprofenamides have been reported to exhibit antiproliferation activity through the substituents linked to the amide bond. The amide linkage is involved in the cytostatic activity resulting in greater cell uptake. Fenoprofen and ketoprofen are non-steroidal anti-inflammatory drugs (NSAIDs) used to relieve pain but has been explored for antitumor effects [38]. The unsaturated pungent alkylamides, α-sanshool, hydroxy-α-sanshool, dihydrobugeanool, and dehydro-γ-sanshool contain anaesthetic and insecticidal properties [39]. Some examples of amides found in *Zanthoxylum* are shown in Figure 1.4.

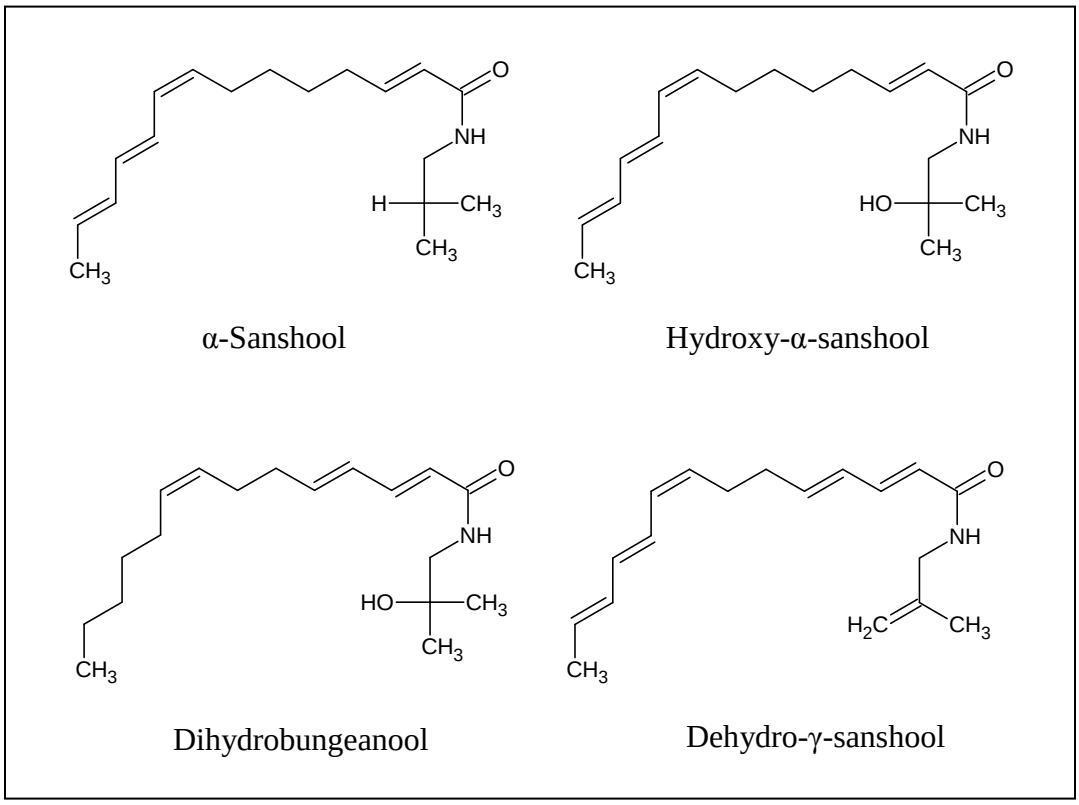

Figure 1.4 Structures of amides from *Zanthoxylum* [39,40].

1.3.5 Flavonoids of *Zanthoxylum*

Flavonoids are secondary metabolite ketone-containing compounds with antioxidant and anticancer properties [41]. Flavonone, 5-methoxy-7-hydroxy flavonone has been reported to show significant antimicrobial activity against bacteria and fungi and cytotoxicity [42]. Quercetin has been shown to exhibit strong radical-scavenging activity that could be used in treating diseases containing free radicals [43]. Hyperoside is the 3-*O*-galactoside of quercetin that is a medicinally active compound with radical-scavenging activity [43]. Hesperidin is also a radical scavenger that has been reported to inhibit

mouse melanoma cells [14]. Some examples of flavonids found in *Zanthoxylum* are shown in Figure 1.5.

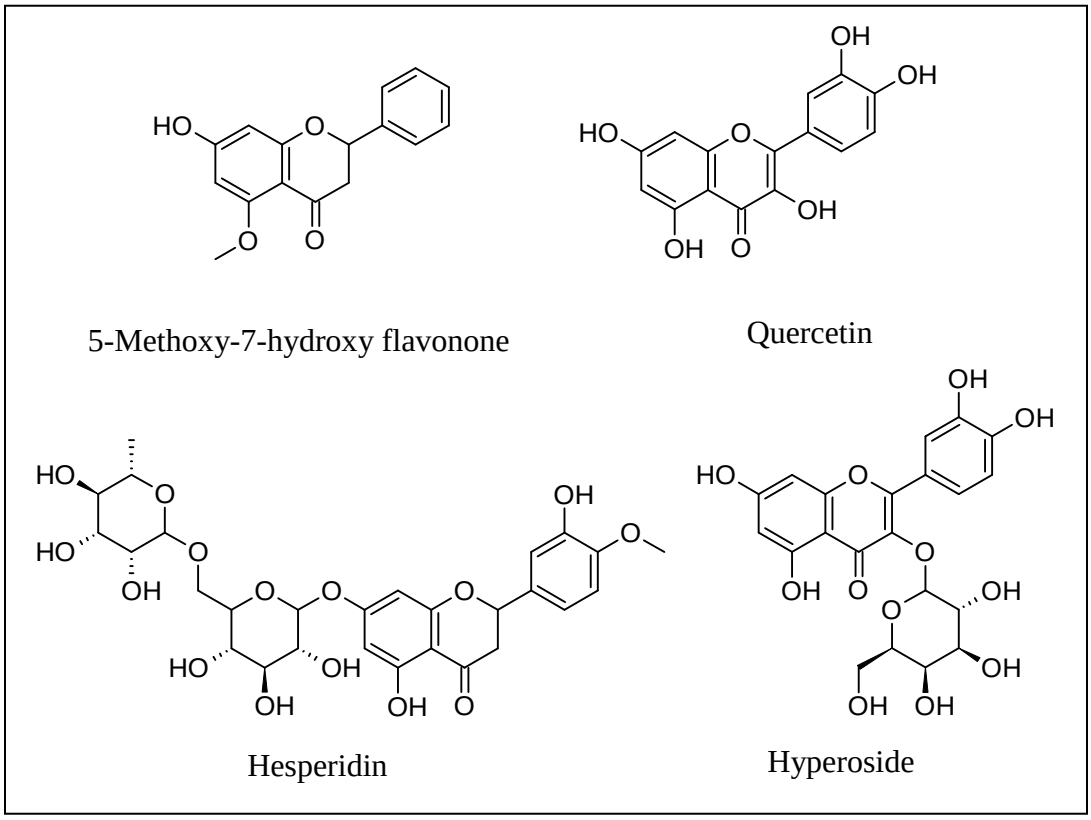

Figure 1.5 Structures of flavonoids from *Zanthoxylum* [42,43].

1.3.6 Terpenes of *Zanthoxylum*

Terpenes are organic compounds produced in plants which when chemically modified through oxidation become terpenoids. Terpenoids, the largest group of natural products, are natural organic chemicals derived from five-carbon isoprene units with antibacterial, antineoplastic, and other pharmaceutical properties. Terpenoids are classified into groups known as monoterpenes, sesquiterpenes, diterpenes, sesterterpenes, triterpenes, tetraterpenes, and polyterpenes based on the number of building blocks [44]. Triterpenoids have been reported to exhibit a variety of pharamaceutical properties such as anti-tumor, anti-virus, anti-hypertension, and anti-hyperglycemia [45]. Lupeol is a cytotoxic triterpene that has been reported to inhibit topoisomerase II relaxation of supercoiled DNA [46]. β-Sitosterol has been reported to be used to treat prostatic hypertrophy and inhibit dihydrotestosterone in prostate disorders [25]. β-Amyrin has been reported to exhibit anti-inflammatory, antinociceptive, and antioxidant properties at non-toxic doses in pancreatic rat model studies [47]. Friedelin has been shown to exhibit anti-tumor, anti-fatigue, anti-hyperlipidemic, and anti-hypertensive activity [45]. Some examples of triterpenoids found in *Zanthoxylum* are shown in Figure 1.6.

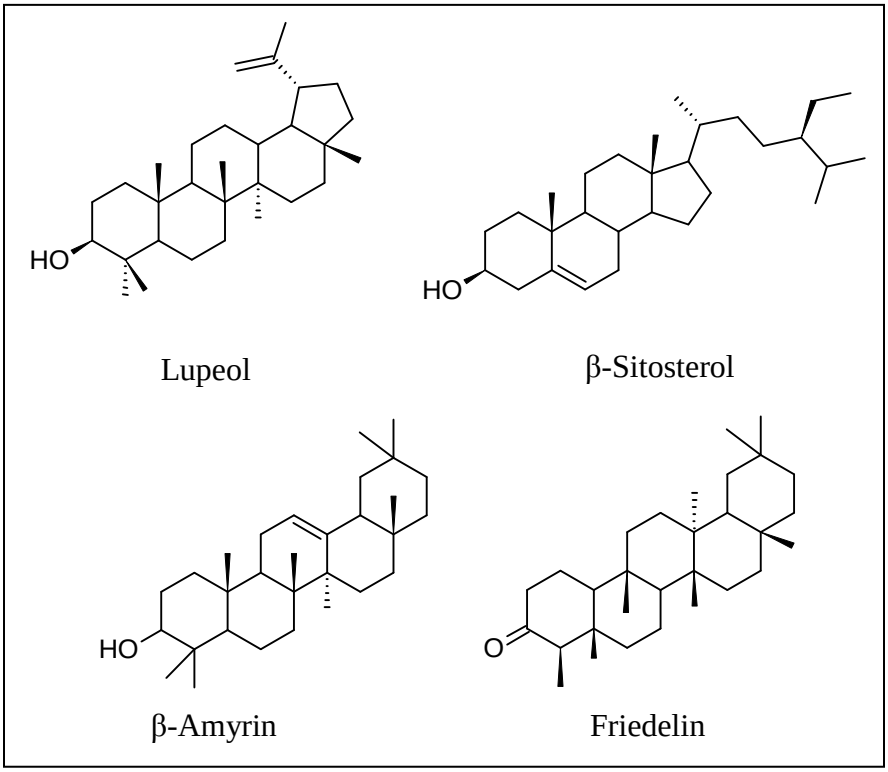

Figure 1.6 Structures of triterpenoids from *Zanthoxylum* [29,48,49].

1.4. *Zanthoxylum setulosum*

Zanthoxylum setulosum P. Wilson is a medium to large tree, 20m tall and 80 cm in diameter; trunk and branches with prickles; leaves alternate, odd-pinnate, 7–17 leaflets, lance-elliptic, 10 cm long by 4 cm wide, apex acuminate, margin crenate, pellucid dots primarily in the sinuses of the crenations, soft pubescent below, inflorescences axillary, 8–16 cm long; flowers white, 5-parted, fruit black, 3–4 mm as shown in Figure 1.8 [78]. Previous phytochemical investigation of *Zanthoxylum setulosum* has shown isolation of compounds shown in Figure 1.7.

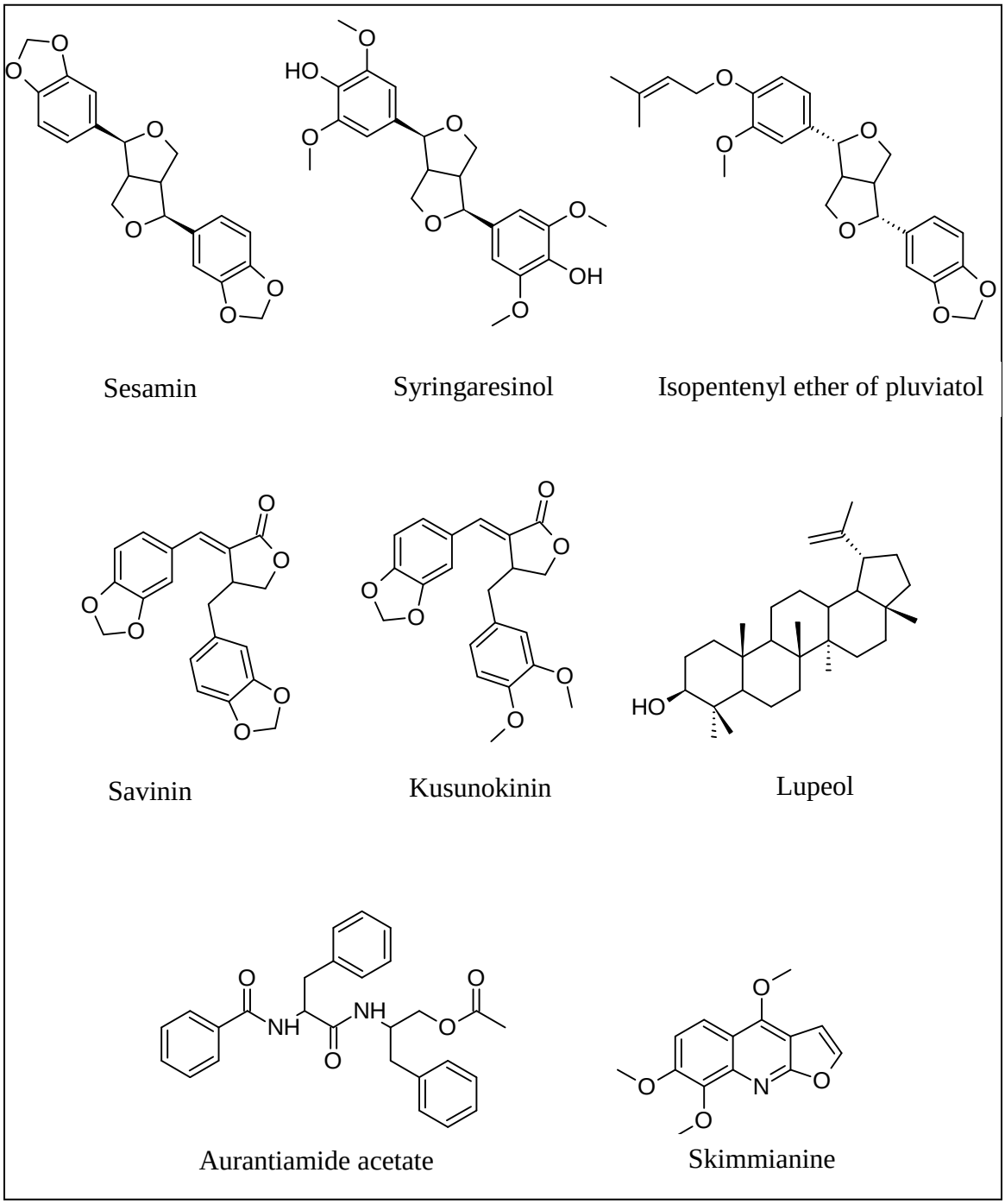

Figure 1.7 Chemical constituents from *Zanthoxylum setulosum* [29].

Figure 1.8 *Zanthoxylum setulosum* deposited in Smithsonian Tropical Research Institute [50].

1.5 Triterpenoids' Antineoplastic Properties

More than 20,000 triterpenoids exist in nature found primarily in plants and various fruits and medicinal herbs such as apples, cranberries, figs, olives, lavender, and thyme [44,51-54]. Plants biosynthesize triterpenoids through cyclization of squalene and triterpenoids are subclassified into diverse groups [44,55]. Some of the subclass of compounds includes lupanes, oleananes, friedelanes, limonoids, and ursanes [56-58]. Triterpenoids exhibit cytotoxicity against a number of tumor cells and have been structurally modified in treatment of cancer. Studies have shown that triterpenoids exhibit antioxidant, antimicrobial, antiviral, antiallergic, and anticancer properties [54,56]. Recent studies have shown that triterpenoids are being structurally modified to optimize bioactivity of the phytochemical properties. Several triterpenoids are currently under phase I of clinical trials for antitumor effects [57].

1.6 DNA Topoisomerases

Topoisomerases are enzymes that regulate deoxyribonucleic acid (DNA) supercoiling. The winding and unwinding of DNA is essential in the function of transcription and replication. There are two classes of topoisomerases, topoisomerase I and topoisomerase II. Class I is involved in the breaking and religating of one DNA strand and class II is involved in double strand breakage. The enzymes function through replication, transcription, and recombinant repair [59]. Topoisomerase II is overexpressed in proliferating cancerous cells and therefore a major target in the creation of antitumor drugs [80].

1.6.1 Anti-cancer DNA Topoisomerase Inhibitors

Topoisomerase inhibitors are drugs designed to interfere with topoisomerases and drugs that inhibit topoisomerases are a popular target for cancer chemotherapy. Topoisomerase inhibitors have been shown to block ligation, which creates breaks in the DNA and lead to cell death. Many chemotherapeutic drugs have been developed to interact with topoisomerases. Camptothecin and topotecan are anticancer drugs that target type I topoisomerase, while etoposide, doxorubicin, and daunorubicin target type II topoisomerase. The structures of the anticancer drugs that inhibit topoisomerases are shown in Figure 1.9 [60]. The X-ray crystal structures of topoisomerase I and II are shown in Figure 1.10 and Figure 1.11, respectively. Some inhibitors of topoisomerase block catalytic activity of DNA topoisomerase but do not stabilize the cleavable complex [59]. These inhibitors include aclarubicin, novobiocin, sobuzoxane, and dexrazoxane. Inhibition using these catalytic agents is expressed by preventing the binding of the enzyme to DNA and by inhibiting the ATPase activity as an uncompetitive inhibitor of adenosine triphosphate (ATP). Topoisomerase II requires ATP as a cofactor and uses the energy released through ATP hydrolysis to induce DNA strand passage. The binding of ATP creates a conformational enzymatic change of an open to a closed clamp form [59]. The inhibitors act by binding to the ATPase domain of the enzyme shown in Figure 1.12 or the DNA binding site, which is shown in Figure 1.11.

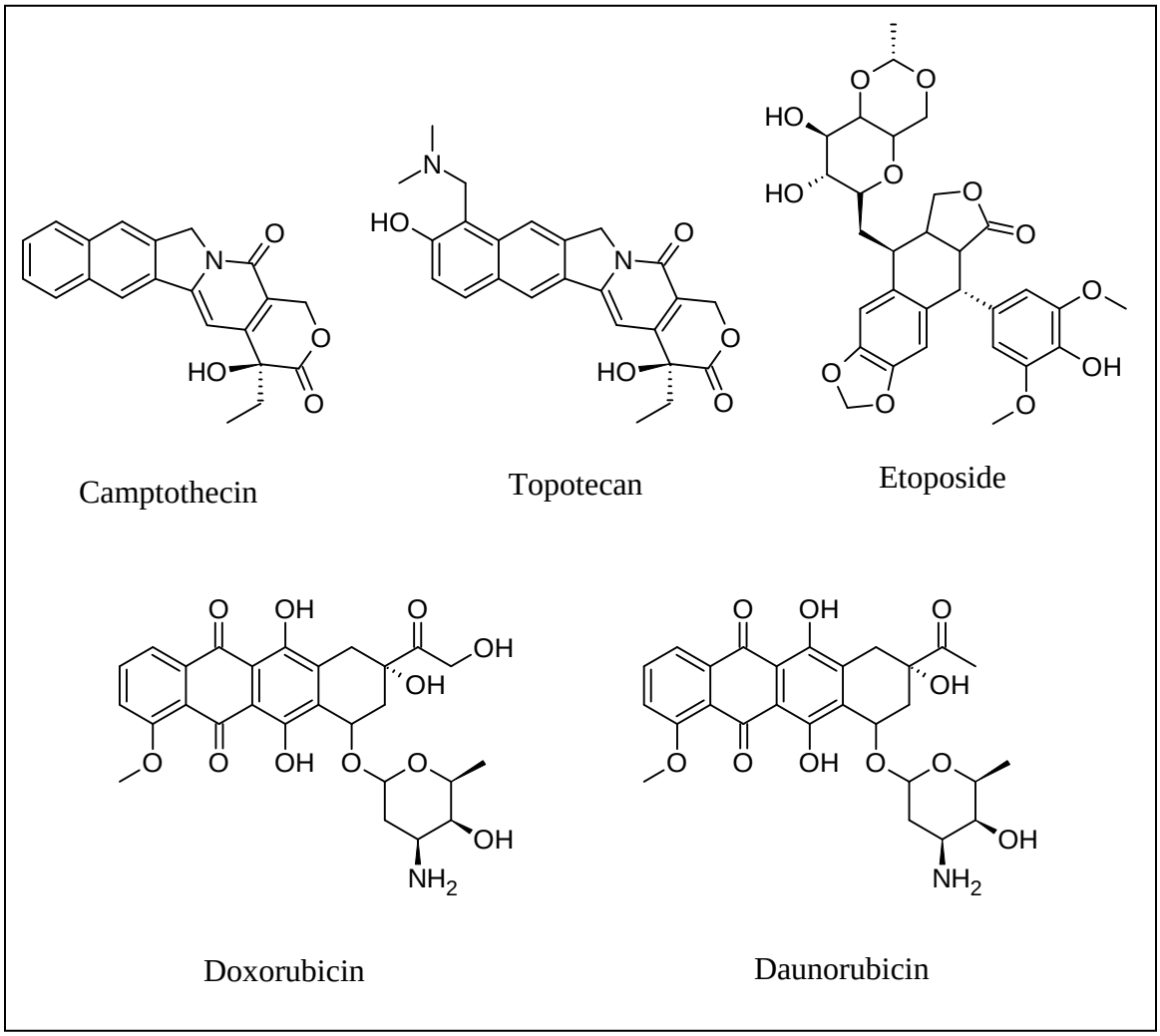

Figure 1.9 Anti-cancer topoisomerase inhibitor drugs [60].

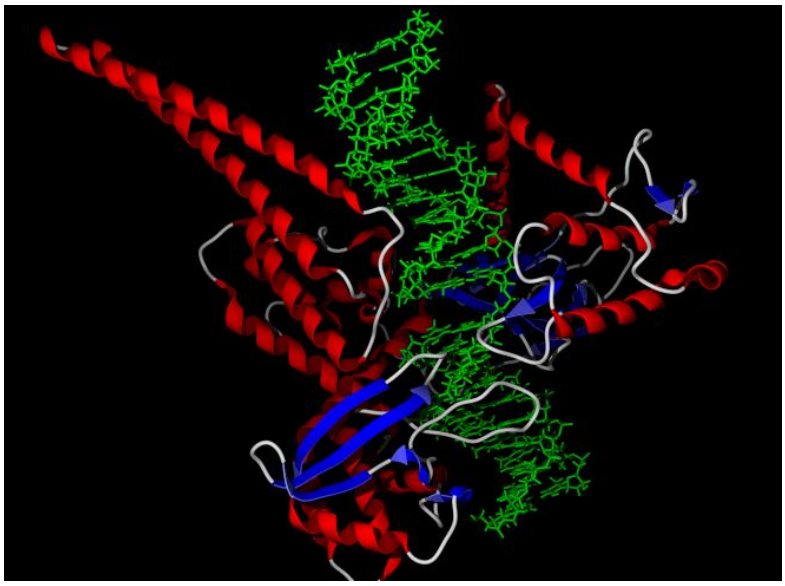

Figure 1.10 X-ray crystal structure of human topoisomerase I bound to DNA (PDB: 1k4t) [62].

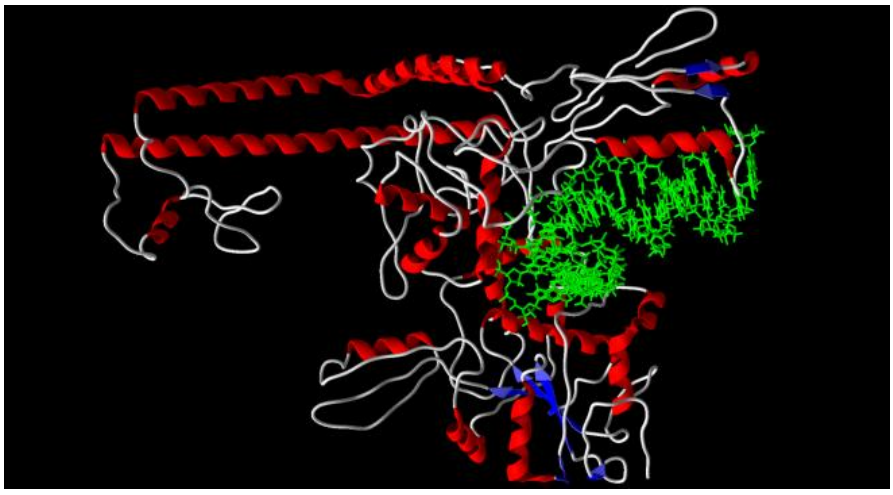

Figure 1.11 X-ray crystal structure of human topoisomerase II bound to DNA (PDB: 2rgr) [59].

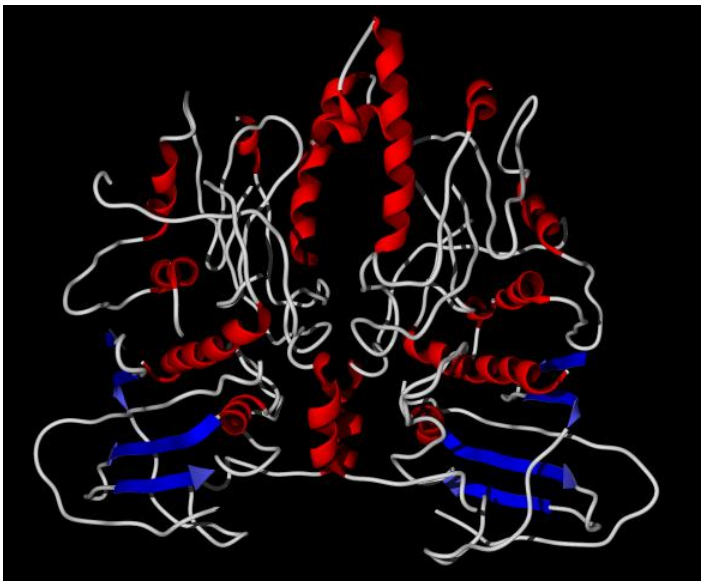

Figure 1.12 X-ray crystal structure of *Saccharomyces cerevisiae* ATPase region of topoisomerase II (PDB: 1pvg) [82].

1.7 Molecular Docking

Docking is the prediction of a ligand orientation relative to the active site of a macromolecule in the development of lead compounds. Docking can be used to design drugs that bind more strongly to a given target than the natural substrate [88]. Docking can be used to cut down on time and cost in comparison to high-throughput screening of compounds in the identification of novel drug agents. Docking can be used as a pre-screening tool used when the three-dimensional structure of a target is known. In vitro experimental studies can be done to further examine drug agents following simulations from docking studies [88]. A docking software program can be used to identify different orientation poses by minimizing the energy of intermolecular interactions [84]. The program uses scoring functions and algorithms to search for various orientations of a

ligand. Docking has been divided into a variety of approaches, rigid docking, flexible ligand-docking, and flexible protein-docking methods. The rigid-docking methods involve making the ligand and protein rigid, whereas in the flexible ligand-docking the ligand is flexible and the protein is rigid. Docking methods also contain ligand docking errors from the search algorithms, scoring functions, the role of water, or flexibility of protein and ligand [84]. Therefore, there have been various docking programs to address these areas that may contain errors, such as Generic Evolutionary Method for molecular DOCKing (GEMDOCK) [84], Genetic Optimization for Ligand Docking (GOLD) [86], FLexX [87], MolDock [88], Grid-base ligand docking with energetics (Glide) [91], and Surflex [92]. Docking accuracy of the programs has been studied to evaluate the docking of flexible ligands to 77 protein targets and MolDock showed the highest docking accuracy. MolDock had a correct binding mode of 87 % compared to 58 % of 76 cases for FlexX, 78 % of 55 cases for GOLD, 82 % for Glide, and 75 % for Surflex [88]. Percentages were calculated using the highest ranked solution compared with the known experimental structure using the Cartesian root-mean-square deviation (RSMD). Successful poses gave a RSMD less than 2.0 Å between the pose and experimentally ligand [88].

1.7.1 Molecular Docking Software

ArgusLab was developed by Dr. Mark Thompson with Planaria Software, Seattle, Washington. The objective of program is to find the most optimal ligand and protein interaction and predict their binding energy. The program predicts the binding energies

of a flexible ligand and flexible protein binding site in under ~5 seconds. The scoring function and algorithms involved in ArgusLab are ShapeDock, a shape-based method; GADock, a Lamarckian genetic algorithm; and AScore, a scoring function [89]. The docking engine of ArgusLab is similar to DOCK and Glide with flexible ligand docking. The ligand is described as a torsion tree where grids are constructed overlaying the binding site. The bonded atoms of the ligand that do not have rotatable bonds are placed on a search point in the binding site and favorable rotations are created. Poses that survive the torsion search are scored and the lowest energy pose are minimized, re-clustered, and ranked [90].

Molecular Vitrual Docker (MVD) is docking software used for the study and prediction of three-dimensional ligand interactions with a macromolecule. Binding is calculated by evaluating the structures of ligand conformations and estimating the energy of their interactions with macromolecules. The MolDock scoring function is a improved derived function from piecewise linear potential (PLP) scoring functions proposed by Gehlharr et al. [83] and extended by Yang et al. [84]. The MolDock function includes new hydrogen bonding term and new charge schemes that take hydrogen bind directionality into account. The algorithm is based on experienced-based techniques search and cavity prediction algorithm. The re-ranking scoring function of MolDock identifies the most promising poses and improves docking accuracy. The search algorithm of MolDock is known as the guided differential evolution that combines a differential evolution optimization technique and a cavity prediction algorithm [88].

CHAPTER II

MATERIALS AND METHODS

2.1 Plant Collection and Extraction

The choice of *Zanthoxylum setulosum* P. Wilson for collection was based on phylogenetic and ecological reasoning with ethnobotanical roots of the *Zanthoxylum* genus. Species of *Zanthoxylum* have been used to treat cough, fever, malaria, pneumonia, rheumatism, and tumors. The bark of *Zanthoxylum* species have been shown to traditionally been used to treat malaria, colds, toothaches, and headaches in Kenya. The bark is also used in Kenya to treat rheumatism [82]. *Zanthoxylum setulosum* was collected on June 19, 2004 in Provinvia Puntarenas, Costa Rica, 6 km SSW of Santa Elena on the main road from Monteverde. *Zanthoxylum setulosum* was identified and authenticated by W.A. Haber and voucher specimens deposited in Missouri Botanical Garden Herbarium. Collection of *Zanthoxylum setulosum* from the cloud forest of Monteverde, Costa Rica is permitted through a Rights Agreement with Costa Rica through the Tropical Science Center in Monteverde. The plant materials were cleaned, macerated, and extracted with percolating methanol followed by ethyl acetate and dichloromethane, respectively, at ambient temperatures for 12-18 hours, following the National Cancer Institute guidelines [98]. The solvent was then evaporated in a fume hood to produce the crude extract. The crude extracts were transported to the University of Alabama in Huntsville and screened for chemical composition and bioactivity.

2.2 Chromatographic Separation

The crude chloroform extract of *Zanthoxylum setulosum* was dissolved with 75 ml of dichloromethane and then 100g of silica gel with a particle distribution of 40-75 μm (200 X 400 mesh) was added to the mixture which was then left to evaporate to dryness in a fume hood. Hexane was then added to the mixture to create a slurry to be used in bioactivity-directed flash chromatography, using a column 70 cm in length x 5 cm diameter. Chromatographic separation of this low-polarity extract (i.e., dichloromethane extract) was carried out on silica gel columns eluting with a solvent gradient (hexane with increasing proportions of ethyl acetate, followed by ethyl acetate with increasing proportions of ethanol). TLC was performed on silica gel precoated aluminum TLC plates with a fluorescent indicator 254 nm for analysis of isolated fractions and spots were detected by illumination with UV light. Fractions were checked by TLC and HPLC analysis and fractions having comparable TLC's were combined to form "superfractions."

2.3 Cytotoxicity Assay

A panel of three breast cancer cell lines have been selected and purchased from the American Type Culture Collection (ATCC) representing breast adenocarcinoma to use for the cytotoxicity assay. The cell lines differ in expression for epidermal growth factor receptor (EGFR), fibroblast growth factor receptor (FGFR), transforming growth factor alpha receptor (TGFαR), and estrogen receptor (ER). MCF-7 is a Caucasian cell line which is ER+ and FGFR+. MDA-MB-231 is a Caucasian cell line which is ER-, EGFR+, and TGFR+. All cells were grown in 5% CO_2 environment at 37 °C in RPMI-1640 medium with L-glutamine, supplemented with 10% fetal bovine serum, 100,000 units of penicillin and 10.0 mg streptomycin per liter of medium, and buffered with $NaHCO_3$ to pH of 7.35. Cells were plated into 96-well cell culture plates at 2.5×10^4 cells per well. The volume in each well was 100 μL. After 48 hrs, supernatant

fluid was removed by suction and replaced with 100 μL growth medium containing 1.0 μL of DMSO solution of extracts or compounds (1% w/v in DMSO), giving a final concentration of 100 μg/mL for each extract or compound. Solutions were added to wells in four replicates. Growth medium with no additions and with DMSO (10 μL DMSO/ml) were used as a negative control, while tingenone (100 μg/ml) was used as a positive control. After addition of compounds, plates were incubated for 48 hrs at 37 °C in 5% CO_2; medium was then removed by suction, and 100 μL of fresh medium was added to each well. In order to establish percent kill rates, the 3-(4,5-dimethylthiazol-2-yl)-2,5-diphenyltetrazolium bromide (MTT) assay for cell viability was carried out. Samples were added to wells in four replicates. After colorimetric readings were recorded (using a Molecular Devices SpectraMAX Plus microplate reader, 570 nm), average absorbances, standard deviations, and percent kill ratios (%killcmpd/%killDMSO) were calculated. LC_{50} values for the pure compounds were determined using serial dilutions of the compounds in DMSO, and calculated using the Reed-Muench method [61].

2.4 Gas Chromatography-Mass Spectrometry

Chemical composition of volatile active extracts were analyzed using GC-MS on an Agilent system consisting of a 6890 Gas Chromatograph, a 5973 Mass selective detector (MSD), and an Agilent ChemStation data system. The GC column was an HP-5ms fused silica capillary consisting of a (5% phenyl)-methylpolysiloxane stationary phase, a film thickness of 0.25 μm, a length of 30 m, and an internal diameter of 0.25 mm. The GC carrier gas was helium and the column had a head pressure of 7.07 psi and a flow rate of 1.0 ml/min. The inlet temperature was 200 °C and the MSD

temperature was 280 °C. The GC oven temperature was programmed as follows: 40 °C initial temperature held for 10 min; increased at 3°/min to 200 °C; increased 2°/min to 220 °C. The extracts were dissolved in dichloromethane and 1 μL of the sample was injected using a split injection method. The mass spectrum of constituents was compared with mass spectra in the literature to verify compound identities.

2.5 Structural Determination

Structures of active components that were isolated and purified were determined using spectroscopic and, whenever necessary, crystallographic techniques. Purified products were analyzed by mass spectrometry and multinuclear nuclear magnetic resonance (NMR) spectroscopy. Fractions subjected to NMR were dissolved in deuterochloroform. Structures were determined using a series of NMR experiments: ^{1}H-NMR, ^{13}C-NMR, gCOSY, gHSQC, and gHMBC with a 500 MHz INOVA spectrometer with a 5 mm Penta (H,C,N,P,D) PFG VT probe.

2.6 Molecular Docking

Protein-ligand docking studies were carried out based on the crystal structures of three models of human DNA topoisomerase I 70 kD with a 22 base pair DNA duplex (PDB: 1k4t [62], 1t8i [62], and 1sc7 [62]), 6 bp DNA (PDB: 1z3f) [63], and self complementary duplex DNA (5'-D(*AP*CP*GP*TP*AP*CP*GP*T)-3') (PDB: 1al9) [64]. All structures were downloaded from the Protein Data Bank (PDB). All solvent molecules and the co-crystallized ligands were removed from the structures. Molecular docking calculations for all compounds with each of the proteins were done using ArgusLab 4.0.1 [65] and Molegro Virtual Docker 2.3 (MVD).

Lichexanthone and compared anticancer drugs were drawn in Spartan '10 [95] and saved as a PDB file and imported into Arguslab by selecting open molecule. The crystal structures of

DNA or human DNA topoisomerase I were downloaded from the PDB by selecting file, query PDB, entering the 4-letter PDB key, and save as. Five crystal structures PDB key: 1k4t, 1z3f, 1al9, 1t8i, and 1sc7 were downloaded in this study, only using one crystal structure per ligand per docking run. The ligand of interest was expanded in the molecule tree view tool and then the residue and misc. folders were expanded, respectively, to visualize the ligand. A ligand group was made by right clicking the ligand and selecting make a ligand group from this residue. The crystal structure was also expanded like the ligand to view the co-crystallized ligands, protein, and DNA. A ligand group of the co-crystallized ligand was made just as previously stated. Then the co-crystallized ligands of the crystal structure were deleted from the misc. folder to allow for proper docking of ligand of interest. A binding site for the new ligand group in the group folder of the crystallized structure was made and the ligand in the group folder was removed. The calculations were set-up using the dock a ligand in the calculation menu option. The ligand of interest was selected along with the binding site that was determined in previous steps. A binding site bounding box of 20 Å was used on all three axes, X, Y, and Z to allow for ligand binding. All other options were used under the default settings and the run ready to start. Different orientations of the ligands were searched and ranked based on their energy scores in a matter of seconds.

A comparison docking study using Molegro Virtual Docker 2.3 was done to verify docking accuracy [66]. Lichexanthone was drawn in Spartan ’10 [95] and saved as a PDB file and imported into MVD by selecting file and import molecules. The crystal structures of DNA or human DNA topoisomerase I were downloaded from the PDB by selecting file, download PDB, and entering the 4-letter PDB key. Five crystal structures PDB key: 1k4t, 1z3f, 1al9, 1t8i, and 1sc7 were downloaded in this study. Lichexanthone and one crystal structure was imported per docking simulation, a total of five docking simulations. Other anticancer drugs, camptothecin,

ellipticine, indenoisquinoline, topotecan, and daunorubicin were also imported into MVD for studies with the five crystal studies, a total of 25 docking simulations. The cofactors, water, and co-crystallized ligands in each docking run were removed from the workspace and the DNA ligands were converted to cofactors. Then all molecules were prepared by selecting prepared and prepare molecules. The potential binding site for the protein was detected by selecting preparation and detect cavities, using a maximum number of five cavities and an expanded Van der Waals molecular surface. The cavity of interest was selecting by choosing the predicted cavity that surrounded the binding site of the co-crystallized ligand of the crystal structure. The docking simulation was done by selecting docking and docking wizard. The ligand of interest to dock was selected and scoring function was chosen and the binding site defined. The scoring function selected was MolDock Score [GRID]. The cavity was chosen under the binding site origin and the radius was set to 20 Å on all three axes, X, Y, and Z. The algorithm selected was MolDock SE with 30 runs and an energy minimization selected after docking. Pose clustering default conditions were selected. The simulation was run in a separate process, file saved before run, and output directory changed from default. Finally, the docking simulation was ready to begin by pressing start. MVD calculated the energy grid and batchjob calculated the lowest binding energy over 30 runs in about 15 minutes. The lowest binding energy poses were viewed by dragging and dropping the DockingResults ion onto the MVD application. The poses were organized based on 2nd re-rank scores and all selected for viewing. The workspace file was saved again with the selected poses. Poses were viewed by unselecting the ligands and constraints in the workspace. Individual poses were visualized by selecting the pose of interest and the energies were shown by selecting the pose organizer, which showed hydrogen bonds as well.

Calculations of *ab initio* molecular structures and energies were carried out using Spartan ’08 along with density functional theory (DFT) M06/6-31G* and Merck Molecular Force Field

(MMFF4). The geometries of lichexanthone were optimized using Gaussian basic set M06/6-31G* level of theory [94]. The calculations of lichexanthone with one C-G base pair were run for a week. Computations are very timely and require large amounts of computer memory.

CHAPTER III

RESULTS

3.1 Chromatographic Separation

Collection and extraction of *Zanthoxylum setulosum* produced 25.02 g of crude chloroform extract and elution was carried out using a hexane/ethyl acetate (EtOAc) gradient illustrated in Figure 3.1. Sixty-six fractions were eluted using flash gravity chromatography and verified by TLC of pure compounds and superfractions. Fractions 29 and 30 crystallized to give 2.05 g sesamin but exhibited no activity against cell lines tested (Figure 3.2). Fraction 14 was separated to give 1.28 g of lupeol and exhibited high cytotoxic activity against cells lines tested (Figure 3.1). Fractions with similar retention factors (R_f) were combined and bioactivity accessed using cytotoxicity assays. All superfractions were furthered separated using smaller column bioactivity-directed flash chromatography. 69 mg of superfraction 20-23 was separated to give 10 mg of lichexanthone (Figure 3.3). 22 mg of superfraction 5-11 was separated to give 10 mg of sesquichamaenol (Figure 3.4).

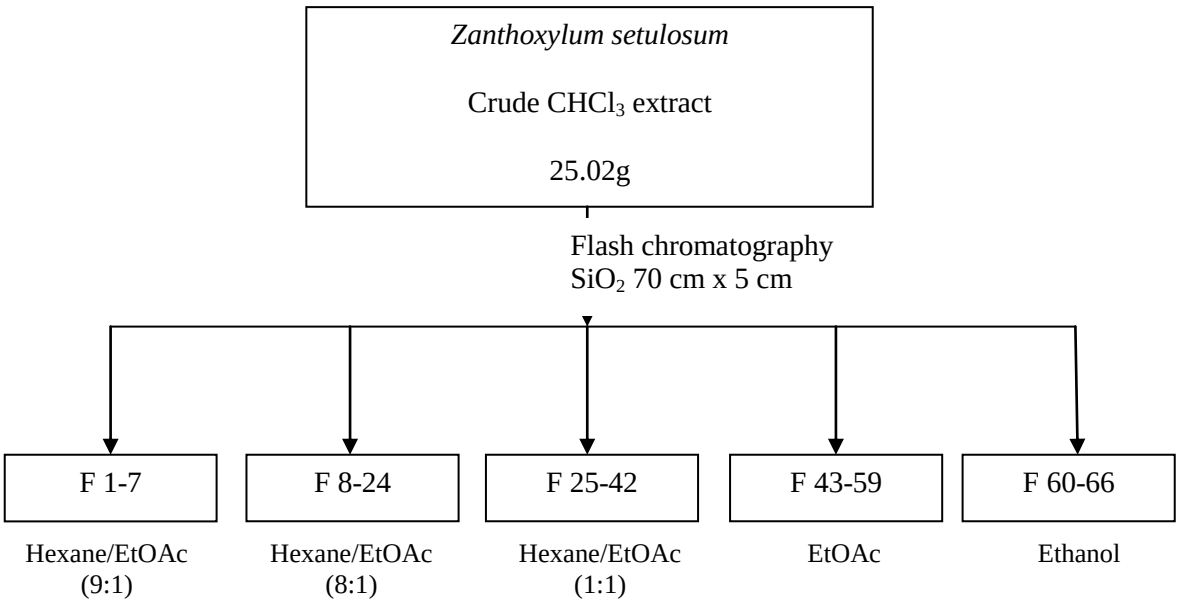

Figure 3.1 Chromatographic separation scheme for *Zanthoxylum setulosum* extract.

3.2 Cytotoxicity Screening Data

Cytotoxicity of pure compounds and superfractions from *Zanthoxylum setulosum* were measured using a MTT assay for cell viability against MCF-7 and MDA-MB-231 breast tumor cell lines. Combined superfractions F12-13, F2-4, F5-11, F20-23, F38-40, and F49-52 exhibited high kill rates against cell lines tested. The six superfractions mentioned above exhibited high kill rates at 100 % against MCF-7 cells. Superfraction 12-13 had a kill rate of 99.28 %, F2-4 87.79 %, F5-11 91.76 %, F20-23 89.54 %, and F38,40 86.54 % against MDA-MB-231 cells. Superfraction 49-52 was not active against MDA-MB-231 cells. Superfraction 16-19 was not active against MCF-7 cells but

exhibited a high rate of 99.16 % against MDA-MB-231 cells. The cytotxicity results are presented in Tables 3.1 and 3.2.

Table 3.1 Cytotoxicity of $CHCl_3$ fractions of *Zanthoxylum setulosum* on MCF-7 cells in culture.

Fraction	% Cells Killed	Standard Deviations
ZASEBC F1	-23.49	1.98
ZASEBC F12-13	100	15.85
ZASEBC F14	100	16.31
ZASEBC F16-19	0.90	24.38
ZASEBC F24-26	7.64	34.16
ZASEBC F31-32	50.38	18.72
ZASEBC F37	85.62	5.06
ZASEBC F41-48	71.47	7.44
ZASEBC F53-56	-10.14	26.85
ZASEBC F29	18.25	18.57
ZASEBC F2-4	100	8.01
ZASEBC F5-11	100	7.27
ZASEBC F15	-63.20	26.39
ZASEBC F20-23	100	6.24
ZASEBC F27-28	14.24	18.35
ZASEBC F33-36	60.55	6.91
ZASEBC F38,40	100	4.20
ZASEBC F49-52	100	2.09
ZASEBC F64-52	-7.60	16.21
ZASEBC F30	45.17	11.81

Table 3.2 Cytotoxicity of $CHCl_3$ fractions of *Zanthoxylum setulosum* on MDA-MB-231 cells in culture.

Fraction	% Cells Killed	Standard Deviations
ZASEBC F1	-11.58	15.37
ZASEBC F12-13	99.38	1.05
ZASEBC F14	100	0.74
ZASEBC F16-19	99.16	1.33
ZASEBC F24-26	88.19	5.36
ZASEBC F31-32	79.32	2.57
ZASEBC F37	76.35	2.55
ZASEBC F41-48	73.18	1.65
ZASEBC F53-56	71.68	9.79
ZASEBC F29	-3.53	7.58
ZASEBC F2-4	87.79	2.65
ZASEBC F5-11	91.76	4.63
ZASEBC F15	60.63	7.87
ZASEBC F20-23	89.56	8.49
ZASEBC F27-28	74.00	14.47
ZASEBC F33-36	82.25	2.78
ZASEBC F38,40	86.54	3.44
ZASEBC F49-52	56.81	33.85
ZASEBC F64-52	72.27	4.58
ZASEBC F30	87.61	4.69

3.3 Spectroscopic Data

Nuclear magnetic resonance, X-ray crystallography, mass spectrometry, and infrared spectroscopy were performed on pure active fractions for structural determination. The structures of lupeol, sesamin, lichexanthone, and sesquichamaenol spectroscopic are shown in Figures 3.2-3.6, respectively. The spectroscopic results are presented in Tables 3.3-3.8.

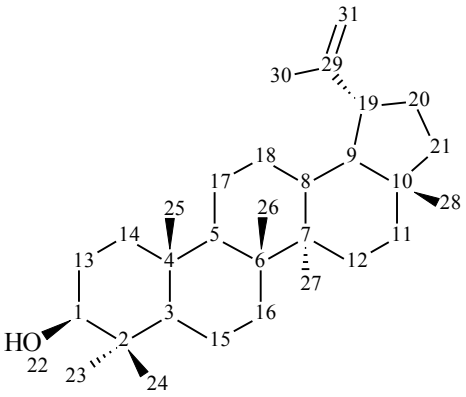

Figure 3.2 Lupeol

Table 3.3 Spectroscopic data for Lupeol (F14).

Spectroscopic Technique	Data	Literature Data [66]
^{1}H NMR ($CDCl_3$)	δ4.70(s,1H,H-31), δ4.57(s,1H,H-31), δ3.21(dd,1H,H-1), δ2.37(m,1H,H-19) δ1.91(m,1H,H-20), δ1.69(s,1H,H-8), δ1.67(s,1H,H-18), δ1.39(s,1H,H-16), δ1.26(s,1H,H-15), δ1.04(s,3H,H-23), δ0.97(s,3H,H-27), δ0.95(s,3H,H-24), δ0.84(s,3H,H-25), δ0.80(s,3H,H-28), δ0.77(s,3H,H-26)	δ4.68(s,1H,H-31), δ4.56(s,1H,H-31), δ3.16(dd,1H,H-1), δ1.25(s,3H,H-30), δ1.02(s,3H,H-23), δ0.95(s,3H,H-27), δ0.93(s,3H,H-24), δ0.82(s,3H,H-25), δ0.78(s,3H,H-28), δ0.75(s,3H,H-26)

Table 3.3 (Continued)

Spectroscopic Technique	Data	Literature Data [66]
^{13}C NMR ($CDCl_3$)	δ153.63(C29), δ111.98(C31), δ81.68(C1), δ57.96(C3), δ53.10(19), δ50.97(C9), δ50.65(C5), δ45.66(C10), δ41.37(C7), δ39.83(C21), δ32.52(C8), δ30.65(C14), δ30.11(C11), δ30.07(C16), δ27.81(C20), δ20.98(C13), δ20.67(C23), δ18.78(C15), δ18.04(C28), δ17.21(C25)	δ151.1(C29), δ109.5(C31), δ79.1(C1), δ55.5(C3), δ50.6(C5), δ48.5(C9), δ48.1(C19), δ43.2(C10), δ43(C7), δ41(C6), δ40.2(C21), δ39(C8), δ38.9(C2), δ38.2(C14), δ37.3(C3), δ35.8(C11), δ34.5(16), δ30(C20), δ28.2(C23), δ27.6(C12), δ27.5(C18), δ25.3(C13), δ21.1(C17), δ19.5(C30), δ18.5(C15), δ18.2(C28), δ16.3(C25), δ16.2(C26), δ15.6(C24), δ14.7(C27)

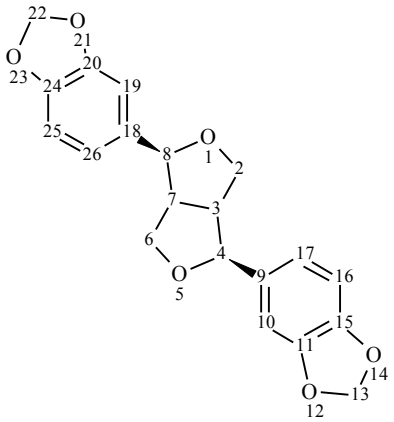

Figure 3.3 Sesamin

Table 3.4 Spectroscopic data for sesamin (F29).

Spectroscopic Technique	Data	Literature Data [67,75]
^{1}H NMR ($CDCl_3$)	δ6.90(d,2H, H-19/H-10), δ6.86(dd,2H,H-26/H-17), δ6.83(d,2H, H-25/H-16), δ6.00(s,4H,H-22/H-13), δ4.77(d,2H, H-4), δ4.28(m,2H,H-8), δ3.92(dd,2H, H-2/H-6), δ3.10(m,2H,H-7/H-3)	δ6.85(d,2H,H-19/H-10), δ6.79(dd,2H,H-26/H-17), δ6.78(d,2H,H-25/H-16), δ5.96(s,4H,H-22/H-13), δ4.71(d,2H,H-4), δ4.23(m,2H,H-8), δ3.86(dd,2H,H-2/H-6), δ3.05(m,2H,H-7/H-3)
^{13}C NMR ($CDCl_3$)	δ148.00(C24/C15), δ147.13(C20/C11), δ135.09(C18/C9), δ119.38(C26/C17), δ108.21(C25/C16), δ106.52(C19/C10), δ101.10(C22/C13), δ85.82(C8/C4), δ71.74(C2/C6), δ54.37(C7/C3)	δ147.97(C24/C15), δ147.11(C20/C11), δ135.09(C18/C9), δ119.33(C26/C17), δ108.17(C25/C16), δ106.48(C19/C10), δ101.05(C22/C13), 85.79(C8/C4), δ71.72(C2/C6), δ54.34(C7/C3)

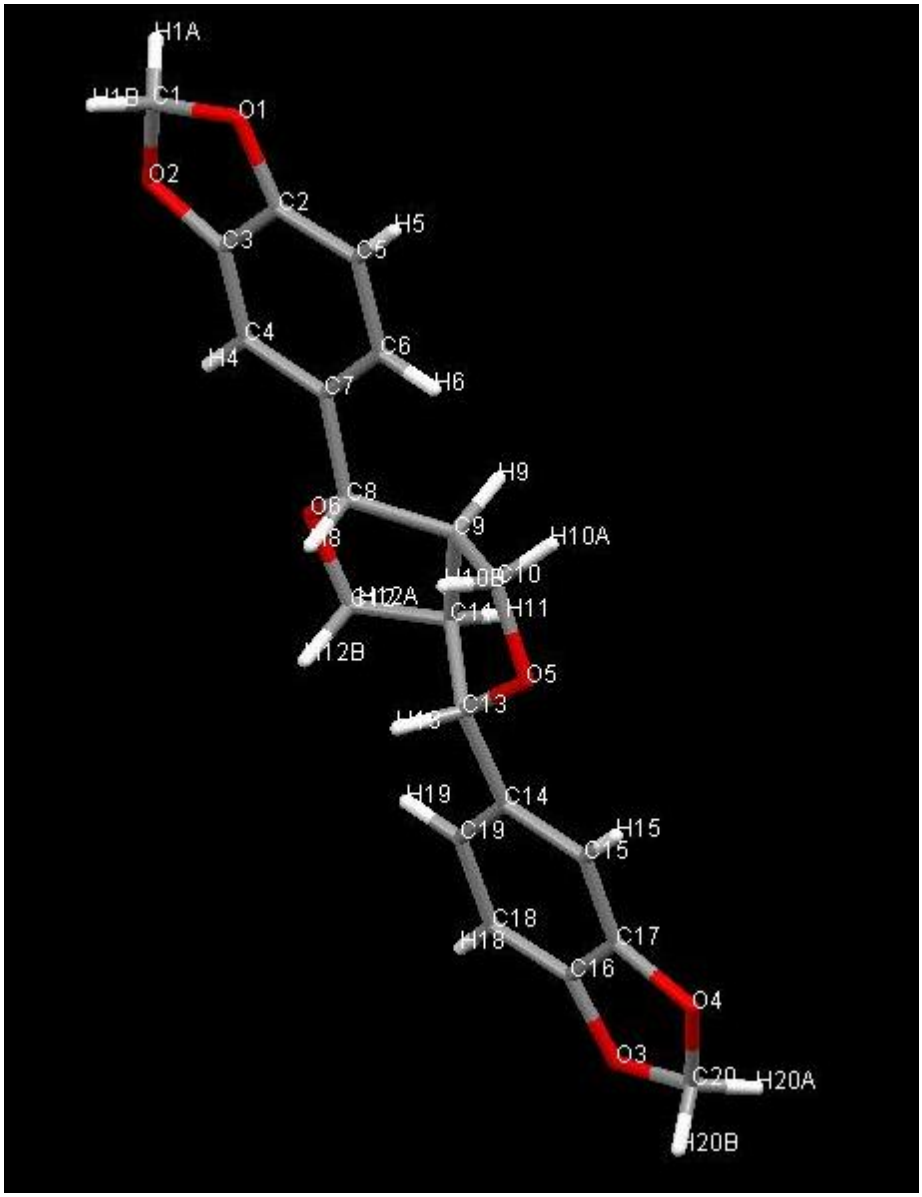

Figure 3.4 X-ray crystal structure of sesamin.

Table 3.5 X-ray atomic coordinates for sesamin.

	X	Y	Z
C(1)	0.0302	-0.0524	0.1305
C(2)	0.1460	0.1327	0.2537
C(3)	0.1609	0.2062	0.1471
C(4)	0.2432	0.3592	0.1296
C(5)	0.2107	0.2095	0.3476
C(6)	0.262	0.3666	0.3310
C(7)	0.3136	0.4387	0.2244
C(8)	0.4160	0.5940	0.2091
C(9)	0.4284	0.7536	0.2961
C(10)	0.5317	0.7152	0.3950
C(11)	0.4913	0.9192	0.2314
C(12)	0.4683	0.8597	0.1089
C(13)	0.6334	0.9236	0.2797
C(14)	0.7068	1.1133	0.2728
C(15)	0.7758	1.1923	0.3669
C(16)	0.8456	1.4492	0.2481
C(17)	0.8438	1.3625	0.3514
C(18)	0.7793	1.3746	0.1546
C(19)	0.7090	1.2037	0.1684
C(20)	0.9690	1.6289	0.3705
O(1)	0.0610	-0.0217	0.2467
O(2)	0.0845	0.1032	0.0697
O(3)	0.9201	1.6156	0.2570
O(4)	0.9174	1.4682	0.4310
O(5)	0.6268	0.8692	0.3939
O(6)	0.3853	0.6947	0.1058
H(1A)	-0.0662	-0.0585	0.1153
H(1B)	0.0687	-0.1727	0.1073
H(4)	0.2520	0.4086	0.0577
H(5)	0.1990	0.1605	0.4191
H(6)	0.3419	0.4230	0.3930
H(8)	0.5040	0.5333	0.2050
H(9)	0.3409	0.7895	0.3225
H(10A)	0.4884	0.7132	0.4657
H(10B)	0.5759	0.5929	0.3854
H(11)	0.4459	1.0407	0.2454
H(12A)	0.4251	0.9627	0.0654
H(12B)	0.5532	0.8380	0.0772
H(13)	0.6843	0.8257	0.2414
H(15)	0.7763	1.1335	0.4371
H(18)	0.7807	1.4346	0.0848

Table 3.5 (Continued)

	X	Y	Z
H(19)	0.6625	1.1489	0.1063
H(20A)	0.9399	1.7484	0.4030
H(20B)	1.0662	1.6264	0.3755

Table 3.6 Atomic bond (Å) lengths for sesamin.

	Bond Length (Å)	Literature Bond Length [67] (Å)		Bond Length (Å)	Literature Bond Length [67] (Å)
C4- H4	0.931		C18- C19	1.398	1.396
C4- C3	1.370	1.358	O3- C16	1.379	1.367
C4- C7	1.405	1.412	O3- C20	1.410	1.441
C6- H6	0.930		O4- C20	1.443	1.420
C6- C5	1.410	1.419	O1- C2	1.370	1.377
C6- C7	1.384	1.388	O1- C1	1.414	1.437
O2- C3	1.364	1.367	C2- C5	1.365	1.360
O2- C1	1.429	1.428	C2-C3	1.384	1.386
C17- O4	1.376	1.371	C14-C15	1.391	1.399
C17- C16	1.370	1.378	C14-C19	1.394	1.394
C17- C15	1.385	1.385	C14-C13	1.517	1.505
C18- H18	0.930		O5-C10	1.434	1.431
C18- C16	1.362	1.370	O5-C13	1.415	1.420
C5-H5	0.930		C13-C11	1.499	1.523
O6-C12	1.417	1.418	C11-H11	0.980	
O6-C8	1.432	1.435	C11-C9	1.542	1.549
C12-H12A	0.970		C20-H20A	0.970	
C12-H12B	0.971		C20-H20B	0.970	
C12-C11	1.518	1.511	C9-H9	0.980	
C15-H15	0.930		C9-C8	1.519	1.523
C10-H10A	0.969		C8-H8	0.980	
C10-H10B	0.970		C1-H1A	0.970	
C10-C9	1.540	1.550	C1-H1B	0.970	
C19-H19	0.930				
C7-C8	1.508	1.501			
C13-H13	0.980				

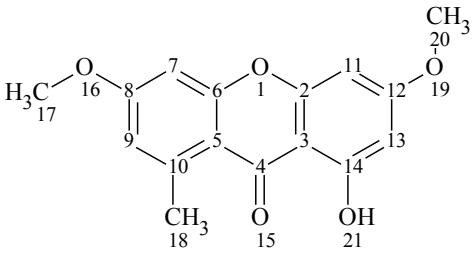

Figure 3.5 Lichexanthone

Table 3.7 Spectroscopic data for lichexanthone (F20-23F1).

Spectroscopic Technique	Data	Literature Data [68,76]
^{1}H NMR ($CDCl_3$)	δ6.3(d,1H,H-7), δ6.1(d,1H,H-9), δ6.27(d,1H,H-11), δ6.24(d,1H,H-13), δ3.83(s,3H,H-20), δ3.80(s,3H,H-17), δ2.79(s,3H,H-18)	δ6.67(d,1H,H-7), δ6.65(d,1H,H-9), δ6.32(d,1H,H-11), δ6.29(d,1H,H-13), δ3.89(s,3H,H-20), δ3.86(s,3H,H-17), δ2.84(s,3H,H-18)
MS: m/z (% abundance)	286(M^+,$C_{16}H_{14}O_5$,100), 257(50), 243(10), 227(1), 213(2), 199(3), 185(2), 143(2), 129(3), 115(10), 103(1), 91(1), 79.1(1), 69(2), 51(1)	286(M^+,$C_{16}H_{14}O_5$,100), 258(40), 243(10)

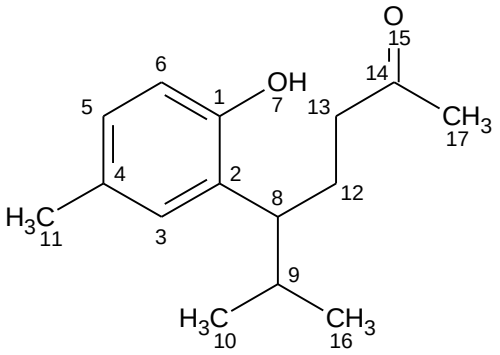

Figure 3.6 Sesquichamaenol

Table 3.8 Spectroscopic data for sesquichamaenol.

Spectroscopic Technique	Data	Literature Data [69]
^{1}H NMR ($CDCl_3$)	δ6.80(d,1H,H-5), δ6.78(dd,1H,H-3), δ6.61(d,1H,H-6), δ4.87(s,1H,OH), δ2.53(m,1H,H-8), δ2.18(s,3H,H-11), δ1.98(s,3H,H-17), δ0.95(d,3H,H-16), δ0.67(d,3H,H-10)	δ6.82(d,1H,H-5), δ6.84(dd,1H,H-3), δ6.65(d,1H,H-6), δ4.95(s,1H,OH), δ2.56(m,1H,H-8), δ2.23(s,3H,H-11), δ2.20(m,2H,H-13), δ2.08(m,1H,H-12a), δ2.03(s,3H,H-17), δ1.83(m,1H,H-9), δ1.73(m,1H,H-12b), δ0.99(d,3H,H-16), δ0.71(d,3H,H-10)
MS: m/z (% abundance)	234.1(M^+,$C_{15}H_{22}O_2$,48), 216(1), 201(1), 191(35), 176(40), 164(58), 147(27), 133(100) , 121(80), 105(25), 91(28), 77(27), 65(15), 55(20), 45(1)	234(M^+,$C_{15}H_{22}O_2$,19), 191(15), 176(18), 165(30), 163(25), 133(75), 121(54), 43(100)

3.4 Molecular Modeling Data

Active pure compounds were examined for potential binding to DNA of human topoisomerase I using ArgusLab and Molegro docking algorithms. The lowest binding energies are summarized in Tables 3.9 and 3.10. The scoring function identifies the energies based on the most favorable ligand conformation when bound to the DNA. The lower the energy scores the better the DNA-ligand binding in comparison to higher energies [88]. The lowest binding energies for Molegro docked ligands; lichexanthone is shown in five crystal structures shown in Figures 3.7-3.11.

Table 3.9 ArgusDock binding energies (kcal/mol) of best binding poses for ligands into DNA of human topoisomerase I.

Ligand	ArgusDock (kcal/mol)				
	1k4t	1z3f	1al9	1t8i	1sc7
Lichexanthone	-5.63	-4.48	-4.52	-6.23	-5.69
Camptothecin[c]	-4.73	-4.72	-4.47	-5.56	-6.73
Ellipticine[d]	-4.12	-4.33	-4.32[a]	-4.85[a]	-5.48
Indenoisquinoline[e]	-4.32	-3.88	-4.06[a]	-5.74[a]	none
Topotecan[f]	-4.57	-4.52	none[b]	-4.90	-5.87
Daunorubicin	-6.38	-4.44	none[b]	-5.00	-5.63

[a]Partial intercalation: molecule does not insert completely. [b]No intercalative binding pose found. [c]Camptothecin is the co-crystallized ligand for crystal structure 1t8i [62]. [d]Ellicipticine is the co-crystallized ligand for crystal structure 1z3f [63]. [e]Indenoisquinoline is the co-crystallized ligand for crystal structure 1sc7 [62]. [f]Topotecan is the co-crystallized ligand for crystal structure 1k4t [62]. [g]Bisdaunorubicin is the co-crystallized ligand for crystal structure 1al9 [64].

Table 3.10 Molegro binding energies (kcal/mol) of best binding poses for ligands into human DNA topoisomerase I.

Ligand	Molegro (kcal/mol)				
	1k4t	1z3f	1al9	1t8i	1sc7
Lichexanthone Rerank	-25.829	-17.911	-19.024	-21.236	-24.229
Camptothecin[c] Rerank	-32.263	-26.701	-1.1259	-23.213	-25.934
Ellipticine[d] Rerank	-23.496	-22.666	-15.086	-18.939	-22.502
Indenoisquinoline[e] Rerank	-32.28	-27.859	-23.364[a]	-26.075	-26.228
Topotecan[f] Rerank	-36.67	-26.416	none[b]	-31.021	-26.201
Daunorubicin Rerank	-18.856	-22.795	3.6813[a]	-16.806	-24.873

[a]Partial intercalation: molecule does not insert completely. [b]No intercalative binding pose found. [c]Camptothecin is the co-crystallized ligand for crystal structure 1t8i [62]. [d]Ellicipticine is the co-crystallized ligand for crystal structure 1z3f [63]. [e]Indenoisquinoline is the co-crystallized ligand for crystal structure 1sc7 [62]. [f]Topotecan is the co-crystallized ligand for crystal structure 1k4t [62]. [g]Bisdaunorubicin is the co-crystallized ligand for crystal structure 1al9 [64].

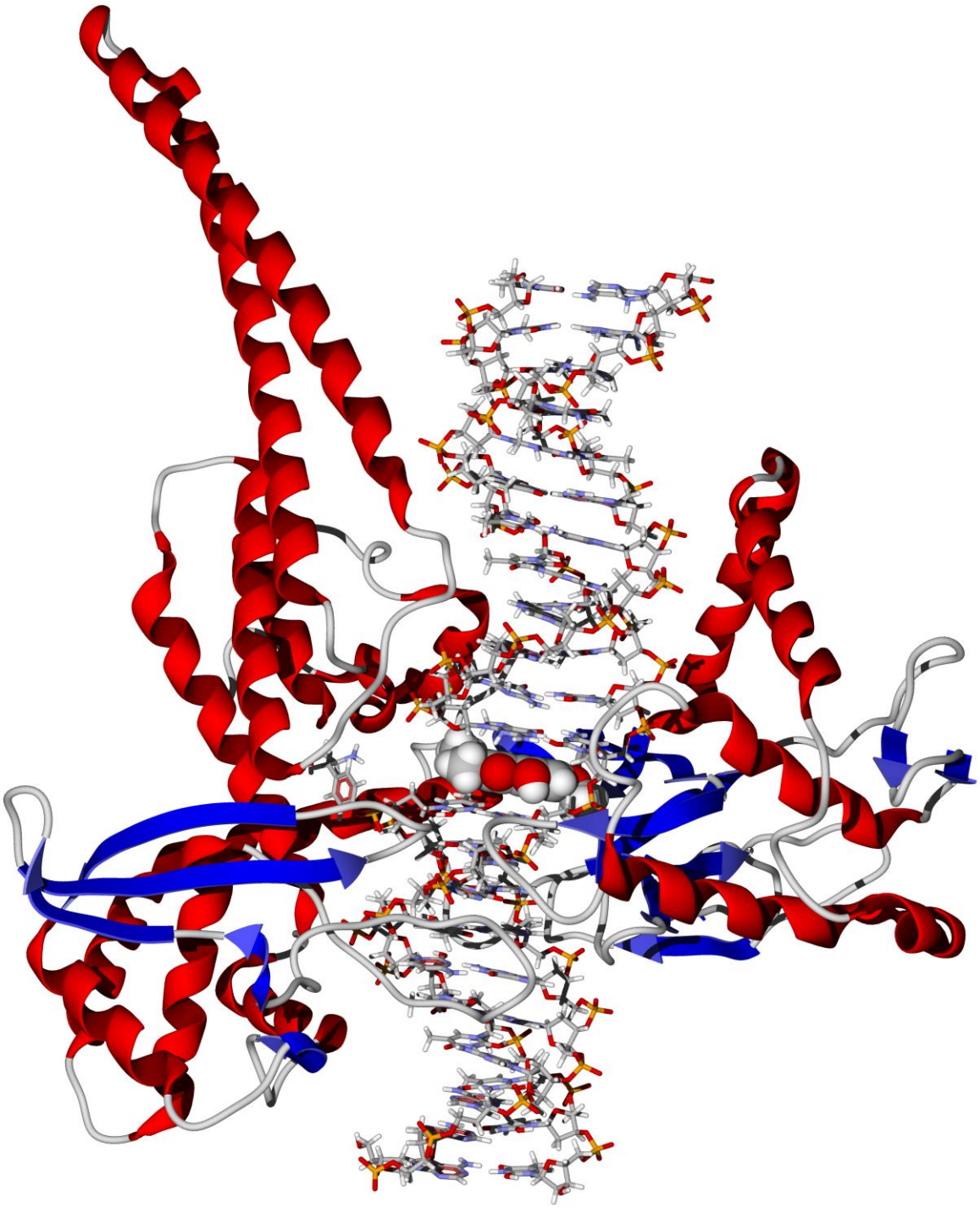

Figure 3.7 X-ray crystal struc I (ribbon structure)-DNA complex (wire figure) PDB: 1k4t with docked lichexanthone (CPK model) from Molegro Virtual Docker molecular docking analysis.

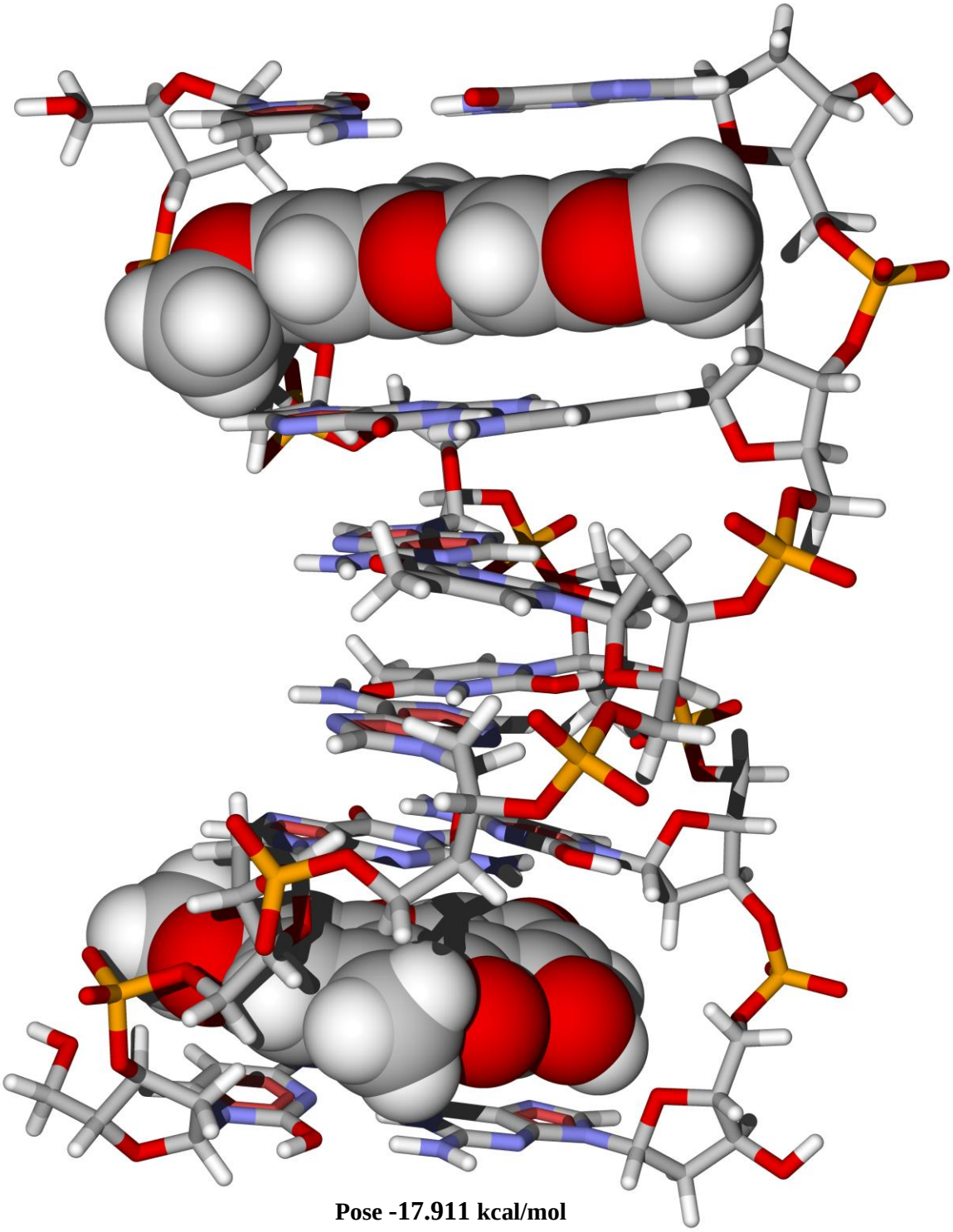

Pose -17.911 kcal/mol

Figure 3.8 X-ray crystal structure of DNA complex (wire figure) PDB: 1z3f with docked lichexanthone (CPK model) from Molegro Virtual Docker molecular docking analysis.

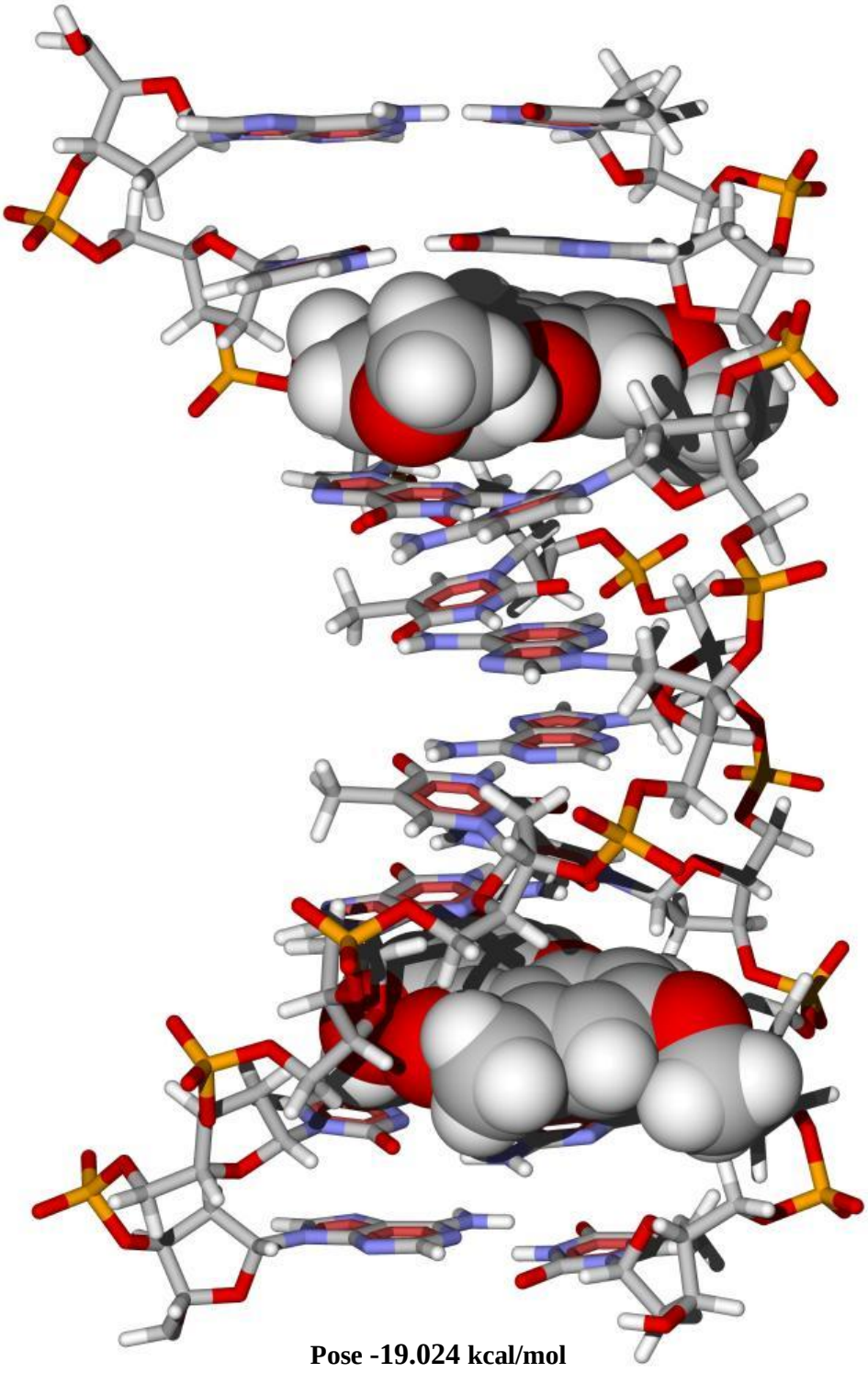

Figure 3.9 X-ray crystal structure of DNA complex (wire figure) PDB: 1al9 with docked lichexanthone (CPK model) from Molegro Virtual Docker molecular docking analysis.

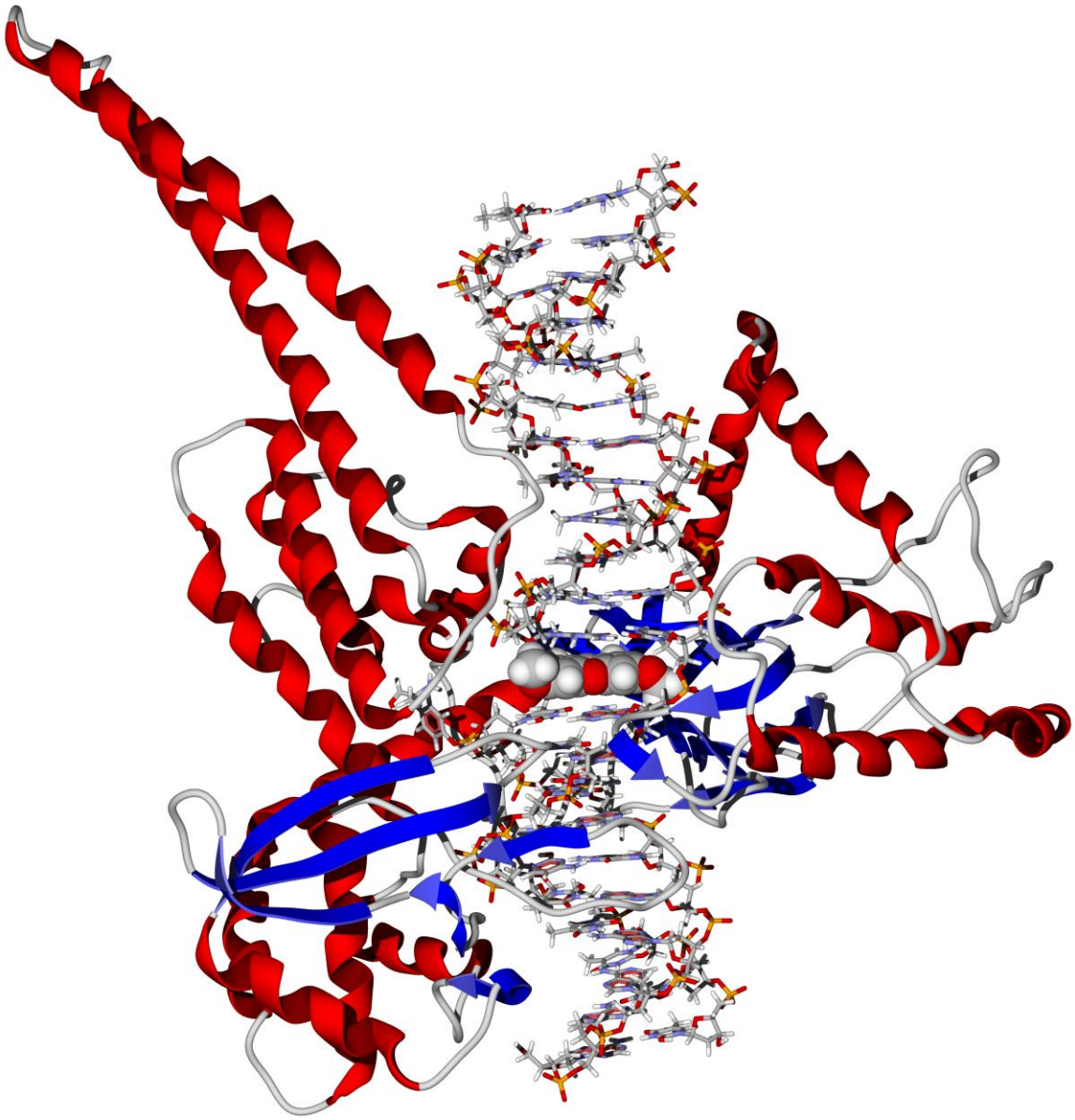

Pose -21.236 kcal/mol

Figure 3.10 X-ray crystal structure of human topoisomerase I (ribbon structure)-DNA complex (wire figure) PDB: 1t8i with docked lichexanthone (CPK model) from Molegro Virtual Docker molecular docking analysis.

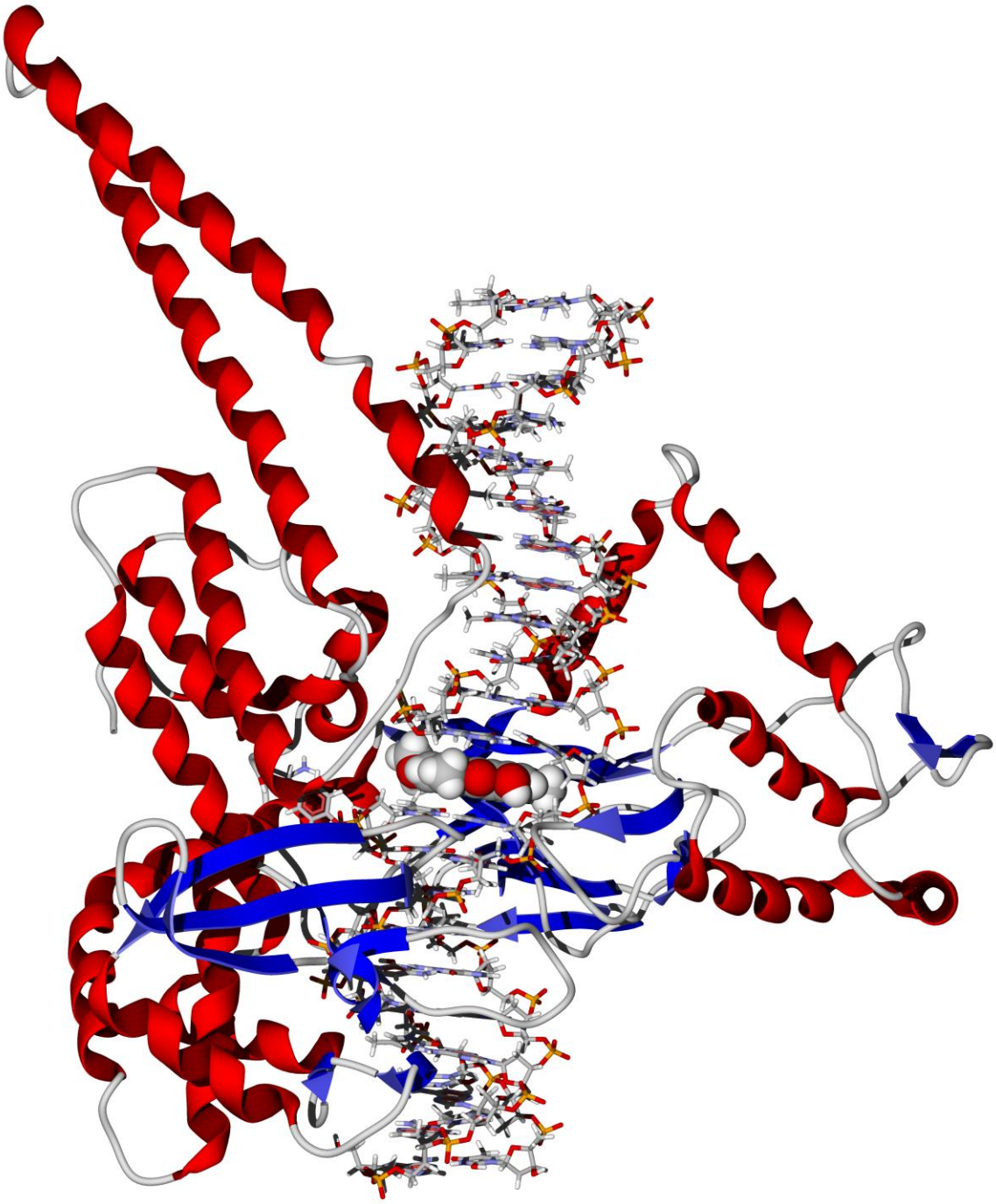

Pose -24.229 kcal/mol

Figure 3.11 X-ray crystal structure of human topoisomerase I (ribbon structure)-DNA complex (wire figure) PDB: 1sc7 with docked lichexanthone (CPK model) from Molegro Virtual Docker molecular docking analysis.

CHAPTER IV

DISCUSSION

4.1 Analysis of Lupeol

Isolated pure compound lupeol (F14) exhibited high kill rates at 100 % against MCF-7 and MDA-MB-231 cell lines. Lupeol ($C_{30}H_{50}O$) is a white powder with a molecular weight of 426.72 g/mol and a melting point of 215ºC-216ºC [68]. The ^{1}H NMR spectrum of Lupeol (F14) is a triterpene that showed seven methyl singlets and one secondary hydroxyl group. Olefinic protons were shown at δ 4.70 and 4.57. ^{13}C NMR of lupeol showed signals that represented seven methyl groups and the carbon bonded to the hydroxyl group C-1 appeared at δ 81.68. The alkenic carbons appeared at δ 153.63 and δ 111.98. The reported data are in agreement with spectroscopic data in the literature [67]. Comparable LC_{50} (concentration required to kill 50 %) values were calculated against cell lines and shown in Table 4.1. Lupeol was generally less toxic than the compared anticancer drugs and has been shown to be an inhibitor of topoisomerase II. Lupeol was also less toxic when compared to other lupane triterpenoids against various cancer cell lines. However, the compared triterpenoid betulinic acid was generally more toxic against the various cell lines (Table 4.2) and anticancer drugs in Table 4.1. Lupane triterpenoids have been shown to inhibit tumor cell proliferation by preventing DNA replication [56]. The cytotxicity may be attributed to the inhibition of topoisomerase II

through hydrogen bonds between the hydroxyl group of lupeol and the carboxylate of Gly 774 and the amide of Gln 739 in the DNA hydrophobic pocket (Figure 4.1). The hydroxyl group of lupeol binds to the ATP site through hydrogen bonding of the amide of Asn 142 and the amide of Arg 141 (Figure 4.2). Therefore, lupeol may inhibit through the DNA or ATP binding site, preventing the binding of DNA [59].

Table 4.1 LC_{50} values of compounds from *Zanthoxylum setulosum* and standard deviation of those values against two tumor cell lines compared to anticancer drugs.

Compound	MCF-7		MDA-MB-231	
	LC_{50} (µM)	Std. Dev.	LC_{50} (µM)	Std. Dev.
Lupeol	85.3	1.92	453.9	15.54
Camptothecin	9.21	1.41	360	74
Colchicine	not active	-	9.30	1.08
Doxorubicin	49.4	3.3	44.6	4.1
Etoposide	not active	-	137	32
Tingenone	40.0	3.9	NT	-
Ellipticine	12.8	0.5	NT	-
Vinblastine	NT	-	235	120
Taxol	NT	-	not active	-

Not active-not active against tested cell line, NT-not tested against cell line

Table 4.2 LC_{50} values of lupane triterpenoids against various cell lines.

Compound	LC_{50},µM	Cell Line	Reference
Lupeol	39.4	MEL-2	[56]
	77	Hep G2	[67]
	>50	MCF-7	[73]
Betulinic acid	2.6	MEL-2	[56]
	34	Hep G2	[56]
	9.61	MDA-MB-231	[56]
	194	MCF-7	[73]

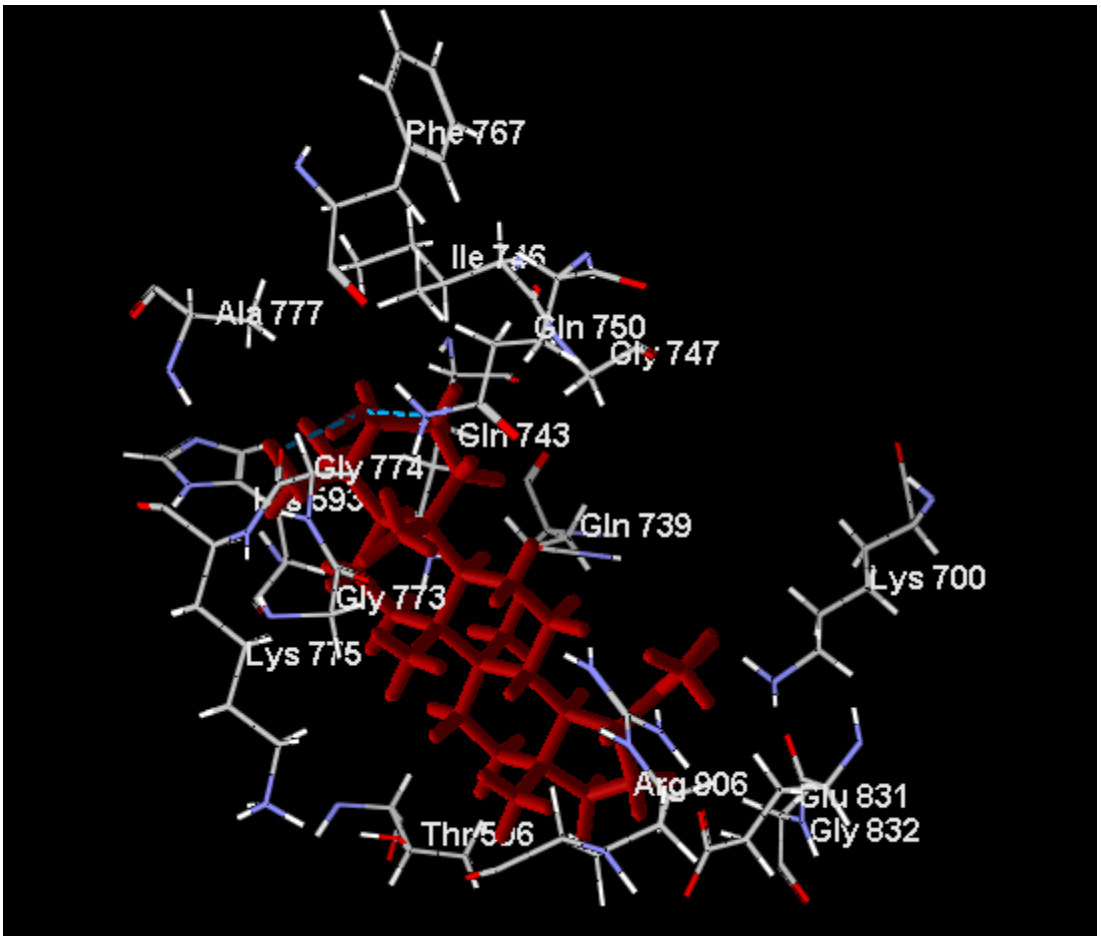

Figure 4.1 Hydrogen bonding (blue dashed lines) of lupeol (red) with amino acids of the DNA binding site of yeast topoisomerase II (PDB: 1bjt).

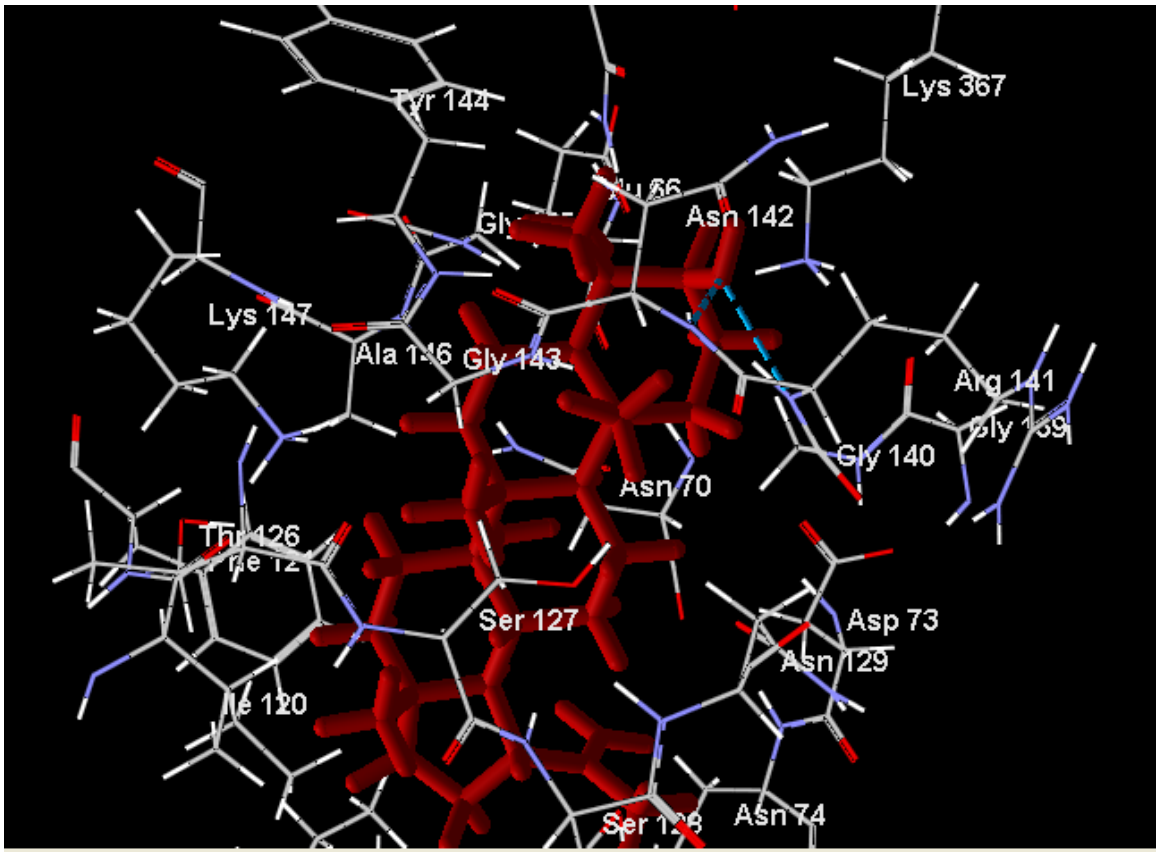

Figure 4.2 Hydrogen bonding (blue dashed lines) of lupeol (red) with amino acids of the ATP binding site of yeast topoisomerase II (PDB: 1pvg).

4.2 Analysis of Sesamin

Crystallized compound sesamin (F29) did not exhibit cytotoxicity and was not active against MCF-7 or MDA-MB-231 cell lines. Sesamin ($C_{20}H_{18}O_6$) is a colorless prism with a molecular weight of 354.35 g/mol and a melting point of 120ºC-128ºC [68]. Sesamin (F29) produced crystals and was analyzed through X-ray crystallography by Madan Gopal. Sesamin contains a monoclinic crystal system with reported unit cell dimesions of a=9.9723 Å b=6.9509 Å and c=11.8965 Å [68]. The furofuran structure of

sesamin has been reported to have a twist of 125.3º and 113.6º to reduce the interactions of the two phenyl substituents in the same plane [24].

^{1}H NMR spectrum showed aromatic protons around δ 6.82-6.90 and the (-O-CH_2-O-)$_2$ was shown at δ 6.00. The ^{13}C NMR spectrum showed the carbon signal at δ 101.1 for the (-O-CH_2-O-)$_2$. Sesamin was in agreement with published results [68].

4.3 Analysis of Lichexanthone

Lichexanthone (F20-23) exhibited high kill rates at 100 % against MCF-7 and 89.56 % against MDA-MB-231 cells. Lichexanthone ($C_{16}H_{14}O_5$) forms beige needles with a molecular weight of 286.28 g/mol and a melting point of 165ºC [69]. However, LC_{50} toxic studies for lichexanthone (F20-23F1) showed no activity against MCF-7 or MDA-MB-231. MS analysis of lichexanthone (F20-23) showed a molecular ion (M^+) at m/z 286. Ion fragments in the mass spectrum of lichexanthone showed (-CHO) at m/z 258, (-CH_2O) at m/z 228, and (-CO) at m/z 200. The ^{1}H NMR showed one methyl singlet at δ 2.79, two singlets at δ 3.83 and δ 3.80, four doublets at δ 6.24, δ 6.27, δ 6.60, and δ 6.63 for the unsaturated rings. The ^{13}C NMR spectrum showed signals between δ 16.76-181.38, indicative of a xanthone structure. Collected data of lichexanthone was compared with literature [69].

Xanthones are a class of oxygenated heterocycles with attributes in medicinal chemistry. Lichexanthone, a xanthone, has been reported to have several pharmacological properties including, antibacterial, antimalarial, antioxidant, and antitumor activity [73]. Xanthones act as metal chelators, free radical scavengers, and

inhibitors of lipid peroxidantion. Xanthones have been reported to inhibit DNA polymerase, human DNA ligase I and to regulate protein kinase C (PKC). Several prenylated xanthones have been shown to inhibit PKC, which are isoenzymes in mammalian cells and tissues involved in tumorigenesis [73].

Literature has shown lichexanthone in the following plants: *Faramea cyanea* Muell. Arg. (Rubiaceae), *Zanthoxylum microcarpum* Griseb. (Rutaceae), *Zanthoxylum valens* (Macbr.) L. Williams (Rutaceae), *Zanthoxylum tetraspermun* Wight & Arn. (Rutaceae), *Henriettella fascicularis* (Melastomataceae), and *Minquartia guianesis* Aubi (Olacaceae) [74]. It is suggested that isolation of lichexanthone from the various plants originate from a lichen source [74]. Lichexanthone has been isolated mainly from a variety of other plant species but is shown in *Zanthoxylum* species of Rutaceae.

4.4 Analysis of Sesquichamaenol

Sesquichamaenol (F5-11) exhibited high kill rates at 100 % against MCF-7 and 91.76 % against MDA-MB-231 cells. Sesquichamaenol ($C_{15}H_{22}O_2$) forms white crystals with a molecular weight of 234.33 g/mol and a melting point of 108ºC-109ºC [70]. Isolated sesquichamaenol LC_{50} toxic studies (F20-23F1) showed no activity against MCF-7 or MDA-MB-231. MS analysis of sesquichamaenol (F5-11) showed a molecular ion (M^+) at m/z 234. The ^{1}H NMR showed doublet of doublets and doublets at δ 6.80, δ 6.78, and δ 6.61, respectively for protons on benzene ring. The four methyl groups appeared at δ 2.53, δ 2.18, δ 0.95, and δ 0.67. Collected data were compared with literature [70]. All spectroscopic data are recorded in Appendices A-B.

Sesquichamaenol is a sesquiterpene that is found in *Pilocarpus* species (Rutaceae) and reported to be a source of various metabolites with pharmacological activities [75]. Sesquichamaenol has also been shown in *Cedrelopsis microfoliata* that was once part of Rutaceae but is currently in the Ptaeroxylaceae [70]. *Juniperus formosana* and *Chamaecyparis formosensis* have also been reported to contain sesquichamaenol [70].

4.5 Analysis of Molecular Docking

Many anticancer drugs are planar aromatic heterocycles that form a complex with DNA and DNA polymererases, topoisomerase I and II [71]. This study focused on the intercalation of ligands with human DNA topoisomerase I. X-ray crystal structures have been solved for various intercalators with DNA including camptothecin, ellipticine, and topotecan. Lichexanthone from *Zanthoxylum setulosum* was examined for potential intercalation into DNA in comparison to intercalative anticancer agents. Molecular docking analysis were carried out using intercalated DNA (PDB: 1z3f and 1al9) and topoisomerase I/DNA complexes (PDB: 1k4t, 1t8i, and 1sc7). ArgusLab and Molegro Virtual Docker 2.3 were used to compare the docking accuracy of ligands. ArgusLab is a free academic molecular modeling software program that runs on Windows operating system. Molegro Virtual Docker was purchased by the dissertation research advisor and readily available and run on Windows operating system. Some of the available docking programs operate on Linux operating systems only and the above facts played a part in the selection of ArgusLab and Molegro Virtual Docker. ArguLab calculated energies in a matter of seconds, while Molegro calculated in several minutes. Molegro gave an option

to increase the amount of runs per simulation which could lead to more accurate results. Also, ArgusLab predicts binding energy without using formal statistical mechanics, which could also play a part in the inaccuracy [89]. ArgusLab has been reported to have a lower docking accuracy in comparative docking studies [90]. The binding energies are summarized in Tables 3.9 and 3.10. Lichexanthone was able to intercalate into all five DNA structures in both docking programs. ArgusLab showed lichexanthone to be the strongest binding ligand (-6.23 kcal/mol) for PDB: 1t8i in comparison to other tested anticancer agents, camptothecin and topotecan. However, the calculated LC_{50} values showed lichexanthone to have no activity against MCF-7 and MDA-MB-231 cells. Molegro outperformed ArgusLab in the binding energies for the co-crystallized ligands and lichexanthone. Therefore, the results will be based on the Molegro Virtual Docker 2^{nd} re-rank score energies that showed lichexanthone as a weak binding ligand when docked into the complexes and compared to the anticancer drugs (Table 3.9). Molegro energies were consistent with the LC_{50} values and the reported inhibition of the anticancer drugs. According to Molegro, the strongest binding ligand for ligands docked in DNA (PDB: 1k4t) was topotecan at -36.67 kcal/mol. Figure 4.3 shows overlay of docked lichexanthone (red) and topotecan (purple) intercalated between DNA base pairs of human topoisomerase I.

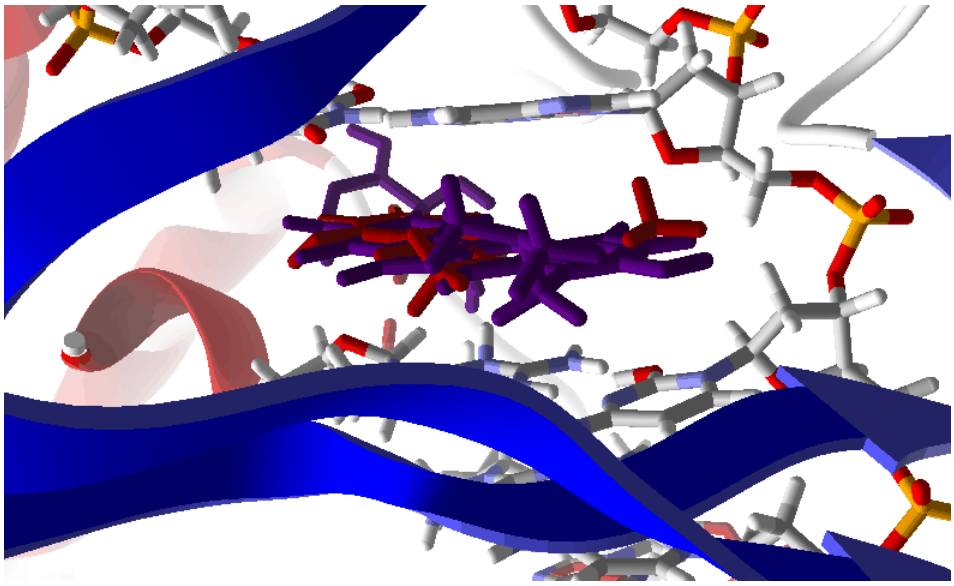

Figure 4.3 Overlay of docked lichexanthone (red) and topotecan (purple) in the DNA of human topoisomerase I (PDB:1k4t).

The strongest binding ligand for ligands docked in DNA (PDB: 1z3f) was indenoisquinoline at -27.859 kcal/mol. The strongest binding ligand for ligands docked in DNA (PDB: 1al9) was partially docked indenoisoquinoline at -23.364 kcal/mol. The strongest binding ligand for ligands docked in DNA (PDB: 1t8i) was topotecan at -31.021 kcal/mol. The strongest binding ligand for ligands docked in DNA (PDB: 1sc7) was indenoisquinoline at -26.228 kcal/mol. Topotecan and indenoisquinoline were the strongest binding ligands with camptothecin very close in energy when compared to both topotecan and indenoisquinoline. The co-crystallized ligands' energies were consistent with the calculated values in Molegro showing intercalation of anticancer drugs in the respective complexes. Daunorubicin had the lowest binding energies against human DNA topoisomerase I and this is consistent with the reported data that daunorubicin has

been shown to inhibit topoisomerase II. The intercalation of lichexanthone (Molegro) with human DNA topoisomerase I are shown in Figures 3.7-3.11.

The electronic structures and properties of lichexanthone, as well as the cytosine-guanine (C-G) base pairs have been calculated using DFT, M06/6-31G* (Table 4.3) for the gas and aqueous phase. M06/6-31G* basis set was chosen to determine the electronic structures of lichexanthone and the C-G base pair. Becke-three-parameter-Lee-Yang-Parr (B3LYP) does not evaluate electronic non-covalent interactions, such as π-π interactions, and does not keep the structures intact; therefore, it was not used. The gas phase lacks the effects of hydrogen bond formation with water that is seen in the aqueous phase. The aqueous phase calculations are necessary to study the chemical reaction of lichexanthone in a biological process carried out in an aqueous environment. Therefore, the ligand is more stabilized in the aqueous phase by forming hydrogen bonding. The hydrogen bond interaction could lead to different hydroxyl group orientations. DFT calculations of lichexanthone resulted in two orientations for interactions with the C-G base pair. The hydrogen bonding of two poses of lichexanthone with the C-G base pair of PDB: 1z3f are shown in Figures 4.4 and 4.5. Figure 4.4 shows hydrogen bonding between the carbonyl and hydroxyl group of lichexanthone with the amine guanine base and the oxygen of deoxyribose. Figure 4.5 shows hydrogen bonding between the heterocyclic oxygen and hydroxyl group of lichexanthone with the amine of cytosine and oxygen's of deoxyribose.

Table 4.3 Calculated electronic properties for lichexanthone and DNA base pair.

Compound	E (kcal/mol)	E_{aq} (kcal/mol)
Lichexanthone	-623,523.24	-623,533.87
Cytosine-Guanine	-637,253.03	-637,276.67
Lichexanthone+C-G (1)	-1,260,793.24	-1,260,839.88
Lichexanthone+C-G (2)	-1,260,795.35	-1,260,841.05

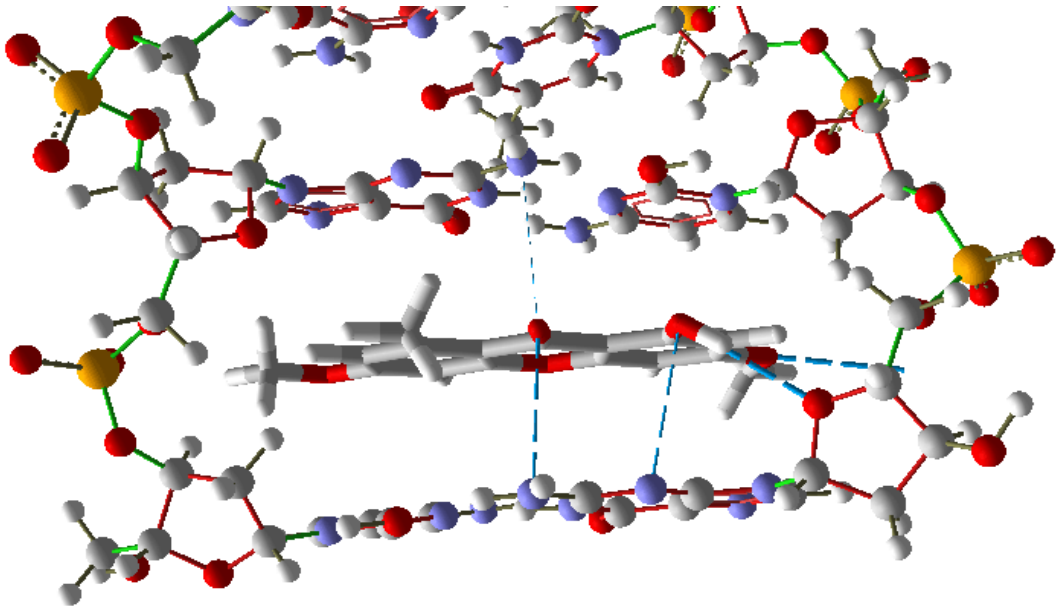

Figure 4.4 Hydrogen bonding between lichexanthone and the C-G base pair of PDB: 1z3f.

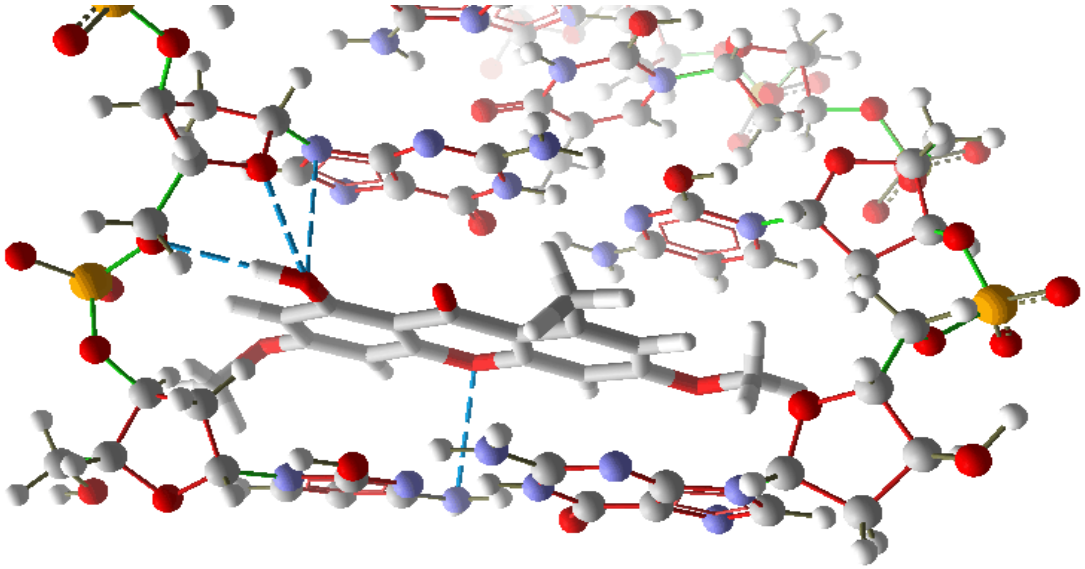

Figure 4.5 Hydrogen bonding between lichexanthone and the C-G base pair of PDB: 1z3f.

π-π interactions play key roles in molecular determination such as stacking of nucleobases [97] and intercalation of drugs into DNA [98]. π-π interaction was calculated using the aqueous energies in Table 4.3 and the following equation: E_{aq}(lichexanthone) + E_{aq}(C-G base pair) – E_{aq}(lichexanthone+C-G base pair). π-π interaction for lichexanthone and C-G base pair orientation 1 was 29.34 kcal/mol and 30.51 kcal/mol for C-G base pair orientation 2 in the aqueous phase. The molecular orbital between the lowest unoccupied molecular orbital (LUMO) of lichexanthone and the highest occupied molecular orbital (HOMO) of guanine-cytosine orientation 1 is shown in Figure 4.6. The LUMO of lichexanthone and HOMO of cytosine-guanine orientation 2 is shown in Figure 4.7. There is no overlap of orbitals in either orientation when the LUMO and HOMO are placed above one another. This shows that hydrogen

bonding and the π-π interactions play a large role in the interaction of lichexanthone with the C-G base pair. The orientation in Figure 4.8 is the lowest-energy M06/6-31G* face-to-face orientation of lichexanthone with the cytosine-guanine base pair orientations.

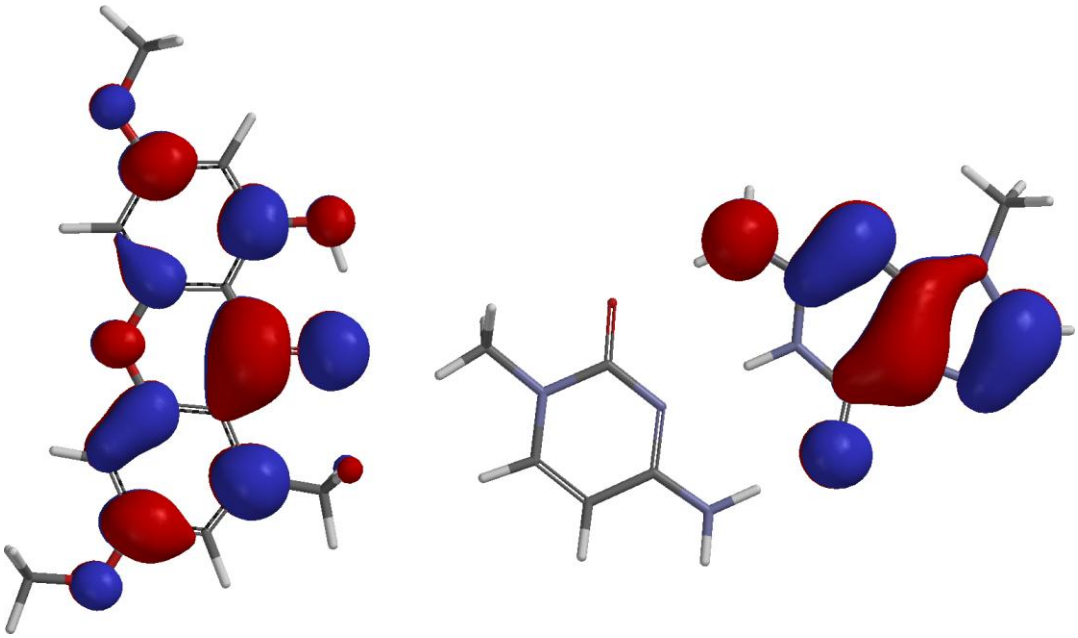

Figure 4.6 LUMO of lichexanthone (left) and HOMO of guanine-cytosine orientation 1 (right) from M06/6-31G* calculations.

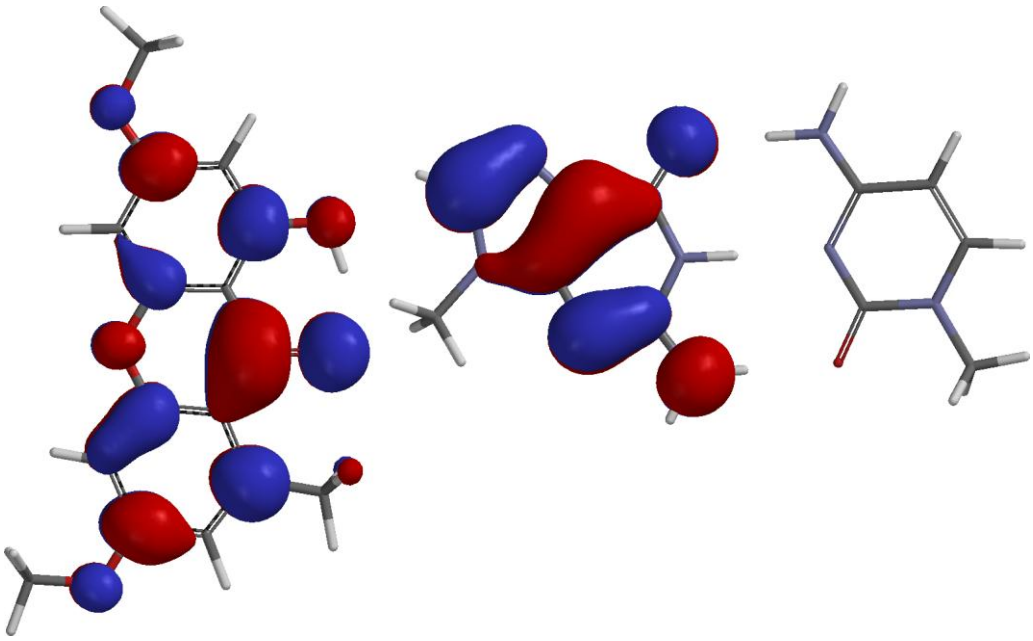

Figure 4.7 LUMO of lichexanthone (left) and HOMO of guanine-cytosine orientation 2 (right) from M06/6-31G* calculations.

Favorable cytosine-guanine orientation 2 (Figure 4.9) π-π interaction is 1.17 kcal/mol higher in energy than orientation 1 (Figure 4.8). The dipole-dipole interaction is in the same direction for orientation 1, whereas the dipole-dipole interactions are in opposite directions for orientation 2. The opposite dipole-dipole interaction creates a greater attraction and makes orientation 2 more favorable. The lower energy orientation showing favorable dipole-dipole interaction between lichexanthone and the C-G base pair is shown in Figure 4.11.

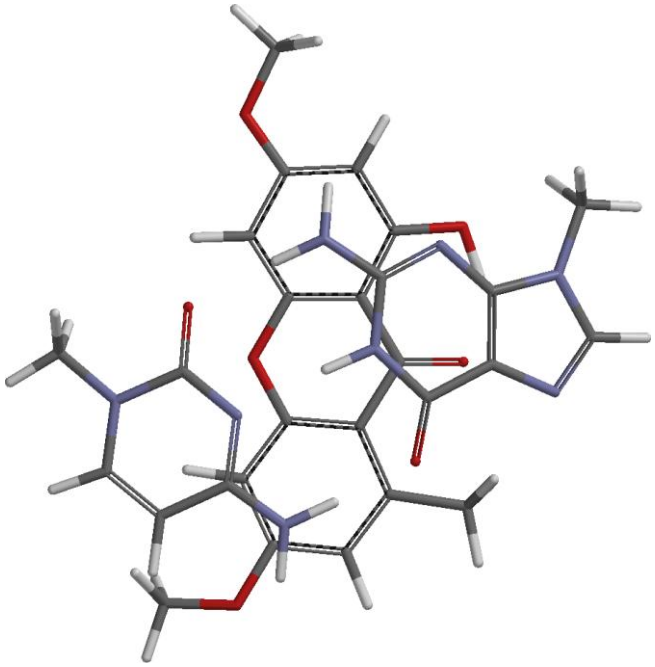

Figure 4.8 Geometry optimized (M06/6-31G*) structure for interactions of lichexanthone with C-G orientation 1.

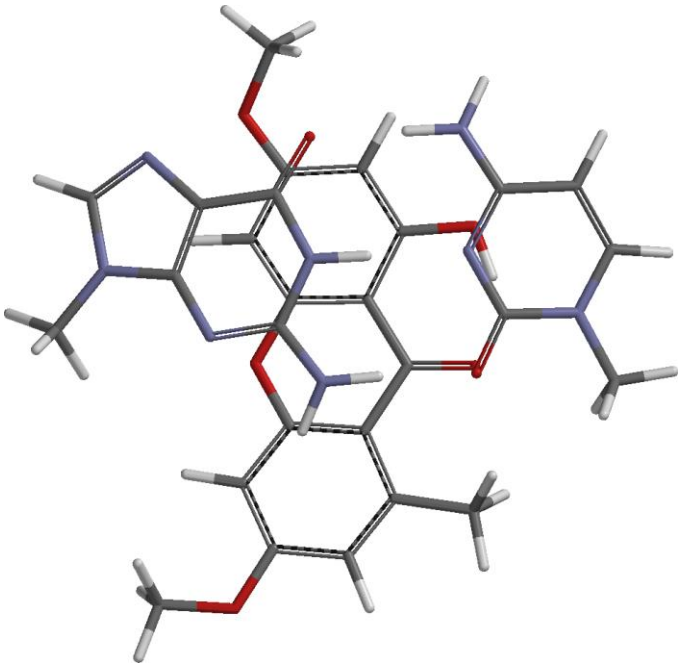

Figure 4.9 Geometry optimized (M06/6-31G*) structure for interactions of lichexanthone with C-G orientation 2.

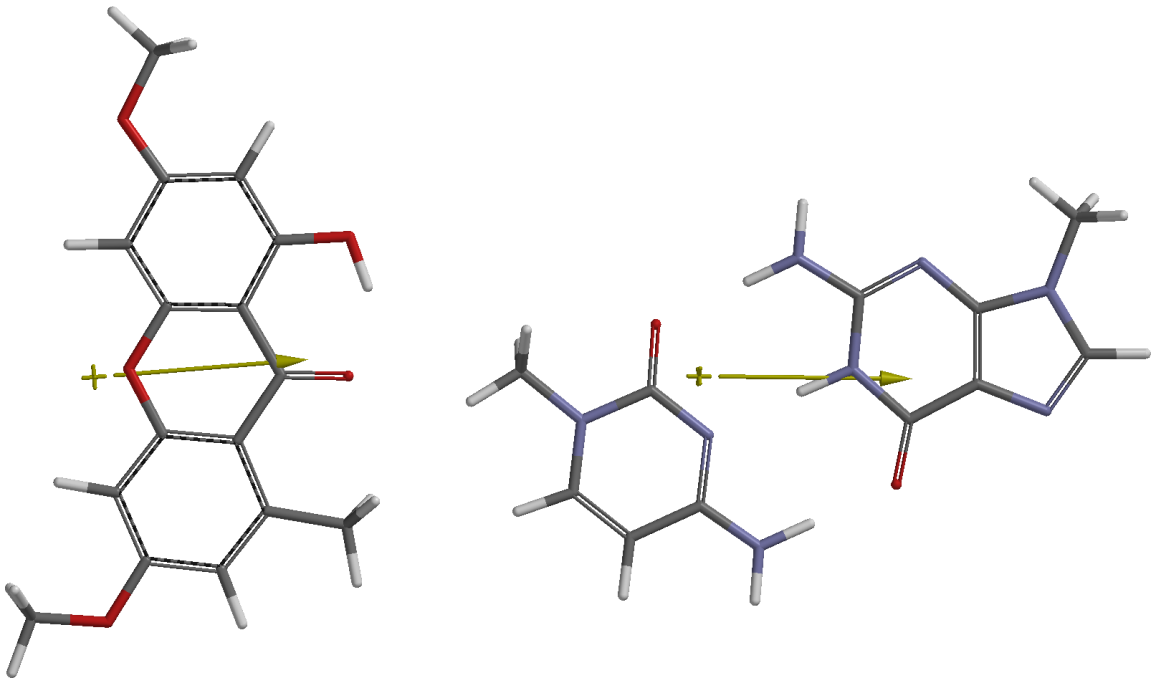

Figure 4.10 Dipole-dipole interactions between lichexanthone and the C-G base pair of orientation 1.

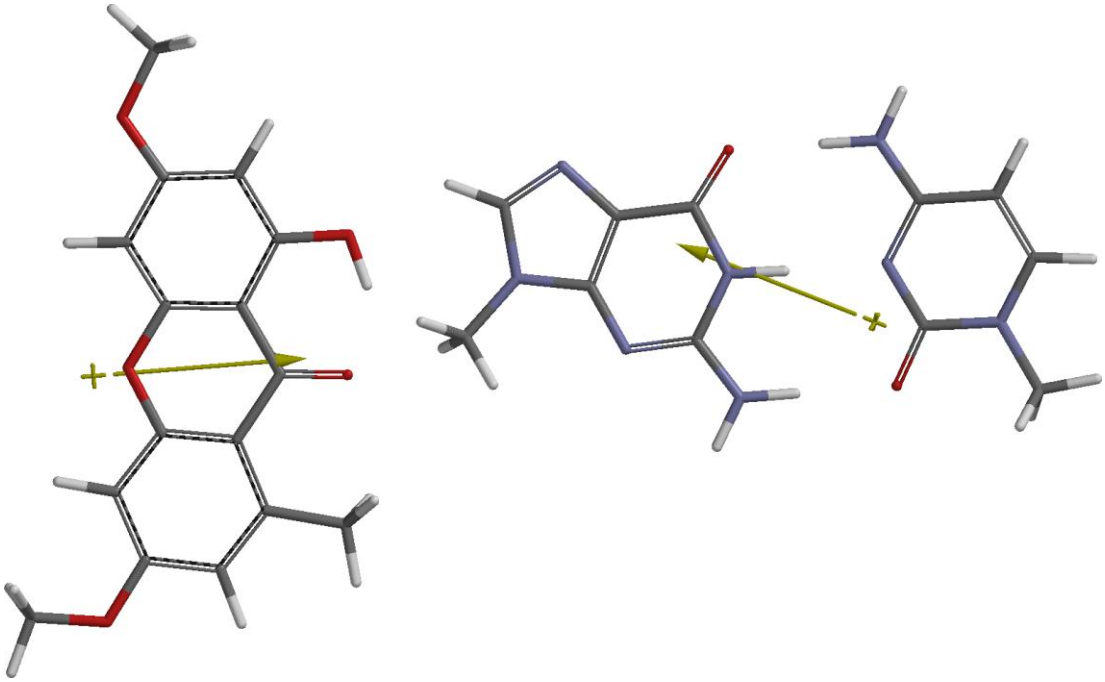

Figure 4.11 Dipole-dipole interactions between lichexanthone and the C-G base pair of orientation 2.

The electrostatic potential maps are constructed to show molecular charge distribution. The electrostatic potential is mapped onto the electron density surface representing different values of electrostatic potential with different colors. Red illustrates the low energy end or most negative electrostatic potential and blue illustrates the most positive electrostatic potential. The colors in between represent intermediate values of electrostatic potential in increasing order: red < orange < yellow < green < blue, according to Spartan [93]. The red corresponds to the oxygen's electron rich region and the blue corresponds to the hydrogen's electron poor region in lichexanthone and the C-G base pair. The electrostatic potential maps for both orientations are shown in Figures 4.12-4.15.

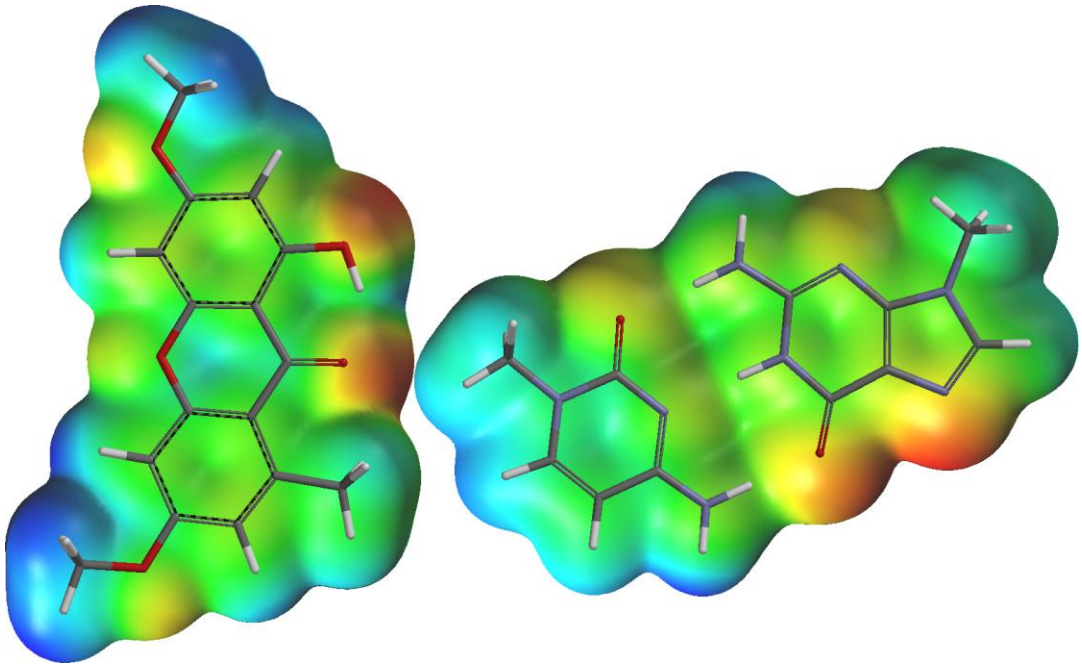

Figure 4.12 Electrostatic potential map for lichexanthone (left) and C-G base pair (right) orientation 1.

A.

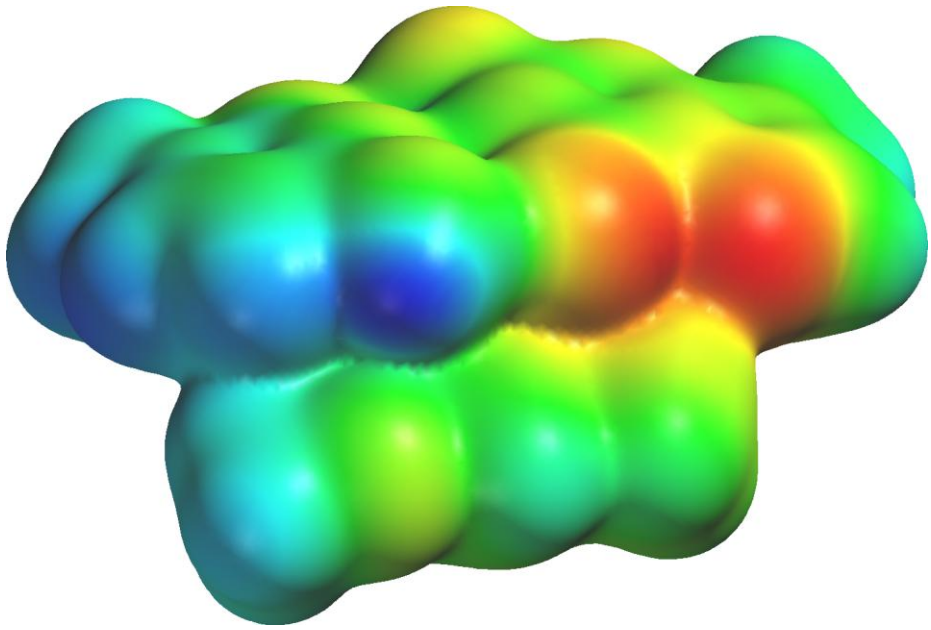

B.

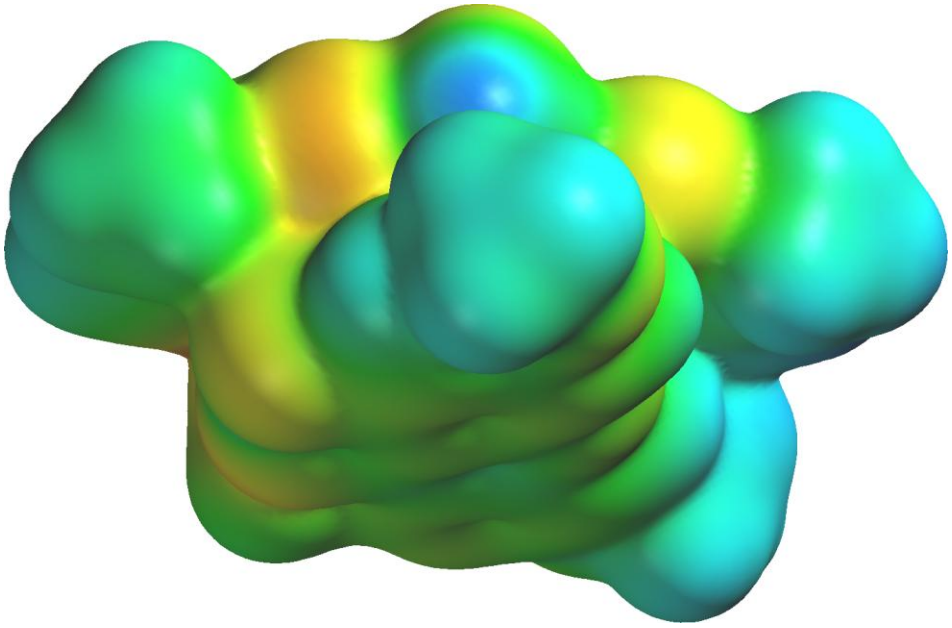

Figure 4.13 A. Electrostatic potential map of the complex lichexanthone (below) and the C-G base Pair (above) for orientation 1. B. Electrostatic potential map of the complex lichexanthone (below) and the C-G base Pair (above) for orientation 1 rotated 180°.

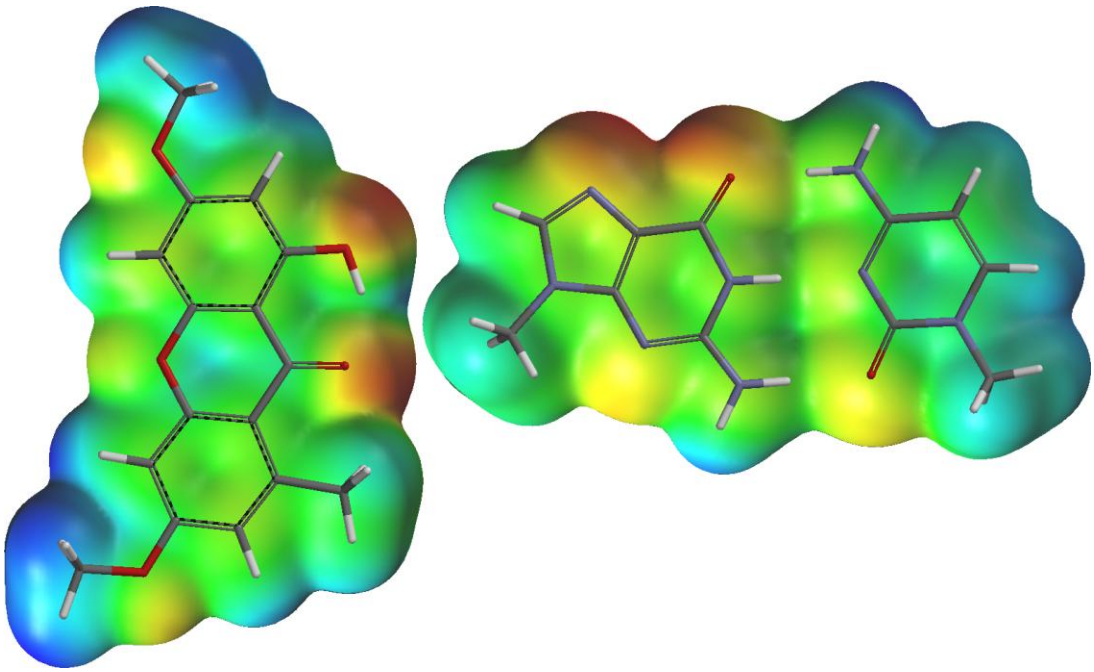

Figure 4.14 Electrostatic potential map for lichexanthone (left) and C-G base pair (right) orientation 2.

A.

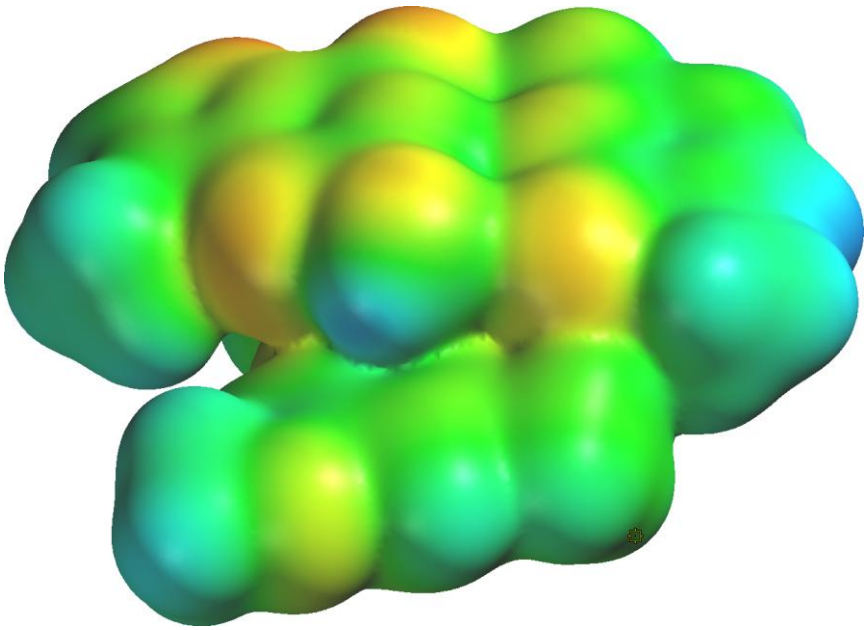

B.

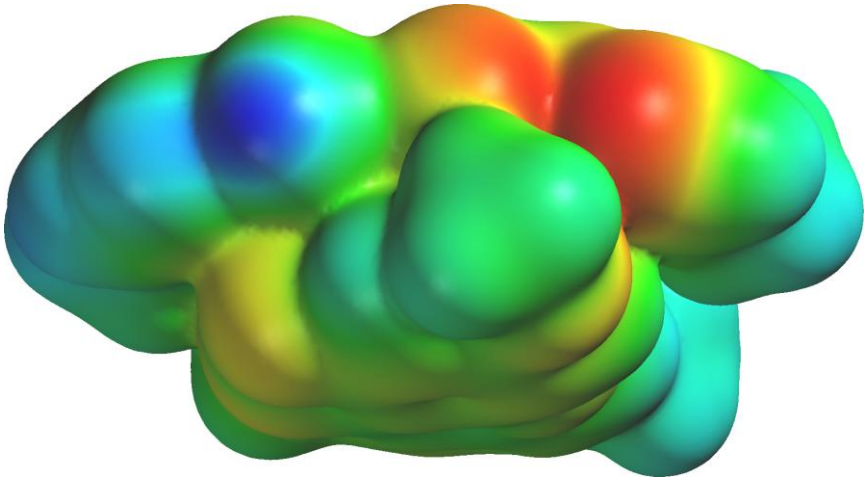

Figure 4.15 A. Electrostatic potential map of the complex lichexanthone (below) and the C-G base Pair (above) for orientation 2. B. Electrostatic potential map of the complex lichexanthone (below) and the C-G base Pair (above) for orientation 2 rotated 180°.

CHAPTER V

CONCLUSIONS

Tropical rainforest plants have evolved chemical defensive mechanisms to avoid herbivory and resist pathogens that have been used as chemical agents for human maladies such as cancer. *Zanthoxylum* is the largest genus in the Rutaceae that contain alkaloids, coumarins, amides, flavonoids, and terpenes with medicinal properties. Therefore, there are beneficial chemical agents present in *Zanthoxylum* that could be used in development of chemotherapeutic drugs. *Zanthoxylum setulosum* produced an alkaloid, lignan, terpene, and xanthone through bio-activity directed fractionation. Active compounds were studied for mechanism of action using human DNA topoisomerase I and II inhibitors as models.

The results indicated that fractions from *Zanthoxylum setulosum* were cytotoxic against MCF-7 and MDA-MB-231 breast cancer cells. Isolation of lupeol from *Zanthoxylum setulosum* exhibited strong cytotoxic effects against MCF-7 and MDA-MB-231 cells at 100 % kill. Sesamin was isolated, crystallized, and determined through X-ray crystallography and NMR but was not active against cell lines tested. Superfraction containing lichexanthone was active against MCF-7 cells at 100 % and 89.56 % kill against MDA-MB-231 cells. Superfraction containing sesquichamaenol was active against MCF-7 cells at 100 % kill and 91.76 % kill against MDA-MB-231. However, isolated purified lichexanthone and sesquichamaenol showed no activity when tested for LC_{50} values. Isolations from superfractions that contained lichexanthone and sesquichamaenol should be rescreened to find the active constituents. On the other hand, lupeol exhibited activity against MCF-7 and MDA-MB-231 to give LC_{50} values of 85.3 and 453.9 µM,

respectively. The toxicity of lupeol is greater than the known anticancer agents and requires more compound for activity. However, mechanistic studies could lead to ways to improve and reduce the effects of the approved anticancer drugs.

The extended planar structure of lichexanthone was similar to known anticancer drugs, camptothecin and topotecan that interacalated human DNA topoisomerase I. Therefore, molecular docking studies were done to find the binding energies of lichexanthone with human DNA topoisomerase I (PDB: 1k4t, 1z3f, 1al9, 1t8i, and 1sc7). Lichexanthone successfully docked into all five DNA crystal structures examined. The study showed lichexanthone to have the lowest binding energy using Molegro Virtual Docker. This result was consistent with the lack of activity in LC_{50} values against MCF-7 and MDA-MB-231 cells. There was no electrostatic overlapping of orbitals but there were opposite dipole-dipole interactions between lichexanthone and the C-G base pair orientation 2 that could be responsible for intercalation. The π-π interactions are also involved in the intercalation of lichexanthone with DNA base pairs. Topotecan and indenoisquinoline exhibited the strongest binding energies from the studied anticancer drugs. Lupeol and sesquichamaenol are not planar molecules and do not intercalate DNA.

The goal of this research was to isolate compounds from *Zanthoxylum setulosum* that has natural chemical defenses that could be studied for the development of chemotherapeutic drugs. As hypothesized *Zanthoxylum* contain a variety of compounds with medicinal properties that can be used for mechanistic models for inhibition of DNA topoisomerases. A known inhibitor of DNA topoisomerase II, lupeol was isolated and is shown as the major constituents in other plant species. An intercalator of DNA topoisomerase I, lichexanthone was also isolated: a compound found in other *Zanthoxylum* species but not yet reported in *Zanthoxylum setulosum*. Sesquichamaenol was also an isolate of *Zanthoxylum* that is not yet reported in *Zanthoxylum*

setulosum. Therefore, *Zanthoxylum* is a genus that may be very fruitful in investigation for novel chemotherapeutic agents and the study of their mechanism of action. Future studies should include screening fractions against other breast tumor cell lines, MDA-MB-468, further isolation of active fractions, structural determination of isolated compounds, and enzymatic assays of isolated compounds. MDA-MB-468 is a black cell line which is epidermal growth factor receptor (EGFR) positive and transforming growth factor receptor (TGFR) positive. Screening the isolated fractions against cell lines expressing other receptors may lead to other mechanisms of action. Overall, this research may lead to new breast cancer chemotherapeutic agents with novel structures and/or mechanisms of action.

APPENDICES

APPENDIX A

NMR SPECTRA

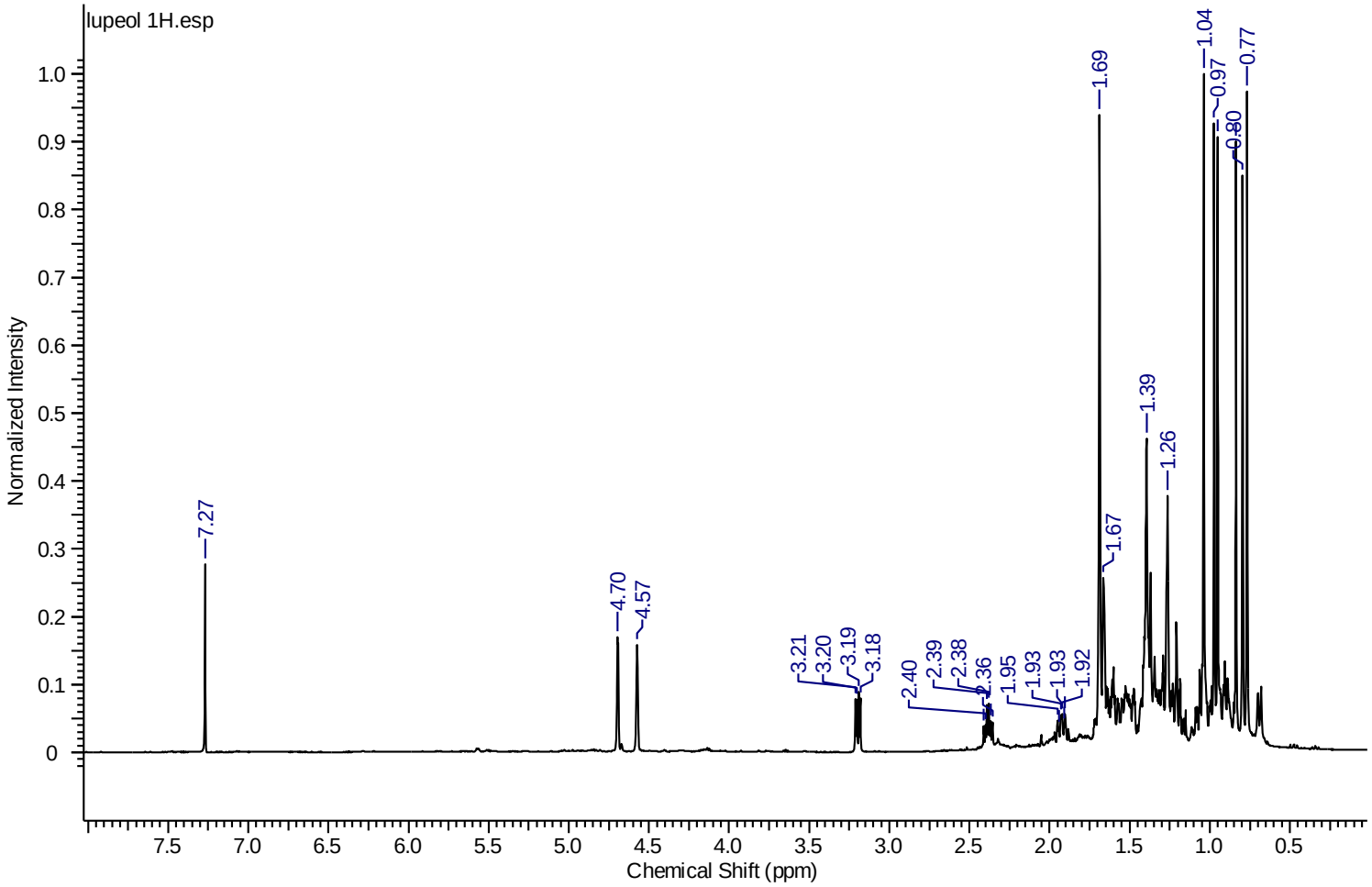

Figure A.1 ^{1}H NMR for lupeol in $CDCl_3$.

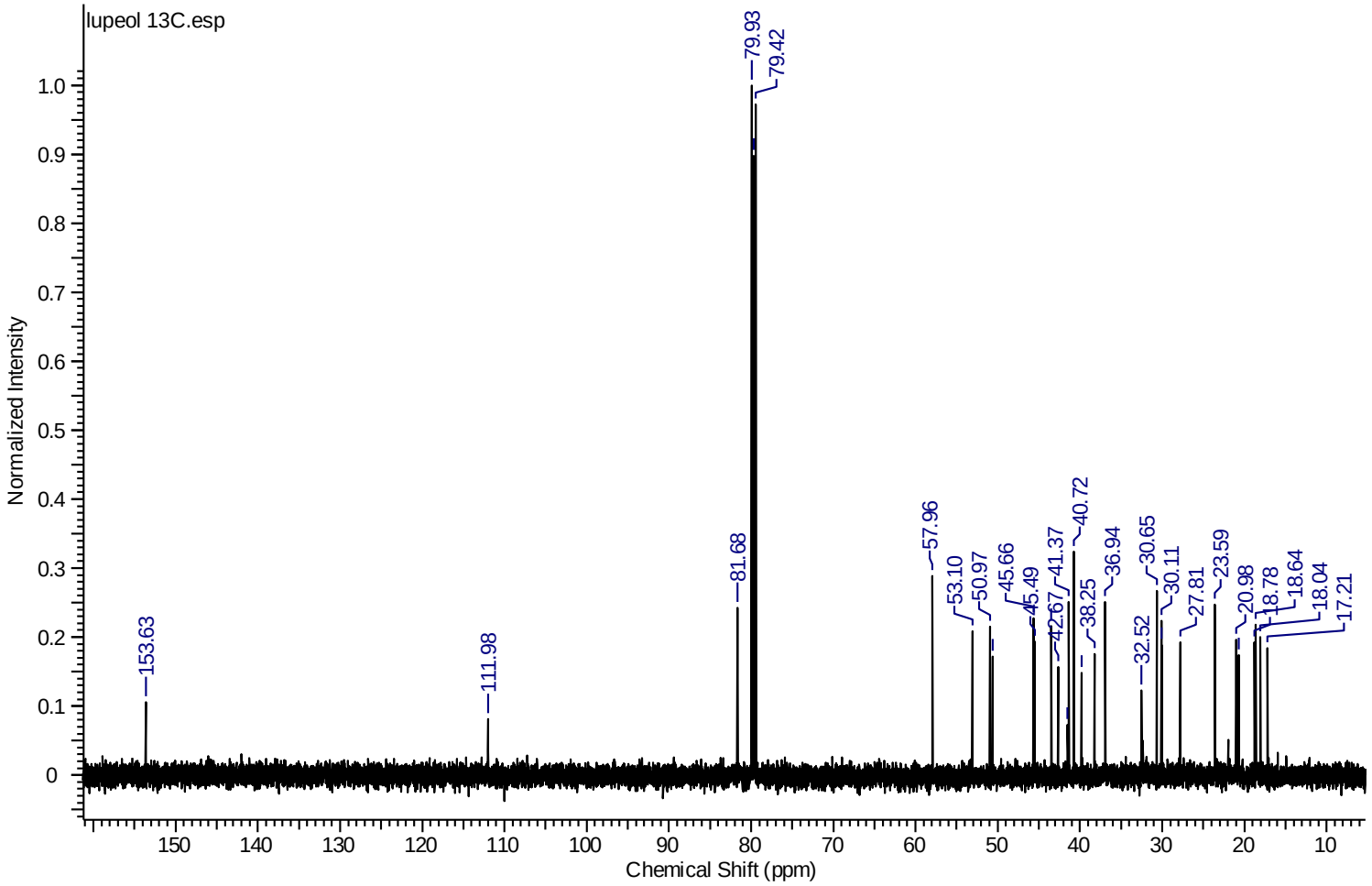

Figure A.2 ^{13}C NMR for lupeol in $CDCl_3$.

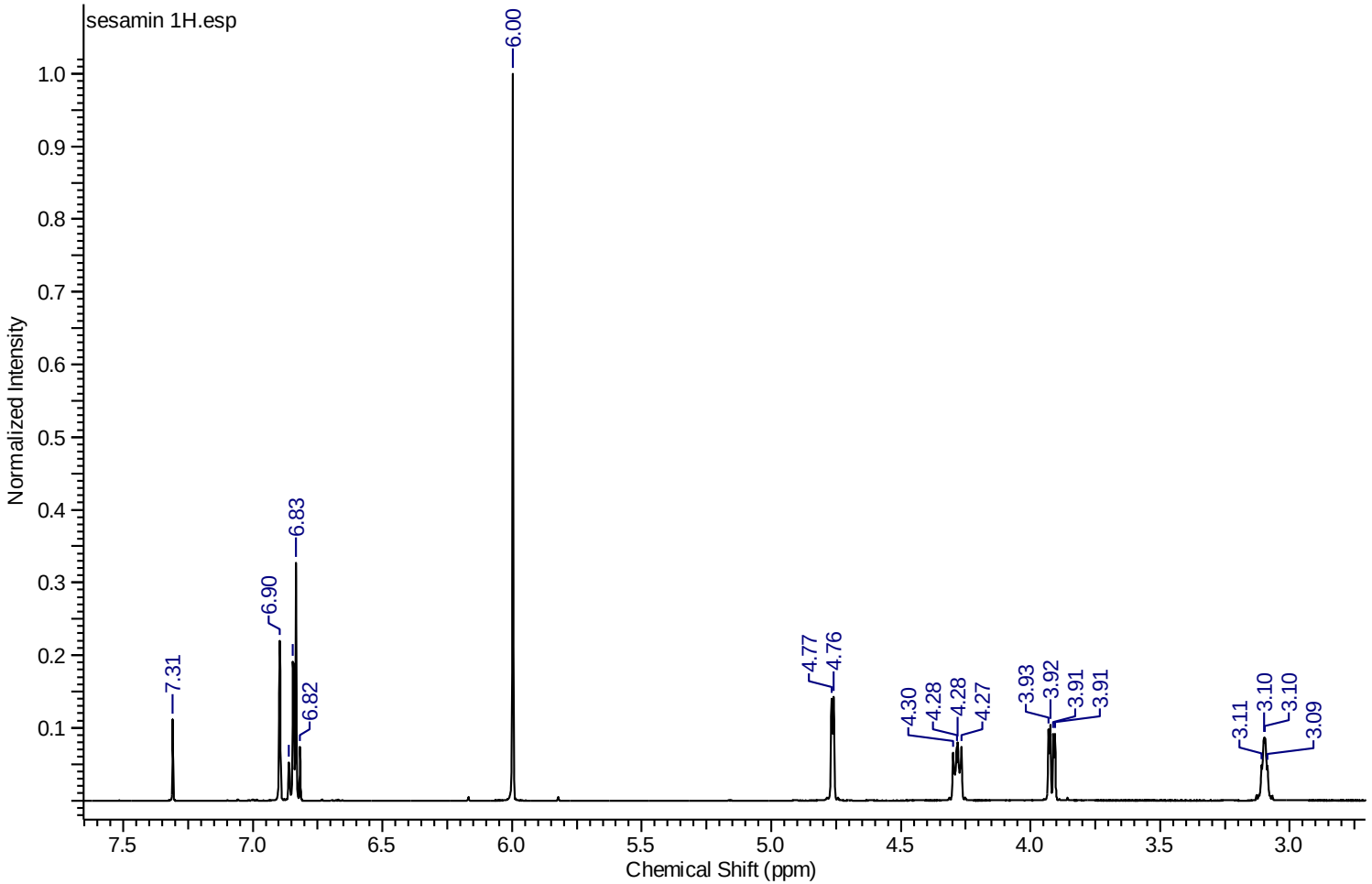

Figure A.3 ^{1}H NMR for sesamin in $CDCl_3$.

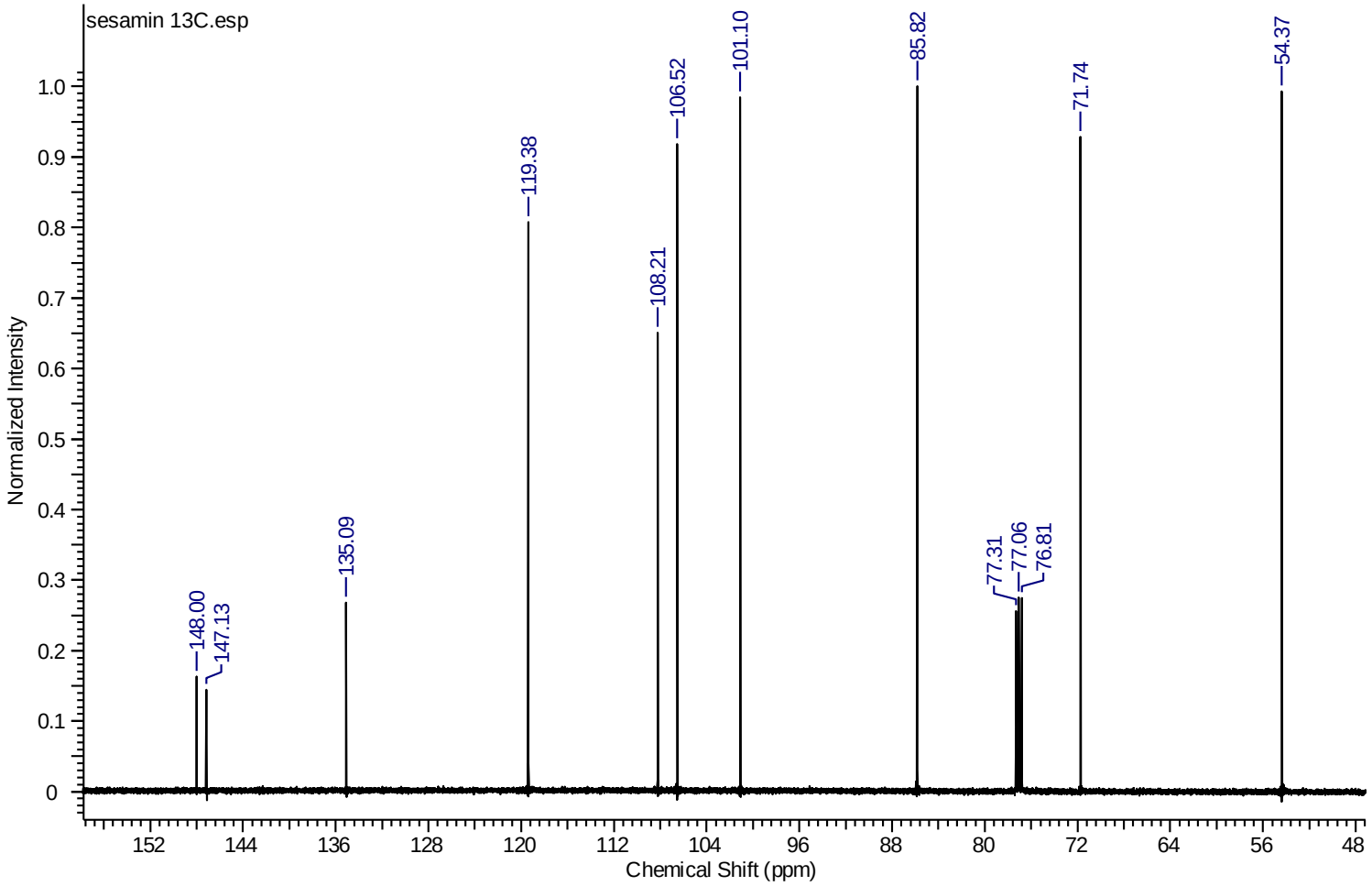

Figure A.4 ^{13}C NMR for sesamin in $CDCl_3$.

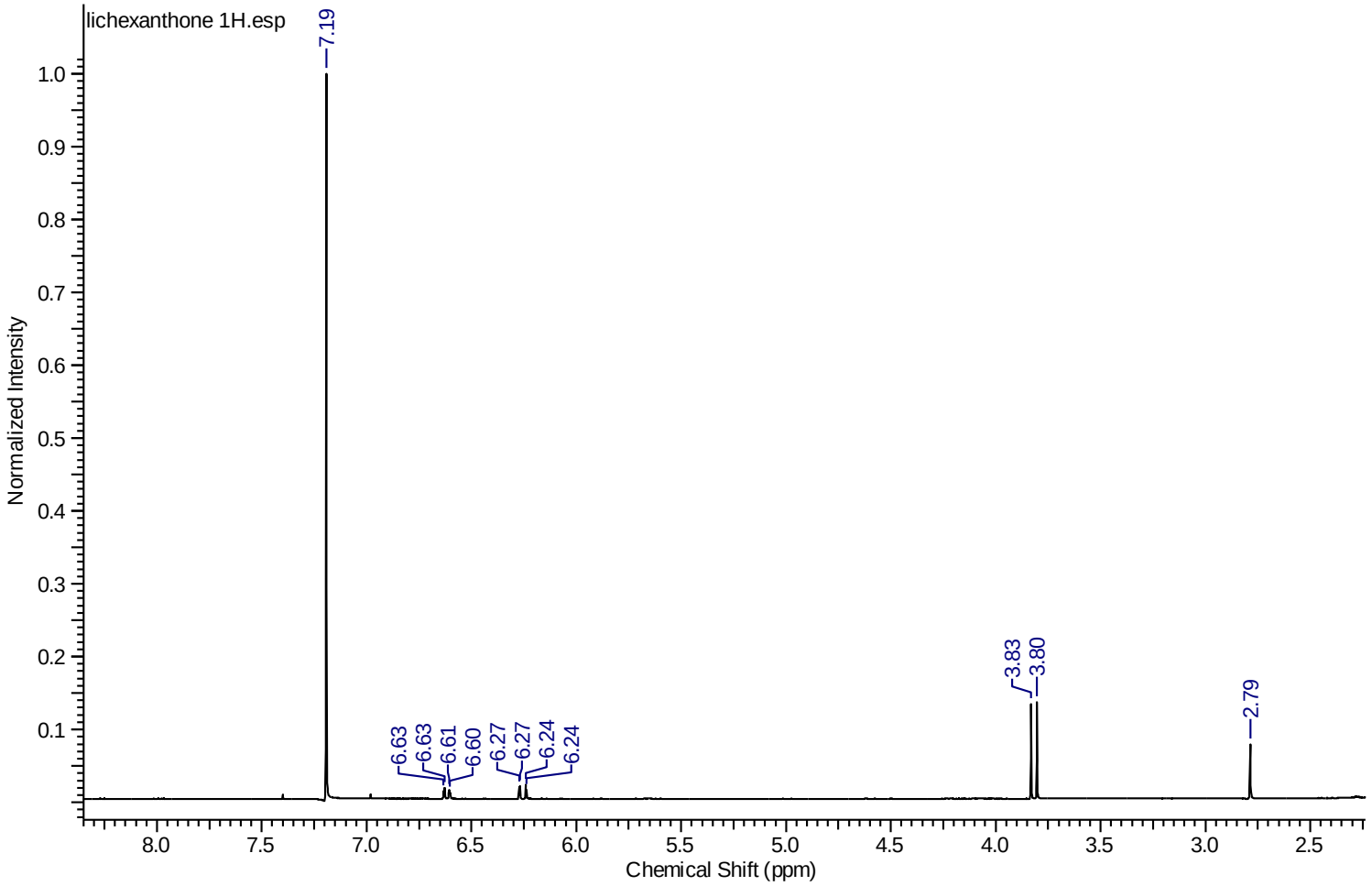

Figure A.5 ^{1}H NMR for lichexanthone in $CDCl_3$.

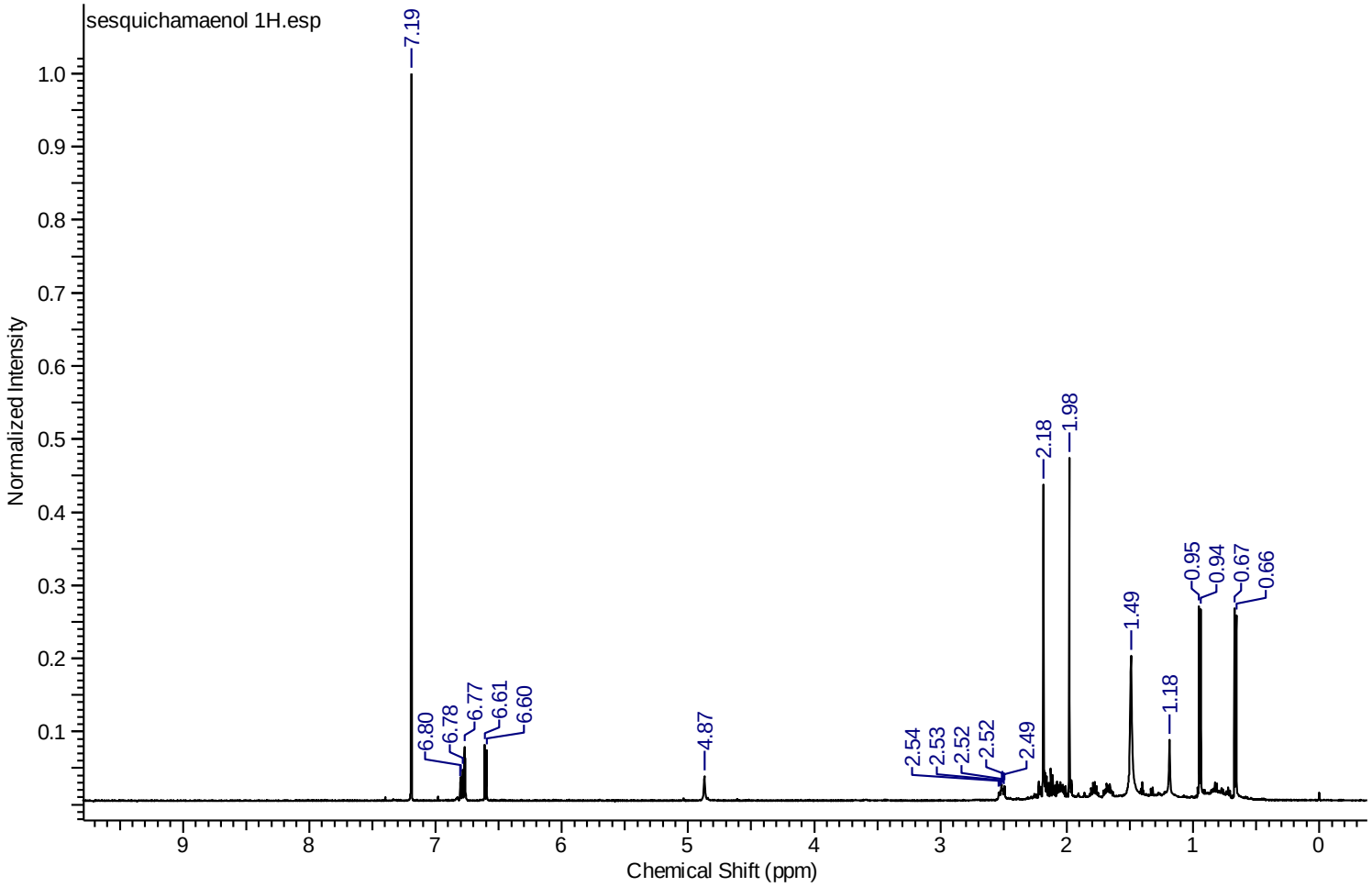

Figure A.6 ^{1}H NMR for sesquichamaenol in $CDCl_3$.

APPENDIX B

MASS SPECTRA

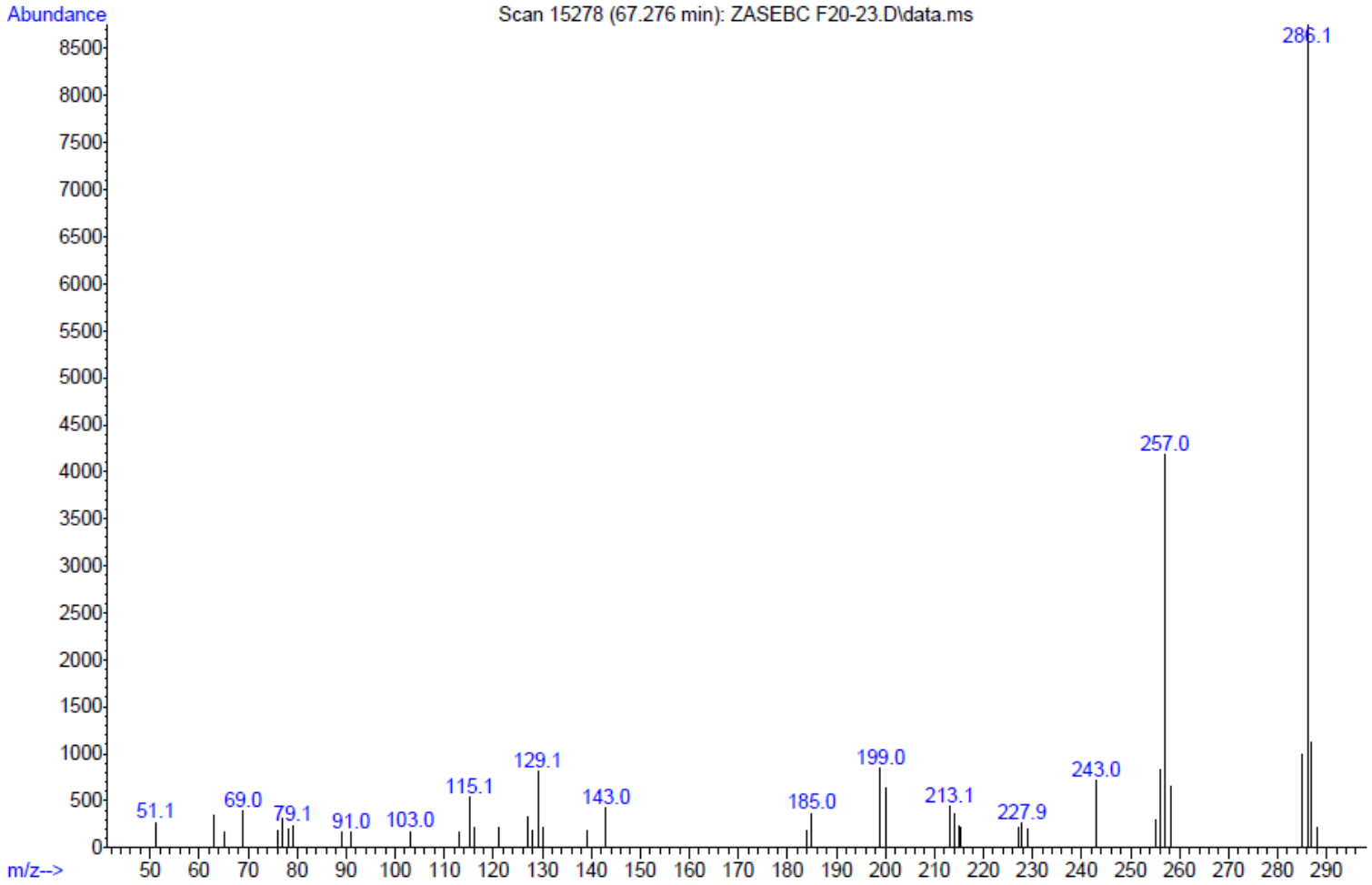

Figure B.1 Mass spectrum of lichexanthone.

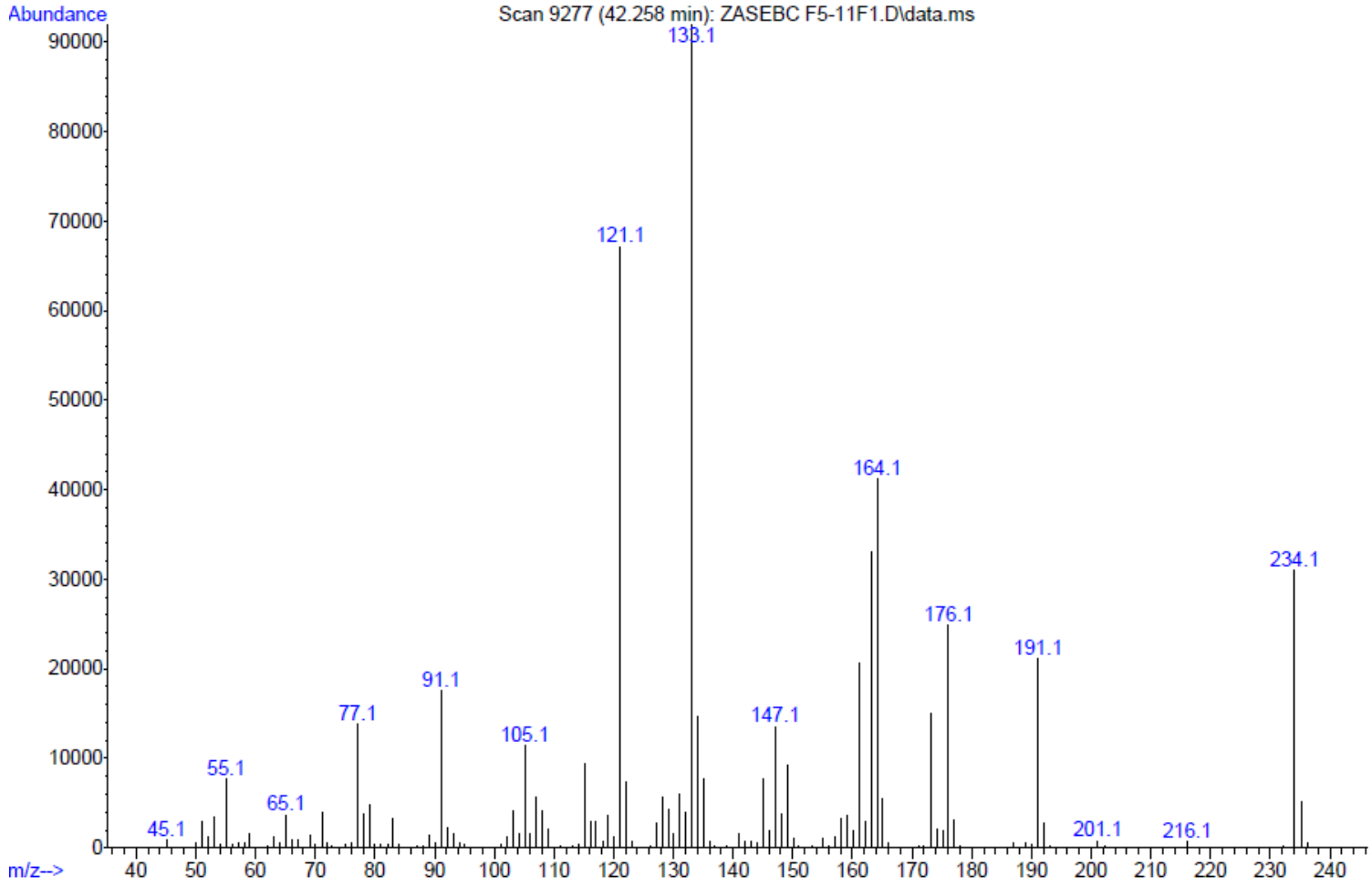

Figure B.2 Mass spectrum of sesquichamaenol.

REFERENCES

[1] American Cancer Society, *Cancer Facts & Figures 2010*, Atlanta: American Cancer Society, 2010.

[2] P. Anand, A.B. Kunnumakkara, A.B. Kunnumakara, C. Sundaram, K.B. Harikumar, S.T. Tharakan, O.S. Lai, B. Sung, and B.B. Aggarwal, "Cancer is a preventable disease that requires major lifestyle changes," *Pharmaceutical Research*, vol. 25, 2008, pp. 2097-2116.

[3] G.M. Cooper, *Elements of Human Cancer*, Boston: Jones & Bartlett, 1992, pp. 178-184.

[4] A. Jemal, R. Siegel, J. Xu, and E. Ward, "Cancer statistics, 2010," *CA: A Cancer Journal for Clinicians*, vol. 60, 2010, pp. 277-300.

[5] American Cancer Society, "What are the key statistics about breast cancer?" *American Cancer Society, Inc.*, 2010, www.cancer.org/Cancer/BreastCancer/DetailedGuide/breast-cancer-key-statistics.

[6] D.J. Blackman and C.M. Masi, "Racial and ethnic disparities in breast cancer mortality: are we doing enough to address the root causes?," *Journal of Clinical Oncology*, vol. 24, 2006, pp. 2170-2178.

[7] M. Cyrus-David, J. King, T. Bevers, and E. Robinson, "Validity assessment of the breast cancer risk reduction health belief scale," *Cancer*, vol. 115, 2009, pp. 4907-4916.

[8] E. Cavalieri, D. Chakravarti, J. Guttenplan, E. Hart, J. Ingle, R. Jankowiak, P. Muti, E. Rogan, J. Russo, R. Santen, and T. Sutter, "Catechol estrogen quinones as initiators of breast and other human cancers: implications for biomarkers of susceptibility and cancer prevention," *Biochimica et Biophysica Acta*, vol. 1766, 2006, pp. 63-78.

[9] H. Lodish, *Molecular Cell Biology*, New York: W.H. Freeman and Co., 2003, pp. 973.

[10] V.G. Vogel, "Chemoprevention Strategies 2006," *Current Treatment Options in Oncology*, vol. 8, 2007, pp. 74-88.

[11] S. Sutherland, S. Ashley, D. Miles, S. Chan, A. Wardley, N. Davidson, R. Bhatti, M. Shehata, H. Nouras, T. Camburn, and S.R. Johnston, "Treatment of HER2-positive metastatic breast cancer with lapatinib and capecitabine in the lapatinib expanded access programme, including efficacy in brain metastases - the UK experience," *British Journal of Cancer*, vol. 102, 2010, pp. 995-1002.

[12] A.H. Gentry, "Chapter 2: Tropical forest biodiversity and the potentail for new medicinal plants," *Human Medicinal Agents from Plants*, American Chemical Society Symposium Series 534, Washington, D.C. 1993, pp. 13-24.

[13] M.F. Balandrin, A.D. Kinghorn, and N.R. Farnsworth, "Chapter 1: Plant-derived natural products in drug discovery and development," *Human Medicinal Agents from Plants*, American Chemical Society Symposium Series 534, Washington, D.C. 1993, pp. 2-12.

[14] L. Reddy, B. Odhav, and K.D. Bhoola, "Natural products for cancer prevention: A global perspective," *Pharmacology & Therapeutics*, vol. 99, Jul. 2003, pp. 1-13.

[15] A. Hager, "Einfluss von Lima und Topographie auf Struktur, Zusammensetzung und Dynamik eines tropischen Wolkenwaldes in Monteverde, Costa Rica (Influence of climate and topography on structure, composition, and dynamics of a tropical cloud forest in Monteverde, Costa Rica)", Ph.D. thesis, Georg August Universitat Gottingen, 2006.

[16] H.F. Howe and L.C. Westley, *Ecological Relationships of Plants and Animals*, Oxford: Oxford University Press, 1990.

[17] A.H. Gentry, *A Field Guide to the Families and Genera of Woody Plants of Northwest South America*, University of Chicago Press, Chicago, Illinois, 1993.

[18] F.R. Stermitz and I.A. Sharifi, "Alkaloids of *Zanthoxylum monophyllum* and *Zanthoxylum punctatum*," *Phytochemistry*, vol. 16, 1977, pp. 2003-2006.

[19] R.E. Schultes and R.F. Raffauf, *The Healing Forest. Medicinal and Toxic Plants of the Northwest Amazonia*," Dioscorides Press, Portland, Orgeon, 1990.

[20] W.A. Haber, W. Zuchowski, and E. Bello, *An Introduction to Cloud Forest Trees, Monteverde, Costa Rica*, Mountain Gem Publications, Monteverde de Puntarenas, Costa Rica, 2000.

[21] L.S. Velentzis, J.V. Woodside, M.M. Cantwell, A.J. Leathem, and M.R. Keshtgar, "Do phytoestrogens reduce the risk of breast cancer and breast cancer recurrence? What clinicians need to know," *European Journal of Cancer*, vol. 44, 2008, pp. 1799-1806.

[22] K.C.G. Jeng and R.C.W. Hou, "Sesamin and Sesamolin: Nature's therapeutic lignans," *Current Enzyme Inhibition*, vol. 1, 2005, pp. 11-20.

[23] K.B. Harikumar, B. Sung, S.T. Tharakan, M.K. Pandey, B. Joy, S. Guha, S. Krishnan, and B.B. Aggarwal, "Sesamin manifests chemopreventive effects through the suppression of NF-kappaB-regulated cell survival, proliferation, invasion, and angiogenic gene products," *Molecular Cancer Research*, vol. 8, 2010, pp. 751-761.

[24] C.Y. Li, T.J. Chow, and T.S. Wu, "The epimerization of sesamin and asarinin," *Journal of Natural Products*, vol. 68, 2005, pp. 1622-1624.

[25] K.H. Lee, H.K. Wang, H. Itokawa, and S.L. Morris-Natschke, "Current perspectives on Chinese medicines and dietary supplements in China, Japan and the United States," *Journal of Food and Drug Analysis*, vol. 8, 2000, pp. 219-228.

[26] G.X. Zhao, Y.H. Hui, J.K. Rupprecht, J.L. McLaughlin, and K.V.J Wood, "Additional bioactive compounds and trilobacin, a novel highly cytotoxic acetogenin, from the bark of *Asimina triloba*," *Journal of Natural Products*, vol. 55, 1992, pp. 347-356.

[27] L.M. Lima, F.F. Perazzo, J.C. Tavares Carvalho, and J.K. Bastos, "Anti-inflammatory and analgesic activities of the ethanolic extracts from *Zanthoxylum riedelianum* (Rutaceae) leaves and stem bark," *The Journal of Pharmacy and Pharmacology*, vol. 59, 2007, pp. 1151-1158.

[28] I.S. Chen, T.L. Chen, Y.L. Chang, C.M. Teng, and W.Y. Lin, "Chemical constituents and biological activities of the fruit of *Zanthoxylum integrifoliolum*," *Journal of Natural Products*, vol. 62, 1999, pp. 833-837.

[29] S. Mora, V. Castro, L. Poveda, M. Chavarria, and R. Murillo, "Chemical constituents from *Zanthoxylum setulosum* (Rutaceae)," *The Latin American and Carribbean Bulletin of Medicinal and Aromatic Plants*, vol. 10, 2011, pp. 155-158.

[30] D.G. Nagle, Y.D. Zhou, F.D. Mora, K.A. Mohammed, and Y.P. Kim, "Mechanism targeted discovery of antitumor marine natural products," *Current Medicinal Chemistry*, vol. 11, 2004, pp. 1725-1756.

[31] R.H.F. Manske, *The Alkaloids: Chemistry and Physiology*, vol. 8, New York: Academic Press, 1965.

[32] C.P. Cordero, S. Gómez-González, C.J. León-Acosta, S.J. Morantes-Medina, and F.A. Aristizabal, "Cytotoxic activity of five compounds isolated from Colombian plants," *Fitoterapia*, vol. 75, 2004, pp. 225-227.

[33] J.P. Michael, "Quinoline, quinazoline and acridone alkaloids," *Natural Product Reports*, vol. 22, 2005, pp. 627-646.

[34] L.K. Wang, R.K. Johnson, and S.M. Hecht, "Inhibition of topoisomerase I function by nitidine and fagaronine," *Chemical Research in Toxicology*, vol. 6, 1993, pp. 813-818.

[35] K. Serghini, A. Perez de Luque, M. Castejon-Munoz, L. Garcia-Toress, and J.V. Jorrin, "Sunflower (*Helianthus annuus* L.) respnose to broomrape (*Orobanche cernua Loefl.*) parasitism: Induced synthesis and excretion of 7-hydroxylated simple coumarins," *Journal of Experimental Botany*, vol. 52, 2001, pp. 2227-2234.

[36] Y. Ju, C.C. Still, J.N. Sacalis, J. Li, C.-tang Ho, and J. Wiley, "Cytotoxic coumarins and lignans from extracts of the northern prickly ash (*Zanthoxylum americanum*)," *Phytotherapy Research*, vol. 15, 2001, pp. 441-443.

[37] A. Greenberg, C.M. Breneman, and J.F. Liebman *The amide linkage: structural significance in chemistry, biochemistry, and materials science*, Wiley-IEEE Press, 2002, pp. 215.

[38] M. Marjanović, B. Zorc, L. Pejnović, M. Zovko, and M. Kralj, "Fenoprofen and ketoprofen amides as potential antitumor agents," *Chemical Biology & Drug Design*, vol. 69, 2007, pp. 222-226.

[39] Q. Xiong, D. Shi, H. Yamamoto, and M. Mizuno, "Alkylamides from pericarps of *Zanthoxylum bungeanum*," *Phytochemistry*, vol. 46, 1997, pp. 1123-1126.

[40] Y. Kashiwada, I. Chikashi, H. Katagiri, I. Mase, K. Komatsu, T. Namba, and Y. Ikeshiro "Amides of the fruit *Zanthoxylum* SPP," *Phytochemistry*, vol. 44, 1997, pp. 1125-1127.

[41] M. Bagchi, M. Milnes, C. Williams, J. Balmoori, X. Ye, S. Stohs, and D. Bagchi, "Acute and chronic stress-induced oxidative gastrointestinal injury in rats, and the protective ability of a novel grape seed proanthocyanidin extract," *Nutrition Research*, vol. 19, 1999, pp. 1189-1199.

[42] A. Islam, A. Sayeed, M.A. Islam, G.R.M. Astaq Mohal Khan, M.H.U. Biswas, and M.S.A. Bhuiyan, "A flavonone from leaves of *Zanthoxylum budrunga*: Its in vitro antimicrobial activity and cytotoxic evaluation," *Journal of Medical Sciences*, 2001, vol. 1, pp. 209-213.

[43] E.J. Cho, T. Yokozawa, D.Y. Rhyu, S.C. Kim, N. Shibahara, and J.C. Park, "Study on the inhibitory effects of Korean medicinal plants and their main compounds on the 1,1-diphenyl-2-picrylhydrazyl radical," *Phytomedicine:International Journal of Phytotherapy and Phytopharmacology*, vol. 10, Jan. 2003, pp. 544-551.

[44] T. Rabi and A. Bishayee, "Terpenoids and breast cancer prevention," *Breast Cancer Research and Treatment*, vol. 115, 2009, pp. 223-239.

[45] B. Lu, L. Liu, X. Zhen, X. Wu, and Y. Zhang, "Anti-tumor activity of triterpenoid-rich extract from bamboo shavings (*Caulis bamfusae* in Taeniam)," *African Journal of Biotechnology*, vol. 9, 2010, pp. 6430-6436.

[46] D.M. Moriarity, J. Huang, C.A. Yancey, P.Z. Zhang, W.N. Setzer, R.O. Lawton, R.B. Bates, and S. Caldera, "Lupeol is the cytotoxic principle in the leaf extract of *Dendropanax cf. querceti*," *Planta Medica*, vol. 64, 1998, pp. 370-372.

[47] C.M. Melo, K.M.M.B. Carvalho, J.C. S. Neves, T.C. Morais, V.S. Rao, F.A. Santos, G.A.C. Brito, and M.H. Chaves, "α,β-amyrin, a natural triterpenoid ameliorates L-arginine-induced acute pancreatitis in rats," *World Journal of Gastroenterology*, vol. 16, 2010, pp. 4272-4280.

[48] I.S. Chen, Y.C. Lin, I.L. Tsai, C.M. Teng, F.N. Ko, T. Ishikawa, and H. Ishii, "Coumarins and anti-platelet aggregation constituents from *Zanthoxylum schinifolium*," *Phytochemistry*, vol. 39, 1995, pp. 1091-1097.

[49] O.A. Binutu and G.A. Cordell, "Constituents of *Zanthoxylum sprucei*," *Pharmaceutical Biology*, vol. 38, 2000, pp. 210-213.

[50] R. Perez, "*Zanthoxylum setulosum* trunk," Smithsonian Tropical Research Institute, http://biogeodb.stri.si.edu/bioinformatics/dfm/metas/view/22146.

[51] M.N. Laszczyk, “Pentacyclic triterpenes of the lupane, oleanane and ursane group as tools in cancer therapy,” *Planta Medica*, vol. 75, 2009, pp. 1549-1560.

[52] Z. Ovensná, A. Vachalková, K. Horváthová, and D. Tothova, “Pentacyclic triterpenoic acids: New chemoprotective compounds. Minireview,” *Neoplasma*, vol. 51, 2004, pp. 327-333.

[53] C.C. Neto, “Cranberry and its phytochemicals: A review in in vitro anticancer studies[1-3],” *Journal of Nutrition*, vol. 137, 2007, pp. 1865-1935.

[54] C. Gerhauser, “Cancer chemopreventive potential of apples, apple juice, and apple components,” *Planta Medica*, vol. 74, 2008, pp. 1608-1624.

[55] S.S. Pereira, L.S. Lopes, R.B. Marques, K.A. Figueiredo, D.A. Costa, M.H. Chaves, and F.R.C. Almeida, “Antinociceptive effect of *Zanthoxylum rhoifolium* Lam. (Rutaceae) in models of acute pain in rodents,” *Journal of Ethnopharmacology*, vol. 129, 2010, pp. 227-231.

[56] W.N. Setzer and M.C. Setzer, “Plant-derived triterpenoids as potential antineoplastic agents,” *Mini Reviews in Medicinal Chemistry*, vol. 3, 2003, pp. 540-556.

[57] A. Petronelli, G. Pannitteri, and U. Testa, “Triterpenoids as new promising anticancer drugs,” *Anti-Cancer Drugs*, vol. 20, 2009, pp. 880-892.

[58] F.B. Mullauer, J.H. Kessler, and J.P. Medema, “Betulinic acid, a natural compound with potent anticancer effects,” *Anti-Cancer Drugs*, vol. 21, 2010, pp. 215-227.

[59] W.N. Setzer, “Non-intercalative triterpenoid inhibitors of topoisomerase II: A molecular docking study,” *The Open Bioactive Compounds Journal*, vol. 1, 2008, pp. 13-17.

[60] Y. Pommier, E. Leo, H.L. Zhang, and C. Marchand, “DNA topoisomerases and their poisoning by anticancer and antibacterial drugs,” *Chemistry & Biology*, vol. 17, 2010, pp. 421-433.

[61] H. Bancroft, J. Ipsen, and P. Feigl, "Bancroft's Introduction to Biostatistics," 2nd Ed. Harper & Row, NY, 1970, Chapter 15.

[62] B.L. Staker, K. Hjerrild, M.D. Feese, C.A. Behnke, A.B. Burgin, and L. Stewart, "The mechanism of topoisomerase I poisoning by a camptothecin analog," *Proceedings of the National Academy of Sciences of the United States of America*, vol. 99, 2002, pp. 15387-15392.

[63] H. Elcock, A. Rodger, and W.G. Richards, "Theoretical studies of the intercalation of 9-hydroxyellipticine in DNA," *Biopolymers*, vol. 39, 1996, pp. 309-326.

[64] G.G. Hu, X. Shui, F. Leng, W. Priebe, J.B. Chaires, and L.D. Williams, "Structure of a DNA-bisdaunomycin complex," *Biochemistry*, vol. 36, 1997, pp. 5940-5946.

[65] M.A. Thompson, "ArgusLab," 2004. Retrieved from http://www.arguslab.com/downloads.htm.

[66] A. Molegro, "Molegro Virtual Docker," 2007. Retrieved from http://www.molegro.com/trial.php?product=mvd.

[67] A.K. Jamal, W.A. Yaacob, and L.B. Din, "A chemical study on *Phyllanthus reticulatus*," *Journal of Physical Science*, vol. 19, 2008, pp. 45-50.

[68] P.W. Baures, M. Miski, and D.S. Eggleston, "Structure of sesamin," *Acta Crystallographica Section C Crystal Structure Comminucations*, vol. 48, 1992, pp. 574-576.

[69] A.B. Díaz, J.R. Vera, V. Cote, J. Bruno-Colmenarez, and G. Diaz de Delgado, "NMR elucidation and crystal structure analysis of 1-hydroxy-3,6- dimethoxy-8-methyl-9h-xanthen-9-one (lichexanthone) isolated from *Vismia baccifera* (Guttiferae)," *Latin American and Caribbean Bulletin of Medicinal and Aromatic Plants*, vol. 9, 2010, pp. 470-474.

[70] N.A. Koorbanally, M. Randrianarivelojosia, D.A. Mulholland, L.Q. van Ufford, and A.J. van den Berg, "Bioactive constituents of *Cedrelopsis microfoliata*," *Journal of Natural Products*, vol. 65, 2002, pp. 1349-1352.

[71] K.G. Byler, C. Wang, and W.N. Setzer, "Quinoline alkaloids as intercalative topoisomerase inhibitors," *Journal of MolecularModeling*, vol. 15, 2009, pp. 1417-1426.

[72] M.B.C. Gallo, and M.J. Sarachine, "Biological activities of lupeol," *International Journal of Biomedical and Pharmaceutical Scicences*, vol. 3, 2009, pp. 46-66.

[73] M.M. Pinto, M.E. Sousa, and M.S Nascimento, "Xanthone derivatives: New insights in biological activity," *Current Medicinal Chemistry*, vol. 12, 2005, pp. 2517-2538.

[74] A.I. Calderon, C. Terreaux, K. Schenk, P. Pattison, J.E. Burdette, J.M. Pezzuto, M.P. Gupta, and K. Hostettmann, "Isolation and structure elucidation of an isoflavone and a sesterterpenoic acid from *Henriettella fascicularis*," *Journal of Natural Products*, vol. 65, 2002, pp. 1749-1753.

[75] A.P. Satos, and P.R.H. Moreno, "*Pilocarpus* spp.: A survey of its chemical constituents and biological activities," *Brazilian Journal of Pharamaceutical Sciences*, vol. 40, 2004, pp. 115-137.

[76] S. Laggoune, I. Brouard, F. Leon, C.A. Calliste, J. Duroux, J. Bermejo, Z. Kabouche, and A. Kabouche, "Lignans and an abundant flavone glycoside with free-radical scavenging activity from the roots of the endemic species *Stachys mialhesi* de Noe," *Records of Natural Products*, vol. 5, 2011, pp. 238-241.

[77] R.M. Letcher, "Chemistry of lichen constituents-VI: Mass spectra of usnic ascid, lichexanthone and their derivatives," *Organic Mass Spectrometry*, vol. 1, 1968, pp. 551-561.

[78] A.K. Boehme, J.A Noletto, W.A. Haber, and W.N. Setzer, "Bioactivity and chemical composition of the leaf essential oils of *Zanthoxylum rhoifolium* and *Zanthoxylum setulosum* from Monteverde, Costa Rica," *Natural Product Research*, vol. 22, 2008, pp. 31-36.

[79] K. Fukuda, Y. Hibiya, M. Mutoh, M. Koshiji, S. Akao, and H. Fujiwara, "Inhibition by berberine of cyclooxygenase-2 transcriptional activity in human colon cancer cells," *Journal of Ethnopharmacology*, vol. 66, 1999, pp. 227-233.

[80] M.M.S. Heck and W.C. Earnshaw, "Topoisomerase II: A specific marker for cell proliferation," *Journal of Cell Biology*, vol. 103, 1986, pp. 2569-2581.

[81] S. Classen, S. Olland, and J.M. Berger, "Structure of the topoisomerase II ATPase region and its mechanism of inhibition by the chemotherapeutic agent ICRF-187," *Proceedings of the National Academy of Sciences of the United States of America*, vol. 100, 2003, pp. 10629-10634.

[82] E.N. Matu and J.V. Staden, "Antibacterial and anti-inflammatory activities of some plants used for medicinal purposes in Kenya," *Journal of Ethnopharmacology*, vol. 87, 2003, pp. 35-41.

[83] D.K. Gehlhaar, D. Bouzida, and P.A. Rejto, "Fully automated and rapid flexible docking of inhibitors covalently bound to serine proteases," *Proceedings of the Seventh International Conference on Evolutionary Programming*, 1998, pp. 449-461.

[84] J.M. Yang and C.C. Chen, "GEMDOCK: A generic evoluntionary method for molecular docking," *Proteins: Structure, Function, and Bioinformatics*, vol. 55, 2004, pp. 288-304.

[85] Molegro ApS, "Molegro virtual docker user manual MVD 2011.4.3 for Windows, Linux, and Mac OS X," 2011, http://www.molegro.com/MVD_Manual.pdf.

[86] G. Jones, P. WIllett, R.C. Glen, A.R. Leach, and R. Taylor, "Development and validation of a generic algorithm for flexible docking." *Journal of Computational Cjemistry*, vol. 267, 1997, pp. 727-748.

[87] B. Kramer, M. Rarey, and T. Lengauer, "Evaluation of the FlexX incremental construction algorithm for protein-ligand docking," *Proteins: Structure, Function, and Bioinformatics*, vol. 37, 199, pp. 228-241.

[88] R. Thomsen and M.H. Christensen, "MolDock: A new technique for high accuracy molecular docking," *Journal of Medicinal Chemistry*, vol. 29, 2006, pp. 3315-3321.

[89] M.A. Thompson, "Molecular docking using ArgusLab, an efficient shape-based search algorithm and the AScore scoring function. *ACS Meeting*, Philadelphia, 172, CINF 42, PA, 2204.

[90] S. Joy, P.S. Nair, R. Hariharan, and M.R. Pillai, "Detailed comparison of the protein-ligand docking efficiencies of GOLD, a commercial package and ArgusLab, a licensable freeware," *In Silico Biology*, vol. 6, 2006, pp. 601-605.

[91] R.A. Friesner, J.L. Banks, R.B. Murphy, and T.A. Halgren, "Glide: A new approach for rapid accurate docking and scoring, 1. method and assessment of docking accuracy," *Journal of Medicinal Chemistry*, vol. 47, 2004, pp. 1739-1749.

[92] A.N. Jain, "Surflex: Fully automatic molecular docking using a molecular similarity-based search engine," *Journal of Medicinal Chemistry*, vol. 46, 2003, pp. 499-511.

[93] Spartan'10 for Windows, Macintosh and Linux Tutorial and User's Guide, Wavefunction, Inc., 2011, http://downloads.wavefun.com/Spartan10Manual.pdf.

[94] Y. Shao, L.F. Molnar, Y. Jung, J. Kussmann, C. Ochsenfeld, S.T. Brown, A.T.B. Gilbert, L.V. Slipchenko, S.V. Levchenko, D.P. O'Neill, R.A. DiStasio Jr., R.C. Lochan, T. Wang, G.J.O. Beran, N.A. Besley, J.M. Herbert, C.Y. Lin, T. Van Voorhis, S.H. Chien, A. Sodt, R.P. Steele, V.A. Rassolov, P.E. Maslen, P.P. Korambath, R.D. Adamson, B. Austin, J. Baker, E.F.C. Byrd, H. Dachsel, R.J. Doerksen, A. Dreuw, B.D. Dunietz, A.D. Dutoi, T.R. Furlani, S.R. Gwaltney, A. Heyden, S. Hirata, C-P. Hsu, G. Kedziora, R.Z. Khalliulin, P. Klunzinger, A.M. Lee, M.S. Lee, W.Z. Liang, I. Lotan, N. Nair, B. Peters, E.I. Proynov, P.A. Pieniazek, Y.M. Rhee, J. Ritchie, E. Rosta, C.D. Sherrill, A.C. Simmonett, J.E. Subotnik, H.L. Woodcock III, W. Zhang, A.T. Bell, A.K. Chakraborty, D.M. Chipman, F.J. Keil, A.Warshel, W.J. Hehre, H.F. Schaefer, J. Kong, A.I. Krylov, P.M.W. Gill and M. Head-Gordon, *Physical Chemistry Chemical Physics*, 8, 2006, pp. 3172.

[95] Spartan'10, Wavefunction, Inc., Irvin, CA. Retrieved from http://downloads.wavefun.com/zipped/Spartan10v101Installer.zip.

[96] W. Saenger, *Principles of Nucleic Acid Structure*, Springer-Verlag: New York, 1984, pp. 132-140.

[97] L.P.G. Wakelin, "Polyfunctional DNA intercalating agents," *Medicinal Research Reviews*, vol. 6, 1986, pp. 275-340.

[98] R.W. Spjut, "Limitations of a random screen: Search for new anticancer drugs in higher plants," *Economic Botany*, vol. 39, 1985, pp. 266-288.